EEG and ECoG features for Brain Computer Interface in Stroke Rehabilitation

Dissertation

zur Erlangung des Grades eines
Doktors der Naturwissenschaften

der Mathematisch-Naturwissenschaftlichen Fakultät
und
der Medizinischen Fakultät
der Eberhard-Karls-Universität Tübingen

vorgelegt
von

Farid Shiman

aus Masjedsoleiman, Iran

August - 2017

Tag der mündlichen Prüfung:	22.01.2018
Dekan der Math.-Nat. Fakultät:	Prof. Dr. W. Rosenstiel
Dekan der Medizinischen Fakultät:	Prof. Dr. I. B. Autenrieth
1. Berichterstatter:	Prof. Dr. Dr. hc. mult. Niels Birbaumer
2. Berichterstatter:	Prof. Dr. Martin Bogdan

Prüfungskommission:

Prof. Dr. Dr. hc. mult. Niels Birbaumer

Prof. Dr. Christoph Braun

Prof. Dr. Martin Bogdan

Prof. Dr. Boris Kotchoubey

I hereby declare that I have produced the work entitled “EEG and ECoG features for Brain Computer Interface in Stroke Rehabilitation”, submitted for the award of a doctorate, on my own (without external help), have used only the sources and aids indicated and have marked passages included from other works, whether verbatim or in content, as such. I swear upon oath that these statements are true and that I have not concealed anything. I am aware that making a false declaration under oath is punishable by a term of imprisonment of up to three years or by a fine.

Tübingen, den ....

Datum / Date Unterschrift /Signature

This thesis is dedicated to my parents.

For their endless love, support and encouragement

Acknowledgements

I would like to express my sincere gratitude to my supervisors, Prof. Dr. Dr. hc. mult. Niles Birbaumer, and Dr. Ander Ramos-Murguialday for supporting me during my research and their enthusiasm and motivation. Their guidance helped me in all the time of research and writing of this thesis. Dear Niels, I am proud that I worked with you during my PhD. I learn a lot from you on both research and personal matter. Dear Ander, I appreciate your persistent help and supervison. You were my primary resource for getting my science questions answered.

I would like to thank to my PhD advisor Prof. Christoph Braun and Prof. Martin Bogdan, for their support, encouragement, and insightful comments. Very special thanks goes to Dr. Eduardo López-Larraz and Dr. Martin Spüler for their guidance and support over the years. My sincere thanks also goes to my dear colleagues Nerea Irastorza-Landa, Andrea Sarasola-Sanz, and Angela Straub for their support during my PhD.

I would like to gratefully acknowledge Dr. Petya Georgieva and Dr. Tina Lampe for coordinating doctoral program. Dear Petya and Dear Tina thanks for your assistance and great advices during my PhD. I would like to also thank Prof. Dr. Horst Herbert, head of the Graduate Training Centre, and Dr. Katja Thieltges, administration and finance Coordinator.

Contents

Abstract

The ability of non-invasive Brain-Computer Interface (BCI) to control an exoskeleton was used for motor rehabilitation in stroke patients or as an assistive device for the paralyzed. However, there is still a need to create a more reliable BCI that could be used to control several degrees of Freedom (DoFs) that could improve rehabilitation results. Decoding different movements from the same limb, high accuracy and reliability are some of the main difficulties when using conventional EEG-based BCIs and the challenges we tackled in this thesis.

In this PhD thesis, we investigated that the classification of several functional hand reaching movements from the same limb using EEG is possible with acceptable accuracy. Moreover, we investigated how the recalibration could affect the classification results. For this reason, we tested the recalibration in each multi-class decoding for within session, recalibrated between-sessions, and between sessions.

It was shown the great influence of recalibrating the generated classifier with data from the current session to improve stability and reliability of the decoding. Moreover, we used a multiclass extension of the Filter Bank Common Spatial Patterns (FBCSP) to improve the decoding accuracy based on features and compared it to our previous study using CSP.

Sensorimotor-rhythm-based BCI systems have been used within the same frequency ranges as a way to influence brain plasticity or controlling external devices. However, neural oscillations have shown to synchronize activity according to motor and cognitive functions. For this reason, the existence of cross-frequency interactions produces oscillations with different frequencies in neural networks. In this PhD, we investigated for the first time the existence of cross-frequency coupling during rest and movement using ECoG in chronic stroke patients. We found that there is an exaggerated phase-amplitude coupling between the phase of alpha frequency and the amplitude of gamma frequency, which can be used as

feature or target for neurofeedback interventions using BCIs. This coupling has been also reported in another neurological disorder affecting motor function (Parkinson and dystonia) but, to date, it has not been investigated in stroke patients. This finding might change the future design of assistive or therapeuthic BCI systems for motor restoration in stroke patients.

Abstrakt

Eine Gehirn-Computer Schnittstelle (engl. Brain-Computer Interface – BCI) kann verwendet werden um ein Exoskelett zu steuern. So lässt sie sich für die motorische Rehabilitation von Schlaganfallpatienten oder als Assistenzsystem für Gelähmte benutzen. Obwohl dies vielfach gezeigt wurde, ist es immer noch notwendig, die Zuverlässigkeit von BCI-Systemen zu erhöhen, um verschiedene Freiheitsgrade zu steuern und somit die Ergebnisse der Rehabilitation zu verbessern. Die Ausdeutung von verschieden Bewegungen einer Gliedmaße, hohe Genauigkeit und Zuverlässigkeit stellen einige der größten Schwierigkeiten bei der Benutzung von BCIs, die auf konventioneller Elektroenzephalographie (EEG) basieren, dar. Diese drei Themen sind die Herausforderungen, die in der vorliegenden Arbeit bearbeitet wurden.

In dieser Dissertation untersuchten wir, ob die Klassifikation von verschiedenen funktionell orientierten Greifbewegungen des gleichen Arms mit akzeptabler Genauigkeit aus dem EEG möglich ist. Darüberhinaus haben wir untersucht, wie Rekalibrierung die Klassifikationsergebnisse beeinflusst. Aus diesem Grund haben wir die Rekalibrierung bei der Klassifikation von mehreren Klassen innerhalb einer Session und zwischen Sessions getestet. Es konnte gezeigt werden, dass die Rekalibrierung großen Einfluss auf die Dekoder mit Daten der aktuellen Session hatte. Besonders erwähnenswert ist dabei, dass die Stabilität und die Genauigkeit der Klassifizierung verbessert werden konnte.

Ferner benutzten wir eine auf mehrere Klassen erweiterte Version des Filter Bank Common Spatial Patterns-Algorithmus (FBCSP), um die Klassifikationsgenauigkeit auf der Basis von Signalcharakteristika zu verbessern und verglichen diese Methode mit unserer vorherigen Studie, bei der der CSP-Algorithmus eingesetzt wurde.

BCI-Systeme, die auf dem sensorimotorischen Rhythmus basieren, wurden bereits in den gleichen Frequenzbereichen eingesetzt, um neuroplastische Prozesse im Gehirn zu beeinflussen und externe Geräte zu steuern. Es wurde jedoch gezeigt, dass

Nervenpopulationen ihre Schwingungen im Zusammenhang mit Bewegungen und kognitiven Funktionen synchronisieren. Aus diesem Grund entstehen aus Interaktionen von miteinander verschränkten Frequenzen Schwingungen in unterschiedlichen Frequenzbändern in neuronalen Netzwerken. In dieser Dissertation haben wir zum ersten Mal gezeigt, dass derartige Interaktionen von verschränkten Frequenzen auch im Elektrokortikogramm (ECoG) von chronisch gelähmten Schlaganfallpatienten bestehen, und zwar im Ruhezustand und während Bewegungen. Wir beobachteten eine übertriebene Kopplung von Phase und Amplitude zwischen der Phase des Alpha-Frequenzbands und der Amplitude des Gamma-Frequenzbands. Diese Kopplung kann als Feature oder Ziel für Neurofeedbacktherapien mit BCI benutzt werden. Darüberhinaus wurde diese Kopplung auch bei anderen neurologischen Erkrankungen, die die Bewegungsfähigkeit beeinträchtigen, beobachtet (Parkinson und Dystonie), aber bis heute wurde sie bei Schlaganfallpatienten noch nicht untersucht. Unsere Ergebnisse könnten das Design von zukünftigen assistiven oder therapeutischen BCI-Systemen für die Wiederherstellung von Bewegung nach Schlaganfall verändern.

Synopsis

Stroke

A sudden interruption of the blood supply to the brain causes a neurological disorder termed stroke (Hossmann 2006). Stroke is one of the most prevalent causes of motor disability worldwide, and its functional limitations can affect the quality of daily living (Dimyan & Cohen 2011; Murphy & Corbett 2009; Langhorne et al. 2009). In 30% to 66% of stroke patients, severe motor deficits remain without recovery when a chronic state is reached after 6 months (Kwakkel et al. 2003). Physiotherapy following stroke has been shown to restore motor function. However, physiotherapy techniques are not useful for chronic stroke patients with severe paralysis due to the necessity of residual active movement (Wolf et al. 2017; Langhorne et al. 2011). Stroke disrupts the connection between the sensorimotor cortex and the peripheral muscles, but a coincident activation of the primary motor cortex and the sensory feedback loop may induce Hebbian plasticity (Murphy & Corbett 2009) for supporting functional recovery. An example of this would be an orthosis moving the paretic limb. Therefore, researchers aim to develop more effective alternative methods that enhance neuroplasticity for rehabilitation of chronic stroke with motor disabilities.

Recent studies have reported the development of rehabilitation robots (Volpe et al. 2000; Krebs et al. 2009; Articles et al. 2008) and neuroprosthetics coupled with brain computer interface (BCI) for chronic stroke rehabilitation (García-Cossio et al. 2015; Ramos-Murguialday et al. 2012; Buch, Weber, Cohen, Braun, Dimyan, Mellinger, et al. 2008; Ramos-Murguialday et al. 2013; Fukuma et al. 2016; Hiremath et al. 2015; Daly & Wolpaw 2008; Ang, Guan, et al. 2014; Birbaumer & Cohen 2007; Wolpaw, Birbaumer, Mcfarland, et al. 2002). These therapies aim to assist the re-organization of neural circuits following stroke or to induce them if chronic stage is reached, in order to restore motor function (Belda-Lois et al. 2011).

Moreover, there is increasing evidence that BCI technologies are better able to enhance the neuroplasticity of patients by closing the loop between brain and hand movement (Ramos-Murguialday et al. 2012; Ramos-Murguialday et al. 2013; Birbaumer & Cohen 2007; Birbaumer 2006; Buch, Weber, Cohen, Braun, Dimyan, Mellinger, et al. 2008).

Application of BCI

Brain Computer Interface (BCI), sometimes called brain machine interface, is a technology for controlling an external device using brain activity (Rogério et al. 2013; Wolpaw, Birbaumer, Mcfarland, et al. 2002). The first study to use BCI was reported in animals by Wyrwicka et al. in 1968. Their BCI study investigated sensorimotor rhythms, using sensory feedback to increase the generation of sensorimotor rhythms in cats (Wyrwicka & Sterman 1968). Kamiya used human subjects to show the volitional control of brain oscillation in healthy participants (Kamiya 1969). This study reported that participants can learn to change the alpha activity using electroencephalography (EEG) (Kamiya 1969).

Different neurophysiological signals have been used for BCI technologies, including EEG (Ramos-Murguialday et al. 2012; Wolpaw & Mcfarland 2004; Kostov & Polak 2000; Pfurtscheller et al. 2005), electrocorticography (ECoG) (Spüler et al. 2014a; Leuthardt et al. 2004; Miller et al. 2010), electromyography (EMG) (Boostani & Moradi 2003; Chang et al. 1996), functional magnetic resonance imaging (fMRI) (Sitaram et al. 2007; Yoo et al. 2004), magnetoencephalography (MEG) (Mellinger et al. 2007; Buch, Weber, Cohen, Braun, Dimyan, Mellinger, et al. 2008), and near-infrared spectroscopy (NIRS) (Coyle et al. 2007). However, functional MRI and MEG are not appropriate for clinical use due to their expense, complex technical requirements, and poor real-time abilities. EEG-based BCI is the most widely used modality for non-invasive neuroimaging in completely paralyzed patients, because of its high temporal resolution. Furthermore, EMG signals, either alone or in

combination with EEG, might be a new strategy for triggering robot movements to close the loop in motor rehabilitation (Ramos-Murguialday et al. 2012; Lalitharatne et al. 2013; Sarasola-Sanz et al. 2015) .

Recently, researchers have shown more interest in using BCI to help patients who suffer from neurological disorders, such as amyotrophic lateral sclerosis, stroke, or other traumatic brain disorders (Daly and Wolpaw, 2008; Chaudhary, Birbaumer and Ramos-Murguialday, 2016). The primary studies using BCI for motor rehabilitation were presented by Pfurtscheller et al. (Gert Pfurtscheller et al. 2003) for traumatic spinal cord injury and by Birbaumer et al. for stroke patients (Birbaumer & Cohen 2007; Buch et al. 2008; Silvoni et al. 2011). BCI systems provide stroke survivors with a feedback, which can affect the brain activity. For this reason, the movement decoding from the brain can be used as feedback which effect the neural network that are directly or indirectly related to the deficit, thus activating neuroplasticity mechanisms (e.g. Hebbian and instrumental learning) (Jackson & Zimmermann 2012). In addition, BCI can be used to control movement of a computer cursor, orthosis, and prosthesis (Jarosiewicz et al. 2016; Gilja et al. 2016; Hochberg et al. 2012) or to stimulate brain or muscles using direct electrical stimulation (Gert Pfurtscheller et al. 2003).

Ramos-Murguialday et al. reported the first double-blind controlled study showing that BCI rehabilitation to control an orthosis can promote motor recovery in severely paralyzed chronic stroke patients (Ramos-Murguialday et al. 2013). Application of BCI has also been reported in patients with extensive impairments in communication and motor function known as amyotrophic lateral sclerosis (ALS). In a successful initial study, Birbaumer et al. found that noninvasive BCIs can be used for communication in locked-in syndrome patients by controlling slow cortical potentials for speller BCI (Birbaumer et al. 1999). However, this strategy has not been successful in complete locked-in syndrome (CLIS).

There are more difficulties using non-invasive EEG, for example, to analyse higher frequencies with low spatial resolutations. On the other hand, ECoG and intracortical

methods have better topographical resolution and wider frequency ranges. There are only a few studies on ECoG-BCI available from people who have had intracortical implants (Leuthardt et al. 2004; Kennedy et al. 2000; Kennedy & Bakay 1998; Hochberg et al. 2006). Literature have shown that most intracortical BCI obtained from animal studies (Serruya et al. 2002; Taylor et al. 2003; Taylor et al. 2002; Musallam et al. 2004; Carmena et al. 2003; Chapin et al. 1999). The question of plasticity in motor recovery can be addressed more precisely with ECoG-BCI rehabilitation therapy, which provides a higher spatial resolution from intracortical recording. Our group has developed an ECoG-BCI rehabilitation for motor recovery in chronic stroke patients (Spüler et al. 2014b; Walter et al. 2012). These studies have shown the application of BCI as an imprtant tool in neurological disorders. Nonetheless, innovative strategies such as BCI-rehabilitation have received little attention in terms of task specific freedoms for non-invasive methods. Moreover, underestanding the mechanism of functional recovery using BCI-rehabilitation therapy is another issue in motor recovery of chronic stroke patients.

In this PhD thesis, I have worked on both issues in developing noninvasive EEG-BCI, decoding more degrees of freedom towards stroke rehabilitation and checking pathological synchronization in ECoG-BCI study using a novel mechanism called cross-frequency interaction.

Electroencephalography (EEG) based BCIs

Electroencephalography measures electrical activity, which reflects the summation of synchronous brain activity from millions of neurons. The electrical brain activity is the flow of electric currents during synaptic excitations in dendrites of neurons (Baillet et al. 2001). EEG was first introduced in human subjects by Hans Berger in 1924 (Berger 1929). EEG has been widely used as a non-invasive neuroimaging modality because of its high temporal

resolution and portability. However, it has low spatial resolution, as it is restricted by volume conduction due to the skull and scalp. For this reason, extracting frequency information above 40 Hz is not possible from EEG.

Non-invasive EEG-based BCI have successfully been used by severely paralyzed patients to control neuroprostheses and wheelchairs (Rogério et al. 2013; Cincotti et al. 2008; Muller-Putz & Pfurtscheller 2008; Sellers et al. 2010). There are different signals that have been used for BCI control but we are focusing on sensorimotor-rhythm (SMR) and slow cortical potentials (SCPs) related BCIs because they are oscillatory activity directly related to the motor neural network.

Motor related EEG-BCI which can be divided into two types for non-invasive BCI in human beings depending on EEG features. For the first type, SMR-based BCIs have been developed using EEG signals recorded over sensorimotor cortices (Wolpaw, Birbaumer, McFarland, et al. 2002; Wolpaw & McFarland 2004; Kostov & Polak 2000; Pfurtscheller et al. 2005; G. Pfurtscheller et al. 2003; Roberts & Penny 2000; Wolpaw et al. 2003; Wolpaw & McFarland 1994; Wolpaw et al. 1991). Sensorimotor rhythms are 8–13 Hz (μ) and 14–26 Hz (β) oscillations the amplitudes of which change with motor task (execution and imagery) and sensation. Studies have reported that patients were able to control a cursor to select a letter or to control an orthotic device (Wolpaw & McFarland 2004; McFarland et al. 2010). Sensorimotor-rhythm-based BCI systems can also support multidimensional control of movements for a robotic arm.

The second type of BCIs uses SCPs, which last from 300 ms to several seconds (Birbaumer et al. 1999; Kübler et al. 2001; Birbaumer et al. 2000). Negative SCPs reflect preparatory depolarization of the underlying cortical network, and positive SCPs indicate cortical inhabitation. The users can be taught to produce negative or positive SCPs for basic word processing or simple control tasks (Kübler et al. 2001; Birbaumer et al. 2000; Birbaumer et al. 1999). All available BCI systems, based on P300, sensorimotor rhythm, and SCP, rely

mainly on visual stimuli and visual feedback. However, for patients with severe paralysis who might not have the necessary visual acuity, BCI systems that use auditory rather than visual stimuli would be preferable.

Electrocorticography (ECoG) based BCIs

Electrocorticography (ECoG) is an invasive technique that measures the brain's electrical activity directly from the cerebral cortex. ECoG has a higher temporal and spatial resolution than EEG and can be used either placed above the dura (epidural) or on the cortex (subdural). Epidural implantation is more common, as its signal has been shown to be similar to the subdural recording (Slutzky et al. 2010). ECoG can record μ-rhythms, β-rhythms, and the higher frequency gamma (30–200 Hz) rhythms which are not possible in EEG recordings. ECoG electrodes are placed under the skull. For this reason, ECoG has been shown to be less sensitive to artifacts and to have a good signal-to-noise ratio (Ball et al. 2009). ECoG electrodes can be implanted by one or multiple stripes or on a quadratic grid with 16-96 electrodes.

The first studies on ECoG were done on animals and evaluated long-term stability of the signals (Margalit et al. 2003; Bullara et al. 1979; Loeb et al. 1977). ECoG has also been used in humans for the analysis of different frequency bands during voluntary motor tasks (Miller et al. 2007; Crone et al. 1998). Moreover, most ECoG recordings in humans were performed on epilepsy patients undergoing treatment to locate the epileptogenic zone (Edakawa et al. 2016). Spüler et al. have reported the feasibility of decoding seven hand movement intentions using ECoG in chronic stroke patients (Spüler et al. 2014a).

ECoG has also been used in BCI to classify motor actions using event-related potentials (ERP) (Levine et al. 1999). An initial study showed that ECoG-BCI could be used to control a one-dimensional cursor and that this system is quicker and more precise than EEG-based BCIs (Leuthardt et al. 2004). Then, another study by Schalk et al. investigated the ability of two-

dimensional ECoG-BCI to control a cursor (Schalk et al. 2007). Pistohl et al. reported prediction of arm movement trajectories from ECoG recording (Pistohl et al. 2008). These studies showed that ECoG-based BCIs are more effective tools to help people with motor disabilities communicate or control external devices. However, ECoG-based BCI systems still need more development to function safely, possibly by using telemetry instead of using wires that pass through the skin.

EEG-classification for Brain Computer Interface

There is an emerging interest in non-invasive electroencephalography (EEG) BCI rehabilitation coupled with exoskeleton. However, the main limitation in the current state of the art of non-invasive BCI systems for rehabilitation is the low number of movements that can be controlled (Ramos-Murguialday et al. 2013; Ang, Chua, et al. 2014; Ono et al. 2014; Pichiorri et al. 2015). It has been reported that the number of degrees of freedom (DoFs) has an important role in rehabilitation robotic therapies (Turner et al. 2013; Oweiss & Badreldin 2015). Several studies have used motor imagery tasks in Initial EEG-based BCI for left hand, right hand, and foot (Wolpaw & Mcfarland 2004; McFarland et al. 2010). Participants were able to move a cursor with two-dimensional control after several sessions of training with left or right hand motor imagery (Wolpaw & McFarland 2004) . These BCI systems were then extended to three-dimensional cursor control based on motor imagery during foot, left hand, and right hand (McFarland et al. 2010). Furthermore, two-class EEG-BCI studies have also been reported in stroke rehabilitation for left vs right hand motor imagery or, more frequently, rest vs motor imagery using visual and functional electrical stimulation (FES) feedback (Fei Meng et al. 2008; Wing-Kin Tam et al. 2011; Ortner et al. 2012; Prasad et al. 2010), or robot feedback (Ang et al. 2010; Ang et al. 2011; Ang, Guan, et al. 2014; Gomez-Rodriguez et al. 2011; Kai Keng Ang et al. 2009; Ramos et al. 2009). The classification from same limb has also been demonstrated for four different imaginary wrist

movements (flexion, extension, pronation, and supination) but the decoding accuracy was not acceptable, approximately 35% (Navarro et al. 2005) .

Furthermore, this control strategy is not intuitive or "natural", so participants need several sessions learning the process to reach acceptable control performance. Moreover, new methods have been developed to control more DoFs for robots using EEG, such as P300 event related potentials (McCane et al., 2015, Sellers and Donchin, 2006, Escolano et al., 2010), steady state visual evoked potentials (SSVEPs) (Ortner et al. 2011), and error potentials (Iturrate et al. 2015). The issue with these methods is that they ignore motor descending which is an important characteristic in motor rehabilitation BCIs for restoring corticomuscular connections (Ramos-Murguialday et al. 2013). In the first controlled study, Ramos-Murguialday et al. reported that motor execution was only correlated with motor improvement compared to motor imagery during a proprioceptive BCI rehabilitative intervention (Ramos-Murguialday et al. 2013).

Other neuronal population signals like magnetoencephalographic (MEG) (Waldert et al. 2008) and intracranial activity (Georgopoulos et al. 1986) were used to decode movement executions from the motor cortex with acceptable decoding accuracy. Intracortical activity has also been used to control multi degrees of freedom for robotic devices in humans (Hochberg et al., 2012, Collinger et al., 2013) and animals (Carmena et al., 2003, Schwartz et al., 2006). However, hand movement decoding from EEG signals, especially from the same limb, is still challenging due to the low spatial resolution and poor signal-to-noise ratio (Sanes et al., 1995). Decoding from the same limb allows more intuitive and natural control of neuroprosthesis, and would also enable users to learn to control different movements using the same device without considering any artificial association between actual movement and neuroprosthesis movement.

Moreover, most of the BCIs designed for stroke rehabilitation only differentiate two classes, rest and movement. These motor rehabilitation based EEG-BCI systems decode natural

movement using a binary classification (rest vs movement) (Ramos-Murguialday et al. 2013; Ang, Chua, et al. 2014; Lopez-Larraz et al. 2014; López-Larraz et al. 2016; Buch, Weber, Cohen, Braun, Dimyan, Ard, et al. 2008; Cincotti et al. 2012; Broetz et al. 2010; Young et al. 2014; Daly et al. 2009; Kaiser et al. 2012). The 2-class BCIs are designed to control only 1DoF for orthosis, visual, and FES feedback for stroke rehabilitation. However, research is needed to develop more realistic methods for using natural movement and more degrees of freedom based on physiological effects of rehabilitation on stroke.

Research has been achieved the classification of functional hand movement from the same limb using EEG mostly between two movements (Sanes et al. 1995; Yong & Menon 2015a; Waldert et al. 2008). For the binary classification, Liao et al. reported ten different pairs of finger movements using 128-channel EEG with acceptable accuracy of 77% (Liao et al. 2014). Vuckovic et al. and Ghani et al. reported a differention of six combinations of different wrist movements using binary classification (flexion, extension, pronation, and supination) with a reasonably high accuracy of 60% to 80% (Vuckovic & Sepulveda 2008; Ghani et al. 2013). There are some additional studies reporting multi-class BCI using execution and imaginery movements from the same upper limb (Yong & Menon 2015a; Ibáñez et al. 2015; Vuckovic & Sepulveda 2008; Deng et al. 2005; Zhou et al. 2009).

Yong et al. show a classification between rest, imaginary grasp, and elbow movement for 3-class BCI using EEG (Yong & Menon 2015b). Focusing on the upper-limb, we could consider training movements reaching in different directions, and different hand and wrist movements (e.g., grasp, pinch, point, pronation, and supination) (Sarasola-Sanz et al. 2015; Irastorza-Landa et al. 2017).

Classification of hand reaching movement has not been reported in the literature from the same limb using EEG. In this PhD thesis, I have shown the feasibility of five-class EEG decoding for four functional reaching movements and rest from the same limb when the participant's hand was placed in a newly developed 7-DoF IsMore Exoskeleton (Shiman,

Irastorza-Landa, Sarasola-Sanz, Spüler, et al. 2015). In this study, we consider the whole trial (forward and backward movement) based on Common Spatial Patterns (CSP) and a linear discriminant analysis (LDA) classifier. Decoding accuracy has been achieved for 39.5% (chance level being 20%) on average for all the subjects (Shiman, Irastorza-Landa, Sarasola-Sanz, Spüler, et al. 2015).

However, healthy subjects show strong brain activation in the regions contralateral to the moving hand but other areas are being also significantly activated depending on the phase of the movement (planning, onset, execution, cessation) (Ramos-Murguialday and Birbaumer, 2015). These cortical activations captured by EEG are affected after any neural lesion in stroke and maintaining the classification performance we obtained in healthy participants will be more challenging. A recent study reported that chronic stroke patients classified by different lesion locations show different EEG patterns (Park et al. 2016). These findings indicated that EEG spectral analyses should be implemented for each patient, considering their lesion location. For all the reasons mentioned above, we have extended our study to use Filter Bank Common Spatial Patterns (FCSP) to extract different frequencies, which helps to optimize the use of EEG patterns instead of single channel features for all the subjects (Shiman, López-Larraz, Sarasola-Sanz, et al. 2017).

Therefore, in this PhD thesis, we studied different class combinations for functional hand movement from the same limb using EEG (Shiman, López-Larraz, Sarasola-Sanz, et al. 2017). We have shown the feasibility of multi-class combination for four forward reaching movements, backward, and rest movement with dramatically increased decoding accuracy towards a more intuitive and natural control of rehabilitative devices like robotic exoskeletons and FES. The decoding accuracy in our study has shown to be increased using FBCSP (Shiman, López-Larraz, Sarasola-Sanz, et al. 2017), compared to the CSP (Shiman, Irastorza-Landa, Sarasola-Sanz, Spuler, et al. 2015), which was also reported in another study (Yong & Menon 2015a; Ang et al. 2008). Moreover, we investigated the influence of

three recalibration strategies on the decoding of each multi-class combinations. This study constitutes a baseline population, which can afterwards be compared to different typologies of patients with different brain alterations, such as stroke and spinal cord injury. Therefore, a BMI system able to decode different movements could be used to provide coincident proprioceptive feedback in order to provide stroke patients with a multi degree of freedom control of rehabilitation or assistive devices.

Sensorimotor rhythm-based BCI systems have been used as a way to influence brain plasticity like normal motor function in disrupted brain connection. However, researchers have studied neural interactions within the same frequency range (e.g. for alpha, beta or gamma) for designing a BCI system or even measuring of therapethic BCI for motor recovery. However, same and different areas of brain operate at different frequency ranges. For this reason, the existence of cross-frequency neural interactions could propogate the information in neural networks producing oscillations with different frequencies at local and global levels. Moreover, cross-frequency coupling in neurological disorders, such as Parkinson, epilepsy, dystonia, and schizophrenia have been shown to be significantly affected, but to date, this coupling has not been investigated in stroke patients. We hypothesized that chronic stroke patient with cortical and subcortical lesion show abnormal synchronization during rest and/or movement, due to the lesion affecting cortico-thalamic and corticospinal neural networks.

For this reason, we designed a study to investigate the cross-frequency coupling as pathological pattern in stroke patients (Shiman, López-Larraz, Figueiredo, et al. 2017).

Pathological synchronization of Cross-Frequency Coupling in stroke rehabilitation

Neural oscillations across multiple frequency bands mediate a number of functions. Frequency activities include the delta (1–4 Hz), theta (4–8 Hz), alpha (8-13 Hz), beta (13–30 Hz), and gamma (>30 Hz) bands with particular functions (Canolty & Knight 2010). The amplitudes of the gamma, alpha, and beta in particular have been shown to be important for motor preparation and execution (Canolty et al. 2006; Pfurtscheller & Lopes 1999). However, the cross-frequency interactions in motor function are not fully understood. Low-amplitude of alpha activity in motor tasks has been reported for active neural processing (Klimesch et al. 2007), termed event-related desynchronization (ERD), and high-amplitude of alpha activity has been reported as a signature of inhibitions, termed event-related synchronization (ERS) (Pfurtscheller & Lopes 1999) for before and after movement, respectively. ERD and ERS can be seen in the part of the motor regions related to the part of the body involved in the movement (Gert Pfurtscheller et al. 2003). However, Ledberg et al. suggested that an interaction of multiple non-motor regions is required for executing movements (Ledberg et al. 2007). For this reason, cross-frequency interaction as a synchronized activity can be seen in neural oscillations for motor and cognitive functions.

Moreover, cross-frequency interactions, in particular phase-amplitude coupling (PAC), have been shown to have a functional role in learning and neural computation (Canolty & Knight 2010; Canolty et al. 2006; Jensen & Colgin 2007; Tort et al. 2009). Phase-amplitude coupling has been reported for the modulation between the phase of the low frequency activity and the amplitude of the high frequency oscillation for sensory, cognitive, and motor tasks (Canolty & Knight 2010). The theoretical importance of PAC has been highlighted by recent studies in which low-frequencies are generated by external motor and sensory input along with the internal cognitive process (Schroeder & Lakatos 2009). The low-frequency phase in

phase-amplitude coupling provides a plausible mechanism for communication guiding cognition, perception, and action when there are slower external and internal events.

Recently, there has been an increased interest in phase-amplitude coupling. PAC has been observed in animals including macaque neocortex (Lakatos et al. 2005), rodent hippocampus (Wulff et al. 2009; Tort et al. 2008; Buzsáki et al. 2003; Bragin et al. 1995; Lakatos et al. 2005; Tort et al. 2009), and rodent basal ganglia (Tort et al. 2008). Furthermore, phase-amplitude coupling has been observed in humans across multiple cortical and subcortical regions with different experimental conditions (Axmacher et al. 2010a; He et al. 2010; Händel & Haarmeier 2009; Cohen, Christian E. Elger, et al. 2009; Mormann et al. 2005; Vanhatalo et al. 2004; Bruns & Eckhorn 2004; Penny et al. 2008; Canolty et al. 2006; Cohen, Axmacher, et al. 2009)

Cohen et al. have shown that the phase of alpha activity is coupled with the amplitude of gamma oscillations in human nucleus accumbens (Cohen, Axmacher, et al. 2009). Furthermore, Axmacher et al. investigated that phase-amplitude cross-frequency coupling play a functional role in cortical processing (Axmacher et al. 2010b). They reported that phase frequency in phase-amplitude coupling depends on working memory load and it remained within the theta range during a working memory task. Canolty et al. reported the phase-amplitude coupling as a mechanism for the global information which is relayed to local information processing (Canolty & Knight 2010). The aboved-mentioned findings showed that phase-amplitude coupling can be modulated dynamically and independently in multiple task-relevant areas but did not provide a clear link to performance. In this way, a well-known study reported a strong correlation between cross-frequency coupling and performance in a learning task (Tort et al. 2009). They found that the strength of hippocampal CFC increased when the rodent performance improved in the learning task. However, their study reported that both CFC strength and task performance were low in the training phase. For this reason, they mentioned that the CFC is not simply an evidence,

which happens independent of behavior. It has been reported that phase-amplitude cross frequency coupling strength is the most predictive neurophysiological marker of learning and can be used as a valuable tool in the future (Tort et al. 2009; Canolty & Knight 2010).

The PAC has been reported as pathological patterns in neurological disorders such as schizophrenia (Uhlhaas & Singer 2010; Moran & Hong 2011), epilepsy (Edakawa et al. 2016; Yanagisawa et al. 2012b; de Hemptinne et al. 2013a), dystonia (de Hemptinne et al. 2013b), and Parkinson (Hammond et al. 2007; de Hemptinne et al. 2013b; de Hemptinne et al. 2015; Lo et al. 2010). This coupling has been reported as an important pattern that can help with diagnosis or in the use of new treatments, such as therapeutic deep brain stimulation in Parkinson (de Hemptinne et al. 2013a; de Hemptinne et al. 2015).

Furthermore, reduction of Phase-amplitude coupling has shown in motor cortex during movement execution (Miller et al. 2012; Yanagisawa et al. 2012b). Many studies reported that PAC link dynamically for task performance in different cortical areas (Axmacher et al. 2010b; Canolty et al. 2006; Cohen, Christian E Elger, et al. 2009). Hemtinne et al. reported exaggerating of phase-amplitude coupling between the phase of beta oscillation and the amplitude of high gamma activity in primary motor cortex in Parkinson patients (de Hemptinne et al. 2013b). It has been shown that there is larger PAC in Parkinson and dystonia as movement disorder compared to the medically intractable epilepsy without basal gangalia disease (de Hemptinne et al. 2013b). An initial study on sensorimotor cortex has reported larger coupling between phase of alpha frequency and amplitude of gamma frequency during rest period prior to the movement in epilepsy patients (Yanagisawa et al. 2012a). However, the existence of phase-amplitude coupling in the sensorimotor cortex of stroke patients has not been reported.

In this PhD thesis, we hypothesized that chronic stroke patients show pathological synchronization between the phase of low-frequency and the amplitude of high-frequency during rest and movement period in the sensorimotor cortex similar to previous findings on

neurological disorders affecting corticothalamic and corticospinal pathways (Parkinson and dystonia). We described phase-amplitude cross-frequency coupling in chronic stroke patients and investigated its evolution during an ECoG-based proprioceptive BCI rehabilitation (Shiman, López-Larraz, Figueiredo, et al. 2017).

In this PhD thesis, I used data from 3 chronic stroke patients implanted with epidural electrocorticography (ECoG) and undergoing a long-term investigational study for brain computer interface (BCI) rehabilitation training (Shiman, López-Larraz, Figueiredo, et al. 2017). Phase-amplitude coupling (PAC) was calculated using the Tort's modulation index (MI) (Tort et al. 2010). First, we investigated normalized changes in modulation index (MI) between movement and rest across all patients before the intervention. We found that there is a significant increase between the phase of alpha frequency and the amplitude of gamma frequency in paralyzed chronic stroke patients, confirming our hypothesis that dissfunction of cortico-thalamic and corticospinal pathways results in abnormal synchronization.

Secondly, we also investigated the phase-amplitude coupling for both movement and rest difference after a week of BCI-rehabilitation. We showed that there is a significantly larger PAC during rest compared to the movement in the first session that is dramatically decreased for both tasks (rest and movement) after six days of BCI rehabilitation. We investigated phase-amplitude coupling for each patient separately and found significant coupling between alpha (in all three patients) and also beta frequency phase (in two out of three patients) and the amplitude of higher gamma. Furthermore, we demonstrated that BCI training produces a statisticaly significant decrease in PAC across all patients, which is also consistent with prior studies for Parkinson showing the reduced PAC by therapeutic DBS (de Hemptinne et al. 2015).

In this PhD thesis, for the first time, we described the phase-amplitude cross frequency coupling in stroke patients and propose its strength as a valuable feature for stroke recovery and/or developing novel motor rehabilitation BCIs.

References

Ang, K.K. et al., 2011. A large clinical study on the ability of stroke patients to Use an EEG-based motor imagery brain computer interface. *Clin EEG Neurosci*, 42(4), pp.253–258. Available at: http://dx.doi.org/10.1177/155005941104200411.

Ang, K.K., Chua, K.S.G., et al., 2014. A Randomized Controlled Trial of EEG-Based Motor Imagery Brain-Computer Interface Robotic Rehabilitation for Stroke. *Clinical EEG and neuroscience*, 1550059414.

Ang, K.K., Guan, C., et al., 2014. Brain-computer interface-based robotic end effector system for wrist and hand rehabilitation : results of a three-armed randomized controlled trial for chronic stroke. , 7(July), pp.1–9.

Ang, K.K. et al., 2010. Clinical study of neurorehabilitation in stroke using EEG based motor imagery brain-computer interface with robotic feedback. *Proceedings of the 32nd Annual International Conference of the IEEE Engineering in Medicine and Biology Society*, 2010, pp.5549–5552. Available at: http://www.ncbi.nlm.nih.gov/pubmed/21096475.

Ang, K.K. et al., 2008. Filter bank common spatial pattern (FBCSP) in brain-computer interface. In *2008 IEEE International Joint Conference on Neural Networks (IEEE World Congress on Computational Intelligence)*. IEEE, pp. 2390–2397.

Articles, R. et al., 2008. Effects of Robot-Assisted Therapy on Upper Limb Recovery After Stroke: A Systematic Review. , pp.111–121.

Axmacher, N. et al., 2010a. Cross-frequency coupling supports multi-item working memory in the human hippocampus. *Proceedings of the National Academy of Sciences of the United States of America*, 107(7), pp.3228–33. Available at: http://www.ncbi.nlm.nih.gov/pubmed/20133762 [Accessed July 17, 2017].

Axmacher, N. et al., 2010b. Cross-frequency coupling supports multi-item working memory in the human hippocampus. *Proceedings of the National Academy of Sciences of the United States of America*, 107(7), pp.3228–33. Available at: http://www.pubmedcentral.nih.gov/articlerender.fcgi?artid=2840289&tool=pmcentrez&rendertype=abstract.

Baillet, S., Mosher, J.C. & Leahy, R.M., 2001. Sylvain Baillet, John C. Mosher, and Richard M. Leahy. , (November).

Ball, T. et al., 2009. Signal quality of simultaneously recorded invasive and non-invasive EEG. *NeuroImage*, 46(3), pp.708–716. Available at: http://www.ncbi.nlm.nih.gov/pubmed/19264143 [Accessed July 17, 2017].

Belda-Lois, J.-M. et al., 2011. Rehabilitation of gait after stroke: a review towards a top-down approach. *Journal of neuroengineering and rehabilitation*, 8(1), p.66. Available at: http://www.pubmedcentral.nih.gov/articlerender.fcgi?artid=3261106&tool=pmcentrez&rendertype=abstract.

Berger, H., 1929. Uber das Elektrenkephalogramm des Menschen. , 278(1875).

Birbaumer, N. et al., 1999. A spelling device for the paralysed. *Nature*, pp.297–298.

Birbaumer, N., 2006. Breaking the silence : Brain – computer interfaces (BCI) for communication and motor control. , 43, pp.517–532.

Birbaumer, N. et al., 2000. The thought translation device (TTD) for completely paralyzed patients. *IEEE transactions on rehabilitation engineering : a publication of the IEEE Engineering in Medicine and Biology Society*, 8(2), pp.190–3. Available at: http://www.ncbi.nlm.nih.gov/pubmed/10896183 [Accessed July 17, 2017].

Birbaumer, N. & Cohen, L.G., 2007. Brain-computer interfaces: communication and restoration of movement in paralysis. *The Journal of physiology*, 579(Pt 3), pp.621–36. Available at: http://www.pubmedcentral.nih.gov/articlerender.fcgi?artid=2151357&tool=pmcentrez&rendertype=abstract.

Boostani, R. & Moradi, M.H., 2003. Evaluation of the forearm EMG signal features for the control of a prosthetic hand. *Physiological measurement*, 24(2), p.309.

Bragin, A. et al., 1995. Gamma (40-100 Hz) oscillation in the hippocampus of the behaving rat. *The Journal of neuroscience : the official journal of the Society for Neuroscience*, 15(1 Pt 1), pp.47–60. Available at: http://www.ncbi.nlm.nih.gov/pubmed/7823151 [Accessed July 17, 2017].

Broetz, D. et al., 2010. Combination of Brain-Computer Interface Training and Goal-Directed Physical Therapy in Chronic Stroke: A Case Report. *Neurorehabilitation and Neural Repair*, 24(7), pp.674–679. Available at: http://www.ncbi.nlm.nih.gov/pubmed/20519741 [Accessed July 17, 2017].

Bruns, A. & Eckhorn, R., 2004. Task-related coupling from high- to low-frequency signals among visual cortical areas in human subdural recordings. *International Journal of Psychophysiology*, 51(2), pp.97–116. Available at: http://linkinghub.elsevier.com/retrieve/pii/S0167876003001715 [Accessed July 17, 2017].

Buch, E., Weber, C., Cohen, L.G., Braun, C., Dimyan, M.A., Mellinger, J., et al., 2008. Think to Move : a Neuromagnetic Brain-Computer Interface (BCI) System for Chronic Stroke. , pp.910–917.

Buch, E., Weber, C., Cohen, L.G., Braun, C., Dimyan, M.A., Ard, T., et al., 2008. Think to move: a neuromagnetic brain-computer interface (BCI) system for chronic stroke. *Stroke*, 39(3), pp.910–917.

Bullara, L.A. et al., 1979. Evaluation of electrode array material for neural prostheses. *Neurosurgery*, 5(6), pp.681–6. Available at: http://www.ncbi.nlm.nih.gov/pubmed/160513 [Accessed July 17, 2017].

Buzsáki, G. et al., 2003. Hippocampal network patterns of activity in the mouse. *Neuroscience*, 116(1), pp.201–11. Available at: http://www.ncbi.nlm.nih.gov/pubmed/12535953 [Accessed July 17, 2017].

Canolty, R.T. et al., 2006. High Gamma Power is Phase-Locked to Theta Oscillations in Human

Neocortex. *Science (New York, N.Y.)*, 313(5793), pp.1626–1628.

Canolty, R.T. & Knight, R.T., 2010. The functional role of cross-frequency coupling. *Trends in Cognitive Sciences*, 14(11), pp.506–515. Available at: http://dx.doi.org/10.1016/j.tics.2010.09.001.

Carmena, J.M. et al., 2003. Learning to Control a Brain–Machine Interface for Reaching and Grasping by Primates Idan Segev, ed. *PLoS Biology*, 1(2), p.e42. Available at: http://dx.plos.org/10.1371/journal.pbio.0000042 [Accessed July 17, 2017].

Chang, G.-C. et al., 1996. Real-time implementation of electromyogram pattern recognition as a control command of man-machine interface. *Medical engineering & physics*, 18(7), pp.529–537.

Chapin, J.K. et al., 1999. Real-time control of a robot arm using simultaneously recorded neurons in the motor cortex. *Nature Neuroscience*, 2(7), pp.664–670. Available at: http://www.ncbi.nlm.nih.gov/pubmed/10404201 [Accessed July 17, 2017].

Chaudhary, U., Birbaumer, N. & Ramos-murguialday, A., 2016. Brain–computer interfaces for communication and rehabilitation.

Cincotti, F. et al., 2012. EEG-based brain-computer interface to support post-stroke motor rehabilitation of the upper limb. *Proceedings of the Annual International Conference of the IEEE Engineering in Medicine and Biology Society, EMBS*, pp.4112–4115.

Cincotti, F. et al., 2008. Non-invasive brain–computer interface system: Towards its application as assistive technology. *Brain Research Bulletin*, 75(6), pp.796–803. Available at: http://www.ncbi.nlm.nih.gov/pubmed/18394526 [Accessed July 17, 2017].

Cohen, M.X., Axmacher, N., et al., 2009. Good vibrations: cross-frequency coupling in the human nucleus accumbens during reward processing. *Journal of Cognitive Neuroscience*, 21(5), pp.875–889. Available at: http://www.mitpressjournals.org/doi/abs/10.1162/jocn.2009.21062\npapers3://publication/doi/10.1162/jocn.2009.21062.

Cohen, M.X., Elger, C.E. & Fell, J., 2009. Oscillatory Activity and Phase–Amplitude Coupling in the Human Medial Frontal Cortex during Decision Making. *Journal of Cognitive Neuroscience*, 21(2), pp.390–402. Available at: http://www.ncbi.nlm.nih.gov/pubmed/18510444 [Accessed July 17, 2017].

Cohen, M.X., Elger, C.E. & Fell, J., 2009. Oscillatory activity and phase-amplitude coupling in the human medial frontal cortex during decision making. *Journal of Cognitive Neuroscience*, 21(2), pp.390–402. Available at: http://eutils.ncbi.nlm.nih.gov/entrez/eutils/elink.fcgi?dbfrom=pubmed&id=18510444&retmode=ref&cmd=prlinks\npapers3://publication/doi/10.1162/jocn.2008.21020.

Coyle, S.M., Ward, T.E. & Markham, C.M., 2007. Brain–computer interface using a simplified functional near-infrared spectroscopy system. *Journal of Neural Engineering*, 4(3), p.219.

Crone, N.E. et al., 1998. Functional mapping of human sensorimotor cortex with electrocorticographic spectral analysis. I. Alpha and beta event-related desynchronization. *Brain : a journal of neurology*, 121 (Pt 12), pp.2271–99. Available at: http://www.ncbi.nlm.nih.gov/pubmed/9874480 [Accessed July 17, 2017].

Daly, J.J. et al., 2009. Feasibility of a New Application of Noninvasive Brain Computer Interface (BCI): A Case Study of Training for Recovery of Volitional Motor Control After Stroke. *Journal of Neurologic Physical Therapy*, 33(4), pp.203–211. Available at:

http://www.ncbi.nlm.nih.gov/pubmed/20208465 [Accessed July 17, 2017].

Daly, J.J. & Wolpaw, J.R., 2008. Brain-computer interfaces in neurological rehabilitation. *The Lancet Neurology*, 7(11), pp.1032–1043.

Deng, J., Yao, J. & Dewald, J.P.A., 2005. Classification of the intention to generate a shoulder versus elbow torque by means of a time–frequency synthesized spatial patterns BCI algorithm. *Journal of Neural Engineering*, 2(4), pp.131–138. Available at: http://www.ncbi.nlm.nih.gov/pubmed/16317237 [Accessed July 17, 2017].

Dimyan, M.A. & Cohen, L.G., 2011. REvIEwS Neuroplasticity in the context of motor rehabilitation after stroke. *Nature Publishing Group*, 7(2), pp.76–85. Available at: http://dx.doi.org/10.1038/nrneurol.2010.200.

Edakawa, K. et al., 2016. Detection of Epileptic Seizures Using Phase-Amplitude Coupling in Intracranial Electroencephalography. *Scientific reports*, 6(April), p.25422. Available at: http://www.ncbi.nlm.nih.gov/pubmed/27147119.

Fei Meng et al., 2008. BCI-FES training system design and implementation for rehabilitation of stroke patients. In *2008 IEEE International Joint Conference on Neural Networks (IEEE World Congress on Computational Intelligence)*. IEEE, pp. 4103–4106. Available at: http://ieeexplore.ieee.org/document/4634388/ [Accessed July 17, 2017].

Fukuma, R. et al., 2016. Real-Time Control of a Neuroprosthetic Hand by Magnetoencephalographic Signals from Paralysed Patients. *Nature Publishing Group*, (August 2015), pp.1–11. Available at: http://dx.doi.org/10.1038/srep21781.

García-Cossio, E. et al., 2015. Decoding sensorimotor rhythms during robotic-assisted treadmill walking for brain computer interface (BCI) applications. *PLoS ONE*, 10(12), pp.1–21.

Georgopoulos, A.P., Schwartz, A.B.A. & Kettner, R.R.E., 1986. Neuronal Population Coding of Movement Direction. *Science*, 233(4771), pp.1416–1419.

Ghani, F. et al., 2013. Classification of Wrist Movements Using EEG Signals. *Journal of Next Generation Information Technology (JNIT)*, 4. Available at: https://pdfs.semanticscholar.org/b38f/842dee403305682cb7885b1c791fe28b6e41.pdf [Accessed July 17, 2017].

Gilja, V. et al., 2016. HHS Public Access. , 21(10), pp.1142–1145.

Gomez-Rodriguez, M. et al., Closing the Sensorimotor Loop: Haptic Feedback Facilitates Decoding of Arm Movement Imagery. Available at: https://people.mpi-sws.org/~manuelgr/pubs/eeg-smc2010.pdf [Accessed July 17, 2017].

Gomez-Rodriguez, M. et al., 2011. Towards brain-robot interfaces in stroke rehabilitation. In *2011 IEEE International Conference on Rehabilitation Robotics*. IEEE, pp. 1–6. Available at: http://www.ncbi.nlm.nih.gov/pubmed/22275589 [Accessed July 17, 2017].

Hammond, C., Bergman, H. & Brown, P., 2007. Pathological synchronization in Parkinson's disease: networks, models and treatments. *Trends in Neurosciences*, 30(7), pp.357–364.

Händel, B. & Haarmeier, T., 2009. Cross-frequency coupling of brain oscillations indicates the success in visual motion discrimination. *NeuroImage*, 45(3), pp.1040–1046. Available at: http://www.ncbi.nlm.nih.gov/pubmed/19150503 [Accessed July 17, 2017].

He, B.J. et al., 2010. The Temporal Structures and Functional Significance of Scale-free Brain Activity. *Neuron*, 66(3), pp.353–369. Available at: http://www.ncbi.nlm.nih.gov/pubmed/20471349 [Accessed July 17, 2017].

de Hemptinne, C. et al., 2013a. Exaggerated phase-amplitude coupling in the primary motor cortex in Parkinson disease. *Proceedings of the National Academy of Sciences of the United States of America*, 110(12), pp.4780–5. Available at: http://www.pnas.org/content/110/12/4780.abstract.

de Hemptinne, C. et al., 2013b. Exaggerated phase-amplitude coupling in the primary motor cortex in Parkinson disease. *Proceedings of the National Academy of Sciences of the United States of America*, 110(12), pp.4780–5. Available at: http://www.pnas.org/content/110/12/4780.abstract.

de Hemptinne, C. et al., 2015. Therapeutic deep brain stimulation reduces cortical phase-amplitude coupling in Parkinson's disease. *Nature Neuroscience*, 18(5), pp.779–786. Available at: http://dx.doi.org/10.1038/nn.3997.

Hiremath, S. V et al., 2015. Brain computer interface learning for systems based on electrocorticography and intracortical microelectrode arrays. *Frontiers in Integrative Neuroscience*, 9(June), pp.1–10. Available at: http://www.scopus.com/inward/record.url?eid=2-s2.0-84934275208&partnerID=40&md5=b5c68c5f2882ebb57bb9a403ee61817b\nhttp://journal.frontiersin.org/article/10.3389/fnint.2015.00040/pdf.

Hochberg, L.R. et al., 2006. Neuronal ensemble control of prosthetic devices by a human with tetraplegia. *Nature*, 442(7099), pp.164–171. Available at: http://www.nature.com/doifinder/10.1038/nature04970 [Accessed July 16, 2017].

Hochberg, L.R. et al., 2012. Reach and grasp by people with tetraplegia using a neurally controlled robotic arm. *Nature*, 485(7398), pp.372–375. Available at: http://dx.doi.org/10.1038/nature11076.

Hossmann, K., 2006. Pathophysiology and Therapy of Experimental Stroke. , 26(November), pp.1057–1083.

Ibáñez, J. et al., 2015. Predictive classification of self-paced upper-limb analytical movements with EEG. *Medical and Biological Engineering and Computing*, 53(11), pp.1201–1210. Available at: "http://dx.doi.org/10.1007/s11517-015-1311-x.

Irastorza-Landa, N. et al., 2017. EMG Discrete Classification Towards a Myoelectric Control of a Robotic Exoskeleton in Motor Rehabilitation. In Springer, Cham, pp. 159–163. Available at: http://link.springer.com/10.1007/978-3-319-46669-9_29 [Accessed July 17, 2017].

Iturrate, I. et al., 2015. Teaching brain-machine interfaces as an alternative paradigm to neuroprosthetics control. *Nature Publishing Group*, pp.1–10. Available at: http://dx.doi.org/10.1038/srep13893.

Jackson, A. & Zimmermann, J.B., 2012. Neural interfaces for the brain and spinal cord — restoring motor function. *Nature Publishing Group*, 8(12), pp.690–699. Available at: http://dx.doi.org/10.1038/nrneurol.2012.219.

Jarosiewicz, B. et al., 2016. HHS Public Access. , 7(313).

Jensen, O. & Colgin, L.L., 2007. Cross-frequency coupling between neuronal oscillations. *Trends in Cognitive Sciences*, 11(7), pp.267–269.

Kai Keng Ang et al., 2009. A clinical study of motor imagery-based brain-computer interface for upper limb robotic rehabilitation. In *2009 Annual International Conference of the IEEE Engineering in Medicine and Biology Society*. IEEE, pp. 5981–5984. Available at: http://ieeexplore.ieee.org/document/5335381/ [Accessed July 17, 2017].

Kaiser, V. et al., 2012. Relationship Between Electrical Brain Responses to Motor Imagery and Motor Impairment in Stroke. *Stroke*, 43(10), pp.2735–2740. Available at: http://www.ncbi.nlm.nih.gov/pubmed/22895995 [Accessed July 17, 2017].

Kamiya, J., 1969. Altered states of consciousness. , pp.519–529.

Kennedy, P.R. et al., 2000. Direct control of a computer from the human central nervous system. *IEEE transactions on rehabilitation engineering : a publication of the IEEE Engineering in Medicine and Biology Society*, 8(2), pp.198–202. Available at: http://www.ncbi.nlm.nih.gov/pubmed/10896186 [Accessed July 16, 2017].

Kennedy, P.R. & Bakay, R.A., 1998. Restoration of neural output from a paralyzed patient by a direct brain connection. *Neuroreport*, 9(8), pp.1707–11. Available at: http://www.ncbi.nlm.nih.gov/pubmed/9665587 [Accessed July 16, 2017].

Klimesch, W., Sauseng, P. & Hanslmayr, S., 2007. EEG alpha oscillations : The inhibition – timing hypothesis. , 3.

Kostov, A. & Polak, M., 2000. Parallel Man–Machine Training in Development of EEG-Based Cursor Control. , 8(2), pp.203–205.

Krebs, H.I., Volpe, B. & Hogan, N., 2009. A working model of stroke recovery from rehabilitation robotics practitioners. , 8, pp.1–8.

Kübler, A. et al., 2001. Brain-computer communication: self-regulation of slow cortical potentials for verbal communication. *Archives of physical medicine and rehabilitation*, 82(11), pp.1533–9. Available at: http://www.ncbi.nlm.nih.gov/pubmed/11689972 [Accessed July 17, 2017].

Kwakkel, G. et al., 2003. Probability of Regaining Dexterity in the Flaccid Upper Limb.

Lakatos, P. et al., 2005. An Oscillatory Hierarchy Controlling Neuronal Excitability and Stimulus Processing in the Auditory Cortex. *Journal of Neurophysiology*, 94(3), pp.1904–1911. Available at: http://www.ncbi.nlm.nih.gov/pubmed/15901760 [Accessed July 17, 2017].

Lalitharatne, T.D. et al., 2013. Towards Hybrid EEG-EMG-Based Control Approaches to be Used in Bio-robotics Applications : Current Status , Challenges and Future Directions. *Journal of behavioral robotics*, 4(2), pp.147–154.

Langhorne, P. et al., 2011. Stroke Care 2 Stroke rehabilitation. , 377.

Langhorne, P., Coupar, F. & Pollock, A., 2009. Motor recovery after stroke : a systematic review. , (i), pp.741–754.

Ledberg, A. et al., 2007. Large-Scale Visuomotor Integration in the Cerebral Cortex. *Cerebral Cortex*, 17(1), pp.44–62. Available at: http://www.ncbi.nlm.nih.gov/pubmed/16452643 [Accessed July 17, 2017].

Leuthardt, E.C. et al., 2004. A brain-computer interface using electrocorticographic signals in humans.

Levine, S.P. et al., 1999. Identification of electrocorticogram patterns as the basis for a direct brain interface. *Journal of clinical neurophysiology : official publication of the American Electroencephalographic Society*, 16(5), pp.439–47. Available at: http://www.ncbi.nlm.nih.gov/pubmed/10576226 [Accessed July 17, 2017].

Liao, K. et al., 2014. Decoding individual finger movements from one hand using human EEG signals. *PLoS ONE*, 9(1), pp.1–12.

Lo, J. et al., 2010. Coupling between Beta and High-Frequency Activity in the Human

Subthalamic Nucleus May Be a Pathophysiological Mechanism in Parkinson ' s Disease. , 30(19), pp.6667–6677.

Loeb, G.E. et al., 1977. Histological reaction to various conductive and dielectric films chronically implanted in the subdural space. *Journal of Biomedical Materials Research*, 11(2), pp.195–210. Available at: http://www.ncbi.nlm.nih.gov/pubmed/323263 [Accessed July 17, 2017].

Lopez-Larraz, E. et al., 2014. Continuous decoding of movement intention of upper limb self-initiated analytic movements from pre-movement EEG correlates. *Journal of neuroengineering and rehabilitation*, 11(1), p.153.

López-Larraz, E. et al., 2016. Control of an ambulatory exoskeleton with a brain-machine interface for spinal cord injury gait rehabilitation. *Frontiers in Neuroscience*, 10. Available at: http://www.frontiersin.org/Journal/Abstract.aspx?s=763&name=neuroprosthetics&ART_DOI=10.3389/fnins.2016.00359.

Margalit, E. et al., 2003. Visual and electrical evoked response recorded from subdural electrodes implanted above the visual cortex in normal dogs under two methods of anesthesia. *Journal of neuroscience methods*, 123(2), pp.129–37. Available at: http://www.ncbi.nlm.nih.gov/pubmed/12606062 [Accessed July 17, 2017].

McFarland, D.J., Sarnacki, W. a & Wolpaw, J.R., 2010. Electroencephalographic (EEG) control of three-dimensional movement. *Journal of neural engineering*, 7(3), p.036007.

Mellinger, J. et al., 2007. An MEG-based brain – computer interface (BCI). , 36, pp.581–593.

Miller, K.J. et al., 2010. Cortical activity during motor execution, motor imagery, and imagery-based online feedback. *Proceedings of the National Academy of Sciences*, 107(9), pp.4430–4435.

Miller, K.J. et al., 2012. Human Motor Cortical Activity Is Selectively Phase- Entrained on Underlying Rhythms. , 8(9).

Miller, K.J. et al., 2007. Real-time functional brain mapping using electrocorticography. *NeuroImage*, 37(2), pp.504–507. Available at: http://linkinghub.elsevier.com/retrieve/pii/S105381190700417X [Accessed July 17, 2017].

Moran, L. V. & Hong, L.E., 2011. High vs low frequency neural oscillations in schizophrenia. *Schizophrenia Bulletin*, 37(4), pp.659–663.

Mormann, F. et al., 2005. Phase/amplitude reset and theta-gamma interaction in the human medial temporal lobe during a continuous word recognition memory task. *Hippocampus*, 15(7), pp.890–900. Available at: http://www.ncbi.nlm.nih.gov/pubmed/16114010 [Accessed July 17, 2017].

Muller-Putz, G.R. & Pfurtscheller, G., 2008. Control of an Electrical Prosthesis With an SSVEP-Based BCI. *IEEE Transactions on Biomedical Engineering*, 55(1), pp.361–364. Available at: http://ieeexplore.ieee.org/document/4360033/ [Accessed July 17, 2017].

Murphy, T.H. & Corbett, D., 2009. Plasticity during stroke recovery: from synapse to behaviour. *Nature reviews. Neuroscience*, 10(12), pp.861–872. Available at: http://dx.doi.org/10.1038/nrn2735.

Musallam, S. et al., 2004. Cognitive Control Signals for Neural Prosthetics. *Science*, 305(5681). Available at: http://science.sciencemag.org/content/305/5681/258.full [Accessed July 17, 2017].

Navarro, I., Hubais, B. & Sepulveda, F., 2005. A Comparison of Time, Frequency and ICA Based Features and Five Classifiers for Wrist Movement Classification in EEG Signals. In *2005 IEEE Engineering in Medicine and Biology 27th Annual Conference*. IEEE, pp. 2118–2121. Available at: http://www.ncbi.nlm.nih.gov/pubmed/17282647 [Accessed July 17, 2017].

Ono, T. et al., 2014. Brain-computer interface with somatosensory feedback improves functional recovery from severe hemiplegia due to chronic stroke. *Frontiers in neuroengineering*, 7(July), p.19.

Ortner, R. et al., 2012. A motor imagery based brain-computer interface for stroke rehabilitation. *Studies in health technology and informatics*, 181, pp.319–23. Available at: http://www.ncbi.nlm.nih.gov/pubmed/22954880 [Accessed July 17, 2017].

Ortner, R. et al., 2011. An SSVEP BCI to control a hand orthosis for persons with tetraplegia. *Neural Systems and Rehabilitation Engineering, IEEE Transactions on*, 19(1), pp.1–5.

Oweiss, K.G. & Badreldin, I.S., 2015. Neurobiology of Disease Neuroplasticity subserving the operation of brain – machine interfaces. *Neurobiology of Disease*, 83, pp.161–171. Available at: http://dx.doi.org/10.1016/j.nbd.2015.05.001.

Park, W. et al., 2016. EEG response varies with lesion location in patients with chronic stroke. *Journal of NeuroEngineering and Rehabilitation*, 13(1), p.21. Available at: http://www.jneuroengrehab.com/content/13/1/21 [Accessed August 4, 2017].

Penny, W.D. et al., 2008. Testing for nested oscillation. , 174, pp.50–61.

Pfurtscheller, G. et al., 2005. EEG-based neuroprosthesis control : A step towards clinical practice. , 382, pp.169–174.

Pfurtscheller, G. et al., 2003. Graz-BCI: state of the art and clinical applications. *IEEE Transactions on Neural Systems and Rehabilitation Engineering*, 11(2), pp.1–4. Available at: http://www.ncbi.nlm.nih.gov/pubmed/12899267 [Accessed July 17, 2017].

Pfurtscheller, G. & Lopes, F.H., 1999. Event-related EEG / MEG synchronization and desynchronization : basic principles. *Clinical Neurophysiology*, 110, pp.1842–1857.

Pfurtscheller, G., Mu, G.R. & Ju, H., 2003. " Thought " – control of functional electrical stimulation to restore hand grasp in a patient with tetraplegia. , 351, pp.33–36.

Pichiorri, F. et al., 2015. Brain – Computer Interface Boosts Motor Imagery Practice during Stroke Recovery. , pp.851–865.

Pistohl, T. et al., 2008. Prediction of arm movement trajectories from ECoG-recordings in humans. *Journal of neuroscience methods*, 167(1), pp.105–114.

Prasad, G. et al., 2010. Applying a brain-computer interface to support motor imagery practice in people with stroke for upper limb recovery: a feasibility study. *Journal of NeuroEngineering and Rehabilitation*, 7(1), p.60. Available at: http://www.ncbi.nlm.nih.gov/pubmed/21156054 [Accessed July 17, 2017].

Ramos, A., Halder, S. & Birbaumer, N., 2009. Proprioceptive feedback in BCI. In *2009 4th International IEEE/EMBS Conference on Neural Engineering*. IEEE, pp. 279–282. Available at: http://ieeexplore.ieee.org/document/5109287/ [Accessed August 4, 2017].

Ramos-Murguialday, A. et al., 2013. Brain–machine interface in chronic stroke rehabilitation: A controlled study. *Annals of Neurology*, 74(1), pp.100–108. Available at: http://dx.doi.org/10.1002/ana.23879.

Ramos-Murguialday, A. et al., 2012. Proprioceptive Feedback and Brain Computer Interface (BCI) Based Neuroprostheses. *PLoS ONE*, 7(10).

Roberts, S.J. & Penny, W.D., 2000. Real-time brain-computer interfacing: a preliminary study using Bayesian learning. *Medical & biological engineering & computing*, 38(1), pp.56–61. Available at: http://www.ncbi.nlm.nih.gov/pubmed/10829391 [Accessed July 17, 2017].

Rogério, P. et al., 2013. Controlling Assistive Machines in Paralysis Using Brain Waves and Other Biosignals Interfaces : A General Overview. , 2013.

Sanes, J.N. et al., 1995. Shared neural substrates controlling hand movements in human motor cortex. *Science*, 268(5218), p.1775.

Sarasola-Sanz, A. et al., 2015. EMG-based multi-joint kinematics decoding for robot-aided rehabilitation therapies. *IEEE International Conference on Rehabilitation Robotics*, 2015-Septe, pp.229–234.

Schalk, G. et al., 2007. Decoding two-dimensional movement trajectories using electrocorticographic signals in humans. *Journal of Neural Engineering*, 4(3), pp.264–275. Available at: http://www.ncbi.nlm.nih.gov/pubmed/17873429 [Accessed July 17, 2017].

Schroeder, C.E. & Lakatos, P., 2009. Low-frequency neuronal oscillations as instruments of sensory selection. *Trends in Neurosciences*, 32(1), pp.9–18. Available at: http://www.ncbi.nlm.nih.gov/pubmed/19012975 [Accessed July 17, 2017].

Sellers, E.W., Vaughan, T.M. & Wolpaw, J.R., 2010. A brain-computer interface for long-term independent home use. *Amyotrophic Lateral Sclerosis*, 11(5), pp.449–455. Available at: http://www.ncbi.nlm.nih.gov/pubmed/20583947 [Accessed July 17, 2017].

Serruya, M.D. et al., 2002. Brain-machine interface: Instant neural control of a movement signal. *Nature*, 416(6877), pp.141–142. Available at: http://www.ncbi.nlm.nih.gov/pubmed/11894084 [Accessed July 17, 2017].

Shiman, F., López-Larraz, E., Sarasola-Sanz, A., et al., 2017. Classification of different reaching movements from the same limb using EEG. *Journal of Neural Engineering*, 14(4), p.046018. Available at: http://www.ncbi.nlm.nih.gov/pubmed/28467325 [Accessed July 17, 2017].

Shiman, F., López-Larraz, E., Figueiredo, T., et al., 2017. Exaggerating of Phase-amplitude coupling in chronic Stroke during Rehabilitation.

Shiman, F., Irastorza-Landa, N., Sarasola-Sanz, A., Spüler, M., et al., 2015. Towards decoding of functional movements from the same limb using EEG. In *Engineering in Medicine and Biology Society (EMBC), 2015 37th Annual International Conference of the IEEE*. IEEE, pp. 1922–1925.

Shiman, F., Irastorza-Landa, N., Sarasola-Sanz, A., Spuler, M., et al., 2015. Towards decoding of functional movements from the same limb using EEG. In *Engineering in Medicine and Biology Society (EMBC), 2015 37th Annual International Conference of the IEEE*. IEEE, pp. 1922–1925.

Silvoni S, Ramos-Murguialday A, Cavinato M, Volpato C, Cisotto G, Turolla A, Piccione F, B.N., 2011. Brain-computer interface in stroke: a review of progress. *Clin EEG Neuroscience*, 4(4), pp.245–52.

Sitaram, R. et al., 2007. FMRI brain-computer interface: a tool for neuroscientific research and treatment. *Computational intelligence and neuroscience*, 2007.

Slutzky, M.W. et al., 2010. Optimal spacing of surface electrode arrays for brain–machine interface applications. *Journal of Neural Engineering*, 7(2), p.026004. Available at: http://www.ncbi.nlm.nih.gov/pubmed/20197598 [Accessed July 17, 2017].

Spüler, M. et al., 2014a. Decoding of motor intentions from epidural ECoG recordings in severely paralyzed chronic stroke patients. *Journal of neural engineering*, 11(6), p.066008.

Spüler, M. et al., 2014b. Decoding of motor intentions from epidural ECoG recordings in severely paralyzed chronic stroke patients. *Journal of neural engineering*, 11(6), p.066008.

Taylor, D.M., Helms Tillery, S.I. & Schwartz, A.B., 2003. Information conveyed through brain-control: cursor versus robot. *IEEE Transactions on Neural Systems and Rehabilitation Engineering*, 11(2), pp.195–199. Available at: http://ieeexplore.ieee.org/document/1214720/ [Accessed July 17, 2017].

Taylor, D.M., Tillery, S.I.H. & Schwartz, A.B., 2002. Direct Cortical Control of 3D Neuroprosthetic Devices. *Science*, 296(5574). Available at: http://science.sciencemag.org/content/296/5574/1829 [Accessed July 17, 2017].

Tort, A.B.L. et al., 2008. Dynamic cross-frequency couplings of local field potential oscillations in rat striatum and hippocampus during performance of a T-maze task. *Proceedings of the National Academy of Sciences of the United States of America*, 105(51), pp.20517–22. Available at: http://www.ncbi.nlm.nih.gov/pubmed/19074268 [Accessed July 17, 2017].

Tort, A.B.L. et al., 2010. Measuring Phase-Amplitude Coupling Between Neuronal Oscillations of Different Frequencies. , pp.1195–1210.

Tort, A.B.L. et al., 2009. Theta-gamma coupling increases during the learning of item-context associations. *Proceedings of the National Academy of Sciences*, 106(49), pp.20942–20947. Available at: http://www.pubmedcentral.nih.gov/articlerender.fcgi?artid=2791641&tool=pmcentrez&rendertype=abstract.

Turner, D.L. et al., 2013. Neurophysiology of robot-mediated training and therapy: A perspective for future use in clinical populations. *Frontiers in Neurology*, 4 NOV(November), pp.1–11.

Uhlhaas, P.J. & Singer, W., 2010. Abnormal neural oscillations and synchrony in schizophrenia. *Nature reviews. Neuroscience*, 11(2), pp.100–13. Available at: http://www.nature.com/doifinder/10.1038/nrn2774\nhttp://www.ncbi.nlm.nih.gov/pubmed/20087360.

Vanhatalo, S. et al., 2004. Infraslow oscillations modulate excitability and interictal epileptic activity in the human cortex during sleep. *Proceedings of the National Academy of Sciences*, 101(14), pp.5053–5057. Available at: http://www.ncbi.nlm.nih.gov/pubmed/15044698 [Accessed July 17, 2017].

Volpe, B.T. et al., 2000. A novel approach to stroke rehabilitation Robot-aided sensorimotor stimulation.

Vuckovic, A. & Sepulveda, F., 2008. Delta band contribution in cue based single trial classification of real and imaginary wrist movements. *Medical and Biological Engineering and Computing*, 46(6), pp.529–539.

Waldert, S. et al., 2008. Hand movement direction decoded from MEG and EEG. *The Journal of neuroscience : the official journal of the Society for Neuroscience*, 28(4), pp.1000–8.

Available at: http://www.ncbi.nlm.nih.gov/pubmed/18216207.

Walter, A. et al., 2012. Coupling BCI and cortical stimulation for brain-state-dependent stimulation: methods for spectral estimation in the presence of stimulation after-effects. *Frontiers in neural circuits*, 6(November), p.87. Available at: http://www.pubmedcentral.nih.gov/articlerender.fcgi?artid=3499764&tool=pmcentrez&rendertype=abstract.

Wing-Kin Tam et al., 2011. A Minimal Set of Electrodes for Motor Imagery BCI to Control an Assistive Device in Chronic Stroke Subjects: A Multi-Session Study. *IEEE Transactions on Neural Systems and Rehabilitation Engineering*, 19(6), pp.617–627. Available at: http://ieeexplore.ieee.org/document/6034528/ [Accessed July 17, 2017].

Wolf, S.L. et al., 2017. Effect of Constraint-Induced Movement. , 296(17), pp.2095–2104.

Wolpaw, J.R. et al., 1991. An EEG-based brain-computer interface for cursor control. *Electroencephalography and Clinical Neurophysiology*, 78(3), pp.252–259. Available at: http://linkinghub.elsevier.com/retrieve/pii/001346949190040B [Accessed July 17, 2017].

Wolpaw, J.R., Birbaumer, N., Mcfarland, D.J., et al., 2002. Brain – computer interfaces for communication and control. , 113, pp.767–791.

Wolpaw, J.R., Birbaumer, N., McFarland, D.J., et al., 2002. Brain–computer interfaces for communication and control. *Clinical neurophysiology*, 113(6), pp.767–791.

Wolpaw, J.R. et al., 2003. The wadsworth center brain-computer interface (bci) research and development program. *IEEE Transactions on Neural Systems and Rehabilitation Engineering*, 11(2), pp.204–207. Available at: http://www.ncbi.nlm.nih.gov/pubmed/12899275 [Accessed July 17, 2017].

Wolpaw, J.R. & Mcfarland, D.J., 2004. Control of a two-dimensional movement signal by a noninvasive brain – computer interface in humans. , 101(51).

Wolpaw, J.R. & McFarland, D.J., 2004. Control of a two-dimensional movement signal by a noninvasive brain-computer interface in humans. *Proceedings of the National Academy of Sciences of the United States of America*, 101(51), pp.17849–17854.

Wolpaw, J.R. & McFarland, D.J., 1994. Multichannel EEG-based brain-computer communication. *Electroencephalography and Clinical Neurophysiology*, 90(6), pp.444–449. Available at: http://linkinghub.elsevier.com/retrieve/pii/001346949490135X [Accessed July 17, 2017].

Wulff, P. et al., 2009. Hippocampal theta rhythm and its coupling with gamma oscillations require fast inhibition onto parvalbumin-positive interneurons. *Proceedings of the National Academy of Sciences*, 106(9), pp.3561–3566. Available at: http://www.ncbi.nlm.nih.gov/pubmed/19204281 [Accessed July 17, 2017].

Wyrwicka, W. & Sterman, M.B., 1968. Instrumental Conditioning of Sensorimotor Cortex EEG Spindles in the Waking Cat ’. , 3, pp.703–707.

Yanagisawa, T. et al., 2012a. Regulation of Motor Representation by Phase – Amplitude Coupling in the Sensorimotor Cortex. , 32(44), pp.15467–15475.

Yanagisawa, T. et al., 2012b. Regulation of motor representation by phase-amplitude coupling in the sensorimotor cortex. *The Journal of neuroscience : the official journal of the Society for Neuroscience*, 32(44), pp.15467–75. Available at: http://www.ncbi.nlm.nih.gov/pubmed/23115184.

Yong, X. & Menon, C., 2015a. EEG classification of different imaginary movements within the

same limb. *PLoS ONE*, 10(4), pp.1–24. Available at: http://dx.doi.org/10.1371/journal.pone.0121896.

Yong, X. & Menon, C., 2015b. EEG Classification of Different Imaginary Movements within the Same Limb. *PLoS One*, 10(4).

Yoo, S.-S. et al., 2004. Brain–computer interface using fMRI: spatial navigation by thoughts. *Neuroreport*, 15(10), pp.1591–1595.

Young, B.M. et al., 2014. Case report: post-stroke interventional BCI rehabilitation in an individual with preexisting sensorineural disability. *Frontiers in Neuroengineering*, 7, p.18. Available at: http://www.ncbi.nlm.nih.gov/pubmed/25009491 [Accessed July 17, 2017].

Zhou, J. et al., 2009. EEG-based classification for elbow versus shoulder torque intentions involving stroke subjects. *Computers in biology and medicine*, 39(5), pp.443–52. Available at: http://www.ncbi.nlm.nih.gov/pubmed/19380125 [Accessed July 17, 2017].

Presentation of own contributions to papers and manuscripts
(Darstellung des Eigenanteils bei Gemeinschaftsarbeiten nach §9 para. 2)

1. *Shiman, F., López-Larraz, E., Sarasola-Sanz, A., Irastorza-Landa, N., Spüler, M., Birbaumer, N., and Ramos-Murguialday, A.* (2017) 'Classification of different reaching movements from the same limb using EEG', *Journal of Neural Engineering*, 14(4), p. 46018. doi: 10.1088/1741-2552/aa70d2.

Designed the experiment: Shiman, F., Sarasola-Sanz, A., Irastorza-Landa, N., Birbaumer, N., and Ramos-Murguialday, A. Data analysis: Shiman, F. Performed the experiment: Shiman, F., Sarasola-Sanz, A., and Irastorza-Landa, N. Wrote the paper: Shiman, F., and Ramos-Murguialday, A. Manuscript revision: Shiman, F., Ramos-Murguialday, A., López-Larraz, E., Birbaumer, N., and Spüler, M.

2. *Shiman, F., Irastorza-Landa, N., Sarasola-Sanz, A., Spüler, M., Birbaumer, N., and Ramos-Murguialday, A.* (2015) 'Towards decoding of functional movements from the same limb using EEG', in *Engineering in Medicine and Biology Society (EMBC), 2015 37th Annual International Conference of the IEEE*. IEEE, pp. 1922–1925.

Designed the experiment: Shiman, F., Irastorza-Landa, N., Sarasola-Sanz, A., Birbaumer, N., and Ramos-Murguialday, A. Data analysis: Shiman, F. Performed the experiment: Shiman, F., Sarasola-Sanz, A., Irastorza-Landa. Wrote the paper: Shiman, F., Manuscript revision: Shiman, F., Ramos-Murguialday, A., and Birbaumer, N.

3. *Shiman, F., López-Larraz, E., Figueiredo, T., Sarasola-Sanz, A., Irastorza-Landa, N., Spüler, M., Birbaumer, N., and Ramos-Murguialday, A.* Exaggerated Phase-amplitude coupling in chronic Stroke during Rehabilitation. Manuscript is ready to be submitted.

Designed the study: Shiman, F., Ramos-Murguialday, A., and Birbaumer, N. Data analysis: Shiman, F. Wrote the paper: Shiman, F., and Ramos-Murguialday, A. Manuscript revision: Shiman, F., Ramos-Murguialday, Figueiredo, T., A., López-Larraz, E., Sarasola-Sanz, A., Irastorza-Landa, N., Birbaumer, N., and Spüler, M.

4. *Sarasola-Sanz, A., Irastorza-Landa, N., Shiman, F., Spüler, M., Birbaumer, N., and Ramos-Murguialday, A.* (2015) 'EMG-based multi-joint kinematics decoding for robot-aided rehabilitation therapies', *IEEE International Conference on Rehabilitation Robotics*, 2015–Septe, pp. 229–234. doi: 10.1109/ICORR.2015.7281204.

Designed the experiment: Shiman, F., Sarasola-Sanz, A., Irastorza-Landa, N., and Ramos-Murguialday, A. Data analysis: Sarasola-Sanz, A., Irastorza-Landa, N., and Spüler, M. Performed the experiment: Shiman, F., Sarasola-Sanz, A., Irastorza-Landa. Wrote the paper: Sarasola-Sanz, A. Manuscript revision: Shiman, F., Ramos-Murguialday, A., Birbaumer, N.

5. *Irastorza-Landa, N., A. Sarasola-Sanz, Shiman, F., López-Larraz, E., Klein, J., Valencia, D., Belloso, A., Morin, F.O., Birbaumer, N., and Ramos-Murguialday*, A.,(2017) 'EMG Discrete Classification Towards a Myoelectric Control of a Robotic Exoskeleton in Motor Rehabilitation', in. Springer, Cham, pp. 159–163. doi: 10.1007/978-3-319-46669-9_29.

Designed the experiment: Shiman, F., Sarasola-Sanz, A., Irastorza-Landa, *E*., Klein, J., Valencia, D., Belloso, A., Morin, F.O, N., Birbaumer, N., and Ramos-Murguialday, A. Data analysis: Irastorza-Landa, N., Performed the experiment: Shiman, F., Sarasola-Sanz, A., Irastorza-Landa. Wrote the paper: Irastorza-Landa, N., and Ramos-Murguialday, A. Manuscript revision: Shiman, F., Ramos-Murguialday, A., López-Larraz, E., Birbaumer, N.

6. *de Almeida Ribeiro, P. R., Brasil, F. L., Witkowski, M., Shiman, F., Cipriani, C., Vitiello, N., Carrozza, M. C., Soekadar, S. R.* (2013). Controlling assistive machines in paralysis using brain waves and other biosignals. *Advances in Human-Computer Interaction*.

Designed the experiment: Shiman, F., de Almeida Ribeiro, P. R., Brasil, F. L., Witkowski, M., Birbaumer, N., Cipriani, C., Vitiello, N., Carrozza, M. C., Soekadar, S. R., Performed the experiment: Shiman, F., de Almeida Ribeiro, P. R., Wrote the paper: Shiman, F., de Almeida Ribeiro, P. R., Soekadar, S. R., and Carrozza, M. C., Manuscript revision: Shiman, F., Cipriani, C., Vitiello, N., Carrozza, M. C., Soekadar, S. R.

OPEN ACCESS
IOP Publishing
Journal of Neural Engineering
J. Neural Eng. **14** (2017) 046018 (13pp)
https://doi.org/10.1088/1741-2552/aa70d2

Classification of different reaching movements from the same limb using EEG

Farid Shiman[1,2], Eduardo López-Larraz[1], Andrea Sarasola-Sanz[1,2], Nerea Irastorza-Landa[1,2], Martin Spüler[5], Niels Birbaumer[1,3] and Ander Ramos-Murguialday[1,4]

[1] Institute of Medical Psychology and Behavioral Neurobiology, University of Tübingen, Tübingen, Germany
[2] International Max Planck Research School (IMPRS) for Cognitive and Systems Neuroscience, Tübingen, Germany
[3] Wyss Center for Bio-and Neuroengineering, Geneva, Switzerland
[4] TECNALIA, San Sebastian, Spain
[5] Computer Science Department, Wilhelm-Schickard-Institute, University of Tübingen, Tübingen, Germany

E-mail: Ander.ramos-murguialday@uni-tuebingen.de

Received 3 October 2016
Accepted for publication 3 May 2017
Published 12 June 2017

Abstract

Objective. Brain–computer-interfaces (BCIs) have been proposed not only as assistive technologies but also as rehabilitation tools for lost functions. However, due to the stochastic nature, poor spatial resolution and signal to noise ratio from electroencephalography (EEG), multidimensional decoding has been the main obstacle to implement non-invasive BCIs in real-live rehabilitation scenarios. This study explores the classification of several functional reaching movements from the same limb using EEG oscillations in order to create a more versatile BCI for rehabilitation. *Approach.* Nine healthy participants performed four 3D center-out reaching tasks in four different sessions while wearing a passive robotic exoskeleton at their right upper limb. Kinematics data were acquired from the robotic exoskeleton. Multiclass extensions of Filter Bank Common Spatial Patterns (FBCSP) and a linear discriminant analysis (LDA) classifier were used to classify the EEG activity into four forward reaching movements (from a starting position towards four target positions), a backward movement (from any of the targets to the starting position and rest). Recalibrating the classifier using data from previous or the same session was also investigated and compared. *Main results.* Average EEG decoding accuracy were significantly above chance with 67%, 62.75%, and 50.3% when decoding three, four and six tasks from the same limb, respectively. Furthermore, classification accuracy could be increased when using data from the beginning of each session as training data to recalibrate the classifier. *Significance.* Our results demonstrate that classification from several functional movements performed by the same limb is possible with acceptable accuracy using EEG oscillations, especially if data from the same session are used to recalibrate the classifier. Therefore, an ecologically valid decoding could be used to control assistive or rehabilitation mutli-degrees of freedom (DoF) robotic devices using EEG data. These results have important implications towards assistive and rehabilitative neuroprostheses control in paralyzed patients.

Keywords: brain–computer interface (BCI), electroencephalography (EEG), motor rehabilitation

(Some figures may appear in colour only in the online journal)

Introduction

Brain–computer interface (BCI) systems can be used to decode brain activity into commands to control external devices [1, 2]. A recent double-blind controlled study has demonstrated for the first time that BCI control of a rehabilitation robot can promote motor recovery of severely paralyzed chronic stroke patients [3], being these results reproduced and confirmed [4–6]. BCIs can also function as an assistive device to restore a lost function, such as motor control. It's obvious that the number of DoFs that can be volitionally controlled is very relevant for assistive technologies and prosthetics. This has also been suggested to be of paramount importance in rehabilitation robotic therapies [7, 8]. Initial EEG-based BCI studies controlling several DoFs were achieved using motor imagery paradigms involving different limbs (e.g. 3D cursor control using hand versus feet versus tongue motor imagery) [9, 10]. This control strategy, albeit successful, is not based on 'natural' or ecologically valid environments (i.e. based on EEG oscillations produced rapidly and without conscious effort when performing the task) and an extensive learning process is necessary to achieve acceptable control performance. Recently, new strategies have been used to control multi-DoF robots based on EEG error potentials [11], steady state visual evoked potentials (SSVEPs) [12] and P300 potentials, even in ALS patients [13–15]. These strategies require attention but ignore motor descending corticospinal volleys, which seems to be key aspect in motor rehabilitation BCIs aiming at restoring natural corticomuscular connections [3]. Involvement on descending motor commands was suggested as key mechanism in motor rehabilitation because motor execution/attempt brain activity only was correlated with significant motor improvement compared to motor imagery related brain activity during a proprioceptive BCI rehabilitative intervention [3]. Other strategies like trajectory decoding [16] might offer a promising solution, albeit methodological challenges [17].

Neuronal population signals have been used to decode, with acceptable decoding performance, directional movement executions using non-invasive magnetoencephalographic (MEG) [18] and intracranial activity [19] from the motor cortex. Furthermore, intracortical activity has been successfully used to control several degrees of freedom of robotic devices in primates [20, 21] and in humans [22, 23] decoding and/or encoding neural signals. Recently, control over functional electrical stimulation (FES) [24] in humans has been also achieved. Furthermore, intracranial EEG has also been used to continuously decode two-dimensional (2D) hand position [25], wrist movement trajectory [26] and seven different hand movement intentions in severely paralyzed chronic stroke patients [27]. However, invasive and MEG (nowadays too bulky and expensive to be considered as a practical option) data decoding are out of the scope of this paper.

Upper limb and especially hand movement decoding from electroencephalography (EEG) signals is still challenging mainly due to poor signal to noise ratio and spatial resolution [28]. Existing motor rehabilitation oriented BCI systems (i.e. decoding 'natural' movement related EEG oscillations) decode two classes only using simple binary classification between rest and movement [3, 4, 29–32]. These BCI systems only allow a user to control 1 DoF (e.g. orthosis for opening or closing the hand, a predefined functional electrical stimulation (FES) or visual feedback).

Recent studies have achieved classification of the same limb with acceptable performance using EEG data although many of these studies classify only two movements [18, 28, 33, 34]. Liao *et al* investigated the binary classification of ten different pairs of executed finger movements using 128-channel EEG signals achieving a promising average decoding performance of 77.1% [35]. In another study, six different wrist movement pairs (e.g. flexion versus extension or pronation versus supination) were decoded with average accuracy ranging from 60 to 80% [36]. A few other groups have reported some preliminary work on multi-class decoding using motor imagery and execution of movements from the same upper limb [33, 37, 38]. Yong *et al* have shown a 3-class BCI system that discriminates EEG signals corresponding to rest, imaginary grasp, and elbow movement [33]. Furthermore, classification of hand movement directions from the same limb using EEG has not been sufficiently explored in the literature. Our previous work reported five class EEG decoding reported during multiclass classification of four movements directions and rest from the same limb [34].

We believe, discriminating different movements within the same limb would allow more intuitive control of neuroprostheses (e.g. brain controlled exoskeleton) without considering any artificial association between actual movement and neuroprosthetic movement. Therefore, in the here presented work, we aimed at discriminating 6 different functional movements from the same limb with acceptable accuracy levels using EEG data towards a more intuitive and natural control of rehabilitative devices like robotic exoskeletons and FES. Furthermore, we evaluated the impact of different recalibration strategies on the decoding to optimize system stability.

We hypothesize decoding accuracy levels allowing robotic control of rehabilitative devices of up to 6 functional movements from the same limb, could be achieved using EEG activity only.

Materials and methods

Participants

Study participants included nine healthy right-handed subjects (6 male, age: 24 ± 4 years) with no history of neurologic disease. Participants underwent four recording sessions (4 non-consecutive days) within eight days (average time

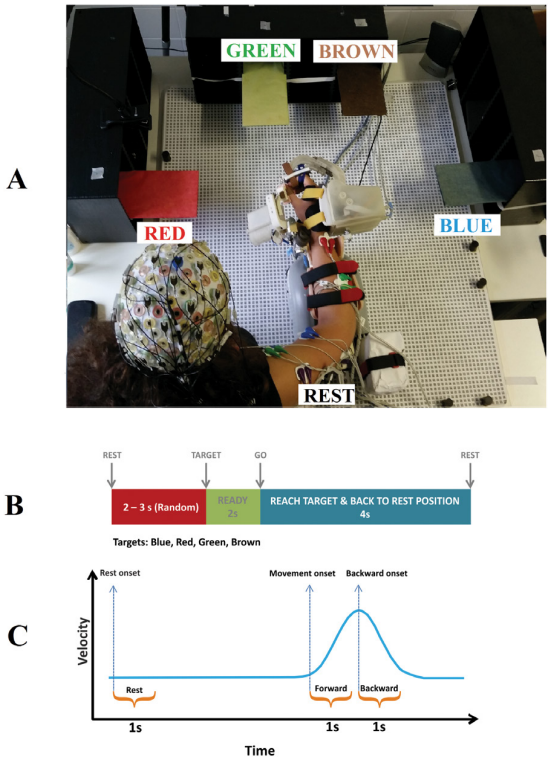

Figure 1. (A) Experimental situation: participant performing a reaching movement from the starting rest position towards the green target. Reaching movements were executed towards the four different targets represented by rectangles coloured in blue, red, green and brown. (B) Timing: to begin, an auditory 'Rest' cue was presented indicating a random resting period between 2 to 3 s. immediately after this period an instructional auditory cue indicated to which target the participant was asked to move (blue, red, green, brown). Two seconds afterwards a 'GO' cue indicated the moment to start the active movement towards the targets at a comfortable pace, having a 4 s time out to perform the reaching movement and come back to the starting position. (C) Movement onsets were identified for forward and backward movements into 1 s epoch for each trial by kinematics data. Rest class was also segmented into 1 s epoch from the beginning of each rest interval.

between each session was 2 d). The experimental procedure was explained to the subjects and they were asked to sign a written consent form. Ethically permission was given by the ethical committee of the Faculty of Medicine, University of Tübingen, Germany.

Experimental setup

Participants were seated in a comfortable chair in front of a desk (see figure 1(A)) especially designed for the experiment. Participants were asked to perform 4 different center-out functional reaching movements and move back to the initial starting position (see figure 1(A)) with their right upper limb attached to an IS-MORE 7-DoF robotic exoskeleton (Tecnalia, San Sebastian, Spain) upon imperative auditory cues (see figure 1(A)). All the participants were instructed to perform the outreaching movements in the same way, and rhythmic auditory cues were used to facilitate movements' timing. The directional colored targets were named as Blue, Red, Green, and Brown. Participants were asked to reach a colored target and return to the rest position at a comfortable pace.

IS-MORE robotic exoskeleton

We decided to use an exoskeleton to record the kinematic data to simulate a realistic scenario condition in which a patient could brain-control the exoskeleton to produce functional movements like reach and grasp. For an optimal stroke rehabilitation paradigm, a realistic environment with different functional movements trained at the same time is very important. Training of reaching movements is key in stroke recovery, as it involves elbow-shoulder coordination [39]. The Exoskeleton was friction-free and motors were disengaged, although produced some mechanical restrictions (e.g. no vertical, or writs movement). Furthermore, the haptics related to the use of the exoskeleton will be present during the real scenario and could also produce some brain activity from afferent origin, which could influence brain oscillatory signature of each motor task.

The exoskeleton can be moved in 7 DoFs including displacement and rotation of the forearm in a 2D horizontal plane (3 proximal DoFs: position in *X*, position in *Y*, and forearm orientation angle), pronation and supination of the wrist (1 distal DoF: wrist angle), flexion and extension of the thumb, index and the group of middle, ring and pinky fingers (3 distal DoFs: thumb angle; index angle; three fingers angle).

Kinematic data (position in *X*, position in *Y*, and forearm orientation angle) of the midpoint of the fore-arm was calculated and recorded via a camera attached to the bottom of the base of the device. The exoskeleton rolls on top of a map with micro optical symbols printed on it, which are used to calculate the instantaneous position (more details can be found in [37, 40]). The rest of the DoFs were recorded using motor encoders and potentiometers. Kinematic data was recorded at 18 Hz. Participants also performed 4 hand grasping movements (pinch grip, key and cylindrical grasp and pointing with the index finger) and reach-and-grasp movements to the 4 targets described in the manuscript combining the different grasping movements using especially designed objects for that purpose. Although we have analyzed the data, we have not included neither the experimental procedure nor the classification results in this manuscript because we did not obtain 'above chance level' classification results for the grasping movements.

Experimental paradigm

Each experimental session was divided in 5 runs, each consisting of 40 trials (10 trials for each target). The experimental timing diagram for each trial is shown in figure 1(B). Each trial consisted of three phases separated by auditory cues: (1) resting interval (random length between 2–3 s); (2) an instructional cue regarding the target to be reached (2 s); (3) 'Go' cue to initiate reaching movements towards the indicated

targets and come back to the starting position at a comfortable pace but always executed in less than 4 s. In order to reduce artifacts, we asked subjects to keep the jaw and face muscles relaxed avoiding eye blinks or swallowing during data recording. Therefore, to increase participants' awareness regarding artifacts, we performed a brief instruction task before the first session instructing subjects to perform face, neck, contralateral arm and eye movements, while raw data was shown to them.

Data acquisition

EEG was recorded according to the international 10–20 system from 32 active electrodes as FP1, FP2, F7, F3, Fz, F4, F8, FC5, FC1, FC2, FC6, T7, C3, Cz, C4, T8, TP9, CP5, CP1, CP2, CP6, TP10, P7, P3, Pz, P4, P8, PO9, O1, Oz, O2, and PO10 (ActiCap, Brain Products GmbH, Germany) and the cap was fixed by a chinstrap to avoid electrode shifts. EOG was recorded with passive electrodes. AFz and FCz were used as the ground and reference electrodes, respectively. The impedance of electrodes was kept below 5 kΩ. EEG data were sampled (BrainAmp, Brain Products GmbH, Germany) at a frequency of 2500 Hz. BCI2000 software was used to record EEG data from the acquisition system and to present the auditory cues [41].

Data analysis

Preprocessing. After offline visual inspection peripheral channels (Fp1, Fp2, T7, T8, TP9, TP10, P7, P8, O1, Oz, O2, PO9, and PO10) were removed from prospective data analysis due to excessive noise and/or artefacts. Blind Source Separation (BSS) algorithm [42] from the automatic artifact removal (AAR) toolbox as an EEGLAB plug-in [43] was used to remove artifacts caused by eye-blinks and eye movements, and muscle activity from face, neck and shoulder movements. Live video streaming with a frontal view from the participants allowed the experimenter to control for systematic or random artifacts, which were reported to the participant if persistent and the correspondent experimental run was disregarded from the analysis. Data was downsampled to 250 Hz, band-pass filtered (0.1–70 Hz), and the power line noise was removed using a 50 Hz notch filter. An open-source MATLAB toolbox, BCILAB, was used to process the EEG data [44].

Time-frequency analysis. Time-frequency analysis for the investigation of spectral changes at distinct time points was performed using wavelet transforms even at the lowest frequency (1 Hz corresponding to 3 cycles during 1 s) as event-related spectral perturbations (ERSPs) [10]. The time window analyzed included 3 s before and 7 s after the auditory 'Go' cue and the time course was obtained by averaging the power change of the frequency bands across all trials during the movement. The time window from −3 to −2 s before the 'Go' cue was used as baseline (see figure 2(B)).

Feature extraction and classification. The kinematics data (position in *X*, position in *Y*, and forearm orientation angle) of the base of the IS-MORE exoskeleton were only analyzed (up-sampled to 250 Hz and synchronized with EEG data), and used to identify sub-movements within a task (forward and backward phases during reaching movements) and hence, to label EEG data. Every EEG trial for movements phase was segmented into two 1 s epochs (figure 1(C)): (a) starting from movement onset identified by kinematics data to forward movement towards the target); and (b) starting movement after target was reached (backward movement towards the starting position). Rest class was also segmented into 1 s epochs from the beginning of each rest interval. Data from all trials for each class were appended and used to extract spatio-frequency features using filter-bank common spatial patterns (FBCSP) [45], which is an extension of the standard common spatial pattern (CSP) algorithm [46]. We applied FBCSP as feature extraction method because it uses frequency filtering into multiple frequency bands, which could benefit the decoding of different motor tasks as demonstrated previously [33]. Furthermore, CSP algorithm has been proven its efficacy calculating optimal spatial filters for motor related BCIs [25, 33, 35]. Spatial filters were created for three frequency windows: 7–15 Hz, 15–25 Hz, and 25–30 Hz. The log-variance of the filtered signal was used as feature for classification.

We set three as the number of spatial filters to use for the CSP algorithm in accordance to prior studies with CSP [33, 45] resulting in 6 features per frequency band and 18 features per channel. The spatial patterns used in feature extraction representing the areas involved in each movement EEG activity were obtained with the help of FCSP patterns (figure 2(A)). We obtained the topographical distribution of the difference in EEG activity during 2 different movement conditions (e.g. reaching towards Blue versus Rest) in specific frequency bands. As depicted with data from a representative participant in figure 2(A), the EEG activity difference is prominent when comparing each movement direction and Rest. However, the difference is not obvious when comparing EEG activity produced during reaching movements towards 2 different targets (e.g. Blue versus Red). Therefore, FCSP patterns of ERD of the mu and beta rhythms were needed to extract distinct features for the different execution movements.

The resulting feature vector was then fed to the Linear Discriminant Analysis (LDA) classifier as multi class classifier. Taking into account the similar performance of LDA and SVM for multiclass classification [33], we chose LDA as our preferred method. It is basically a two-class classifier extended to more classes by one-versus-one voting. For the one-versus-one voting scheme, the classifier was trained for a $K(K-1)/2$ binary classifiers in a K-way multiclass problem [47]. Validation performance was estimated using five-fold blockwise cross-validation with 5 trials safety margin. Thus, each session was split up into five folds, with each fold being used for testing and used the remaining four folds to train the classifier. Decoding accuracy was estimated according to the average over all folds for each session.

To evaluate the statistical significance thresholds for decoding accuracy, we used the chance levels ($p < 0.05$) for an infinite number of trials and classes using the binomial cumulative distribution [48]. From now on, we will refer to

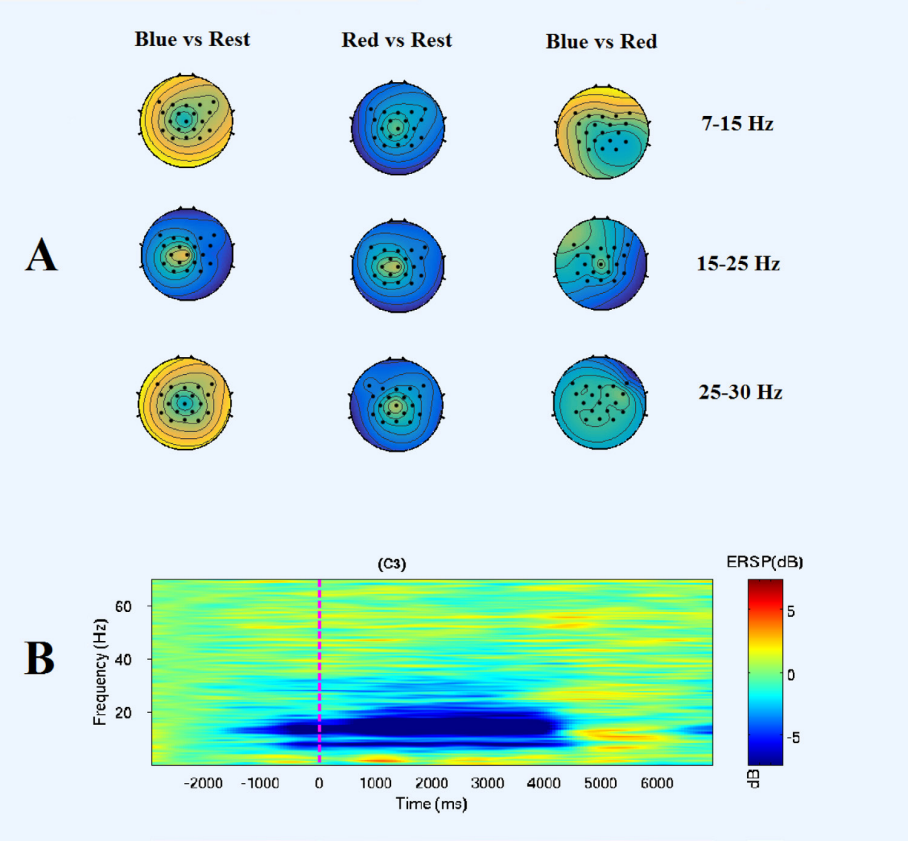

Figure 2. Filter bank common spatial pattern (FBCSP) and time-frequency analysis: EEG data from a representative participant transformed into spatio-frequency topographical maps and into one selected channel time-frequency domain. (A) Highest-ranking common spatial patterns for each pair of movements within the specific frequency band (black dots represent the 19 channels used for classification). BLUE and RED stand for reaching movement towards the blue and red target respectively. (B) Channel C3 time-frequency event-related spectral perturbation (ERSP) during reaching towards the blue target. The vertical dashed line shows the time when the Go cue was presented to the participant.

wthis significance level when reporting classification accuracy results.

The collected EEG data contained nine different states: REST, and eight actual directional movements: four forward (F) (towards BLUE, RED, GREEN, and BROWN targets) and four backward (B) (coming back from each target to the starting position) that we combined in one movement only (coming back to the starting position from any target (BACKWARD)) to reduce the number of classes. In this manuscript, we described the classification of three different complexity cases, decoding 3, 4 and 6 movement classes:

- 3 class (RED, BLUE, REST)
- 4 class (RED, BLUE, BACKWARD, REST)
- 6 class (RED, BLUE, GREEN, BROWN, BACKWARD, REST)

Recalibration. In order to investigate how the recalibration could affect the classification results, we first divided each session in five data blocks that were used later as folds for the cross-validation of the classification and tested three decoding schemes using data from the different four sessions (see table1):

Scheme 1 (within session): We used each session for both training and testing with five-fold cross-validation. The within session decoding accuracy was averaged over all folds.

Scheme 2 (recalibrated between-sessions): Previous and current session data (four folds) were used for training, and only one fold of current session (S2* or S3* or S4*) was used for testing. The recalibrated between sessions decoding accuracy was averaged over all folds.

Scheme 3 (between sessions): All previous session data were used for training and current session was used for testing in between sessions.

Statistical analysis. We performed two separate statistical analyses to evaluate: (i) changes in performance over sessions, and (ii), if any factor (scheme, class, and session) had a significant effect in performance.

- To check for learning effects over sessions, we compared classification accuracy differences between the different sessions using a repeated measures ANOVA separately for the 3-class, 4-class, and 6-class problems. The time (four sessions for scheme 1, and three sessions for schemes

Table 1. Decoding schemes: different sessions were used for training and testing to investigate re-calibration effects on classification performance. If the same session was used for training and testing (in schemes 1 and 2 indicated by *), it was evaluated using a 5-fold cross-validation to ensure that training and test set do not overlap. Scheme 3 trained with previous 'calibration' sessions and tested on current session.

Scheme 1 (within session)		Scheme 2 (recalibrated between-sessions)		Scheme 3 (between sessions)	
Training	Testing	Training	Testing	Training	Testing
S1	S1*				
S2	S2*	**S1-S2**	S2*	**S1**	S2
S3	S3*	**S1-S2-S3**	S3*	**S1-S2**	S3
S4	S4*	**S1-S2-S3-S4**	S4*	**S1-S2-S3**	S4

2 and 3; see table 1) was considered the independent variable and the classification accuracy the dependent variable.

- A three-way ANOVA was performed to study the influence of the three factors (Scheme, Class, Session) in classification accuracy (dependent variable). Factor scheme consisted of 3 levels (Scheme 1, Scheme 2, Scheme 3); factor classification problem included 3 levels (3-, 4-, and 6-classes); and factor session had also 3 levels (S2, S3, S4). Notice that session S1 was removed from this analysis to facilitate comparisons, as it was only tested in scheme 1 (within session). When these factors or their interactions reached significance ($p < 0.05$), subsequent post-hoc *t*-tests were performed, applying a Bonferroni correction for multiple comparisons. These post-hoc comparisons were considered significant if the *p*-value was below 0.05 after correction.

Results

Regardless of the number of movements to be classified and the calibration strategy, the classification results were above significance level in all participants. For clarity, the results section was categorized into three sections according to different decoding schemes (calibration strategy) and complexity of the classification (number of movements to be classified).

Scheme 1 **(within session classification):** Each session was used for training and testing with five-fold cross-validation.

3-movements classification

We obtained an average accuracy of 67 ± 7.33 % (significance level 40%) for classifying 3-classes (Blue versus Red versus Rest) as can be seen in detail from table 2. The maximum classification accuracy over all sessions was observed in Participant1 (75.25 ± 10) and the minimum for Participant 6 (53.25 ± 3). The maximum and minimum classification accuracy for one session was observed in Participant1 (Session 2; 86%) and Participant6 (Session 3; 49%) respectively. The mean average accuracy across participants increased from the first session (64%) to the fourth session (69%) being this difference non-significant ($p = 0.61$). The confusion matrix demonstrated that the 3 classes were similarly classified with no clear confusion between classes.

4-movements classification

Table 2 (in the middle) shows a mean classification accuracy of $62.75 \pm 6.89\%$ (significance level 30%) for all participants when classifying 4-classes (Blue, Red, Backward, and Rest). Maximum classification accuracy over all sessions was observed in Participant2 (73.75 ± 2.7) and the minimum in Participant6 (48 ± 2.1). Same as for the 3-class classification, the maximum and minimum classification in one session was achieved by Participant1 (Session 3; 77%) and Participant6 (Session 3; 46%) respectively. The Average accuracy increased from the first session for 60.6% compared to the fourth-session for 63.6% (see table 2 in the middle), being this difference non-significant ($p = 0.76$).

6-movements classification

Table 2 (in the right) shows an average accuracy of $50.3 \pm 8.76\%$ (significance level 20.33%) for all participants when classifying 5 movements towards different targets (Blue, Red, Green, Brown, and Backward) and Rest. Maximum classification accuracy over all sessions was observed in Participant2 (64 ± 7.7) and the minimum in Participant6 (33.5 ± 4.4). The maximum and minimum classification in one session was observed in Participant2 (Session 3; 70%) and Participant6 (Session 3; 28%) respectively. In the Confusion matrix (figure 3 in the right) can be seen that in contrast to the targets more separated from each other (Blue and Red), neighbor targets are confused by the classifier. Average accuracy did not change significantly between sessions ($p = 0.77$).

Scheme 2 **(recalibrated between-sessions classification):** In this scheme, previous and current sessions were used for training and only the current session was used for testing with five-fold cross-validation.

Table 3 shows the mean decoding performance of multiclass combinations of 3-class, 4-class, and 6-class during 3 different recalibration using different combinations of sessions: a) two sessions were used for training (S1, S2) and tested on unseen data of S2; b) three sessions were used for training (S1, S2, S3) and tested on unseen data of S3; and c) four sessions (S1, S2, S3, S4) were used for training and tested on unseen data of S4. In each recalibration of sessions (table 3) the previous and the current session were used as the training sets, and the current session was used as the testing set.

Table 2. Within session classification results for 3-class (left), 4-class (middle), and 6-class (right) classification accuracy for all participants and sessions. For each participant, average and SD is shown in the last column of the table. In the lower cell of the table significance level of the decoding is shown. Five-fold cross-validation was used to estimate the accuracy. 'P' indicates participant and 'S' for the session.

	3-class					4-class					6-class				
	S1 (%)	**S2** (%)	**S3** (%)	**S4** (%)	**Average** (%)	**S1** (%)	**S2** (%)	**S3** (%)	**S4** (%)	**Average** (%)	**S1** (%)	**S2** (%)	**S3** (%)	**S4** (%)	**Average** (%)
P1	70	86	81	64	75.25 ± 10	59	64	69	59	62.75 ± 4.7	47	54	67	49	54.25 ± 8.9
P2	69	72	78	80	74.75 ± 5.1	72	71	77	75	73.75 ± 2.7	64	53	70	69	64 ± 7.7
P3	65	62	62	73	65.5 ± 5.1	59	62	60	70	62.75 ± 4.9	54	63	49	55	55.25 ± 5.8
P4	64	72	62	65	65.75 ± 4.3	59	60	65	58	60.5 ± 3.1	43	51	53	41	47 ± 5.8
P5	52	60	58	65	58.75 ± 5.3	58	59	55	69	60.25 ± 6	44	41	40	42	41.75 ± 1.7
P6	56	53	49	55	53.25 ± 3	47	51	46	48	48 ± 2.1	38	36	28	32	33.5 ± 4.4
P7	71	61	78	78	72 ± 8	66	62	65	68	65.25 ± 2.5	50	55	58	52	53.75 ± 3.5
P8	64	63	82	75	71 ± 9.1	65	67	74	64	67.5 ± 4.5	49	52	54	47	50.5 ± 3.1
P9	66	65	69	67	66.75 ± 1.7	61	66	67	62	64 ± 2.9	53	52	58	50	53.25 ± 3.4
Average	64.1 ± 6.3	66 ± 9.5	68.7 ± 11.6	69.1 ± 7.9	67 ± 7.33	60.6 ± 6.8	62.4 ± 5.6	64.2 ± 9.5	63.6 ± 8	62.75 ± 6.8	49.1 ± 7.5	50.7 ± 7.9	53 ± 12.9	48.5 ± 10.3	50.3 ± 8.76
Significance level	**40%**					**30%**					**20.33%**				

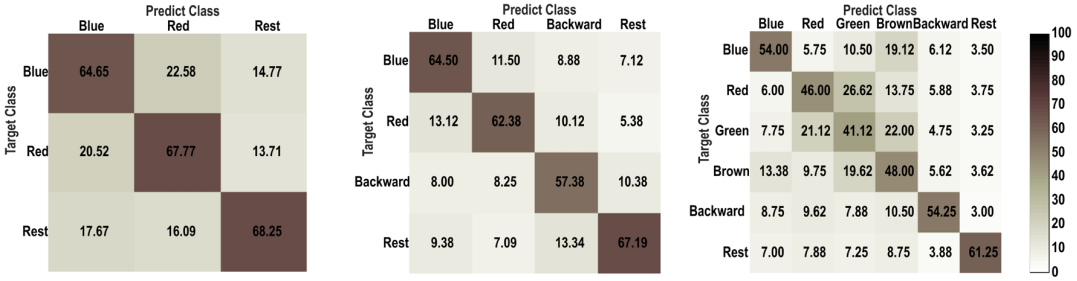

Figure 3. Within session classification results. Confusion matrices showing the mean classification accuracy (%) of all participants for different combination of movements (blue, red, green, brown, backward, and rest).

Table 3. Mean classification accuracy (%) for the offline analysis of multiclass combination during different session calibration and current session with testing on current session. If the same session was used for training and testing (in scheme 1 and 2 indicated by $*$, it was evaluated using a 5-fold cross-validation to ensure that training and test set do not overlap. First recalibration: two sessions were used for training (S1, S2) and tested on unseen data of S2*. Second recalibration: three sessions were used for training (S1, S2, S3) and tested on unseen data of S3*. Third recalibration: four sessions (S1, S2, S3, S4) were used for training and tested on unseen data of S4$*$. 'P' indicates participant.

	3-class			4-class			6-class		
	S1-S2* (%)	**S1-S2-S3*** (%)	**S1-S2-S3-S4*** (%)	**S1-S2*** (%)	**S1-S2-S3*** (%)	**S1-S2-S3-S4*** (%)	**S1-S2*** (%)	**S1-S2-S3*** (%)	**S1-S2-S3-S4*** (%)
P1	79	73.7	48.1	73.6	60.4	33.6	57.2	52.6	44.8
P2	79.6	84.9	84.8	73.7	86.1	82.2	65.2	58.5	67.1
P3	55.3	60.5	62	51.3	48	48.8	38.1	37.5	36.2
P4	66.5	63.2	59.9	68.4	65	54.6	53.8	46	38.2
P5	59	64.2	60.5	62	61.5	64.5	52.5	55.4	56.5
P6	49.3	48.6	45.4	35.6	42.7	34.2	27	28.7	25.7
P7	63.2	67.6	76.4	62.7	49.3	69.8	42.8	36.2	49.4
P8	73.7	72.9	76.5	52.6	66.5	63.1	40.2	46.4	42.1
P9	80	87.5	91	74.4	85	87	50.6	63.1	62
Average	67.2 ± 11.4	69.2 ± 12.13	67.1 ± 15.86	61.5 ± 13	62.7 ± 15.27	59.7 ± 18.9	47.5 ± 11.54	47.15 ± 11.38	46.8 ± 13.23
Significance level	38	37.11	36.5	28.5	28	27.5	19.16	18.77	18.41

As shown in table 3, mean classification accuracies for the first recalibration of sessions (S1 and S2 for training; S2* for testing) were 67.2 ± 11.4%, 61.5 ± 13%, and 47.5 ± 11.54% for 3-class, 4-class, and 6-class respectively. The maximum classification accuracy in the 3-, 4- and 6-class paradigm was 80% (Participant9), 74.4% (Participant9) and 65.2% (Participant2) respectively. The minimum classification accuracy in the 3-, 4- and 6-class paradigm was obtained always for Participant6 and was 49.3%, 35.6%, and 27%, respectively.

During the second recalibration of sessions in table 3, mean classification accuracies (S1, S2, S3 for training; S3* for testing) were 69.2 ± 12.13%, 62.7 ± 15.27%, and 47.15 ± 11.38%. The maximum average accuracy in the 3-, 4- and 6-class paradigm was 87.5% (Participant9), 86.1% (Participant2) and 63.1% (Participant9), respectively. The minimum classification accuracy in the 3-, 4- and 6-class paradigm was obtained for Participant6 and was 48.6%, 42.7%, and 28.7%, respectively.

During the third recalibration of sessions, mean classification accuracies (S1, S2, S3, S4 for training; S4* for testing) were 67.1 ± 15.86, 59.7 ± 18.9, and 46.8 ± 13.23. The maximum classification accuracy was also observed for 3-, 4- and 6-class 91% (Participant9), 87% (Participant9), and 67.1% (Participant2), respectively. The minimum classification accuracy for 3-, 4- and 6-class was obtained for 45.4% (Participant6), 33.6% (Participant 1), and 25.7% (Participant6), respectively. For all combinations the significance level is shown in table 3. Furthermore, we also analyzed the difference in performance for scheme 2 depending on how many sessions' data were included in the recalibration of the classifier (see table 3). Although there was an overall increase in classification accuracy, our ANOVA analysis resulted in not significant results, (3-class p-value = 0.93; 4-class p-value = 0.92; 6-class p-value = 0.98).

***Scheme* 3 (between-sessions classification):** In this scheme, previous sessions were used for training and only current session was used for testing.

Table 4 shows the mean classification accuracy of multiclass combination for 3-class, 4-class, and 6-class for three different combinations (see table 1). We analyzed 3 different recalibration of sessions using the previous session as training set and the current session as test set. a) one session was used for training (S1) and tested on session S2; b) two sessions were used for

Table 4. Mean classification accuracy (%) of the offline analysis of multiclass combination during session calibration and testing on current session. First recalibration: one session was used for training (S1) and tested on session S2. Second recalibration: two sessions were used for training (S1, S2) and tested on session S3. Third recalibration: three sessions (S1, S2, S3) were used for training and tested on session S4. 'P' indicates participant.

	3-class			4-class			6-class		
	S1-S2 (%)	**S1-S2-S3** (%)	**S1-S2-S3-S4** (%)	**S1-S** (%)	**S1-S2-S3** (%)	**S1-S2-S3-S4** (%)	**S1-S2** (%)	**S1-S2-S3** (%)	**S1-S2-S3-S4** (%)
P1	42.8	62.5	41.4	55.3	58.6	32.2	48.7	55.3	37.1
P2	49.3	69.7	71.1	72.4	71.1	74.3	55.9	50	68.4
P3	46.1	51.3	53.9	46.7	41.4	46.1	34.9	39.5	33.6
P4	54.6	46.7	53.9	61.2	58.6	48	50	38.2	32.2
P5	57.2	62.3	65.4	53.5	57.5	60.5	50.2	53.5	52
P6	41.4	42.8	42.8	37.5	40.8	35.5	34	27	25.7
P7	55.3	38.8	71.7	55.3	44.7	67.8	48	32.2	46.7
P8	54	77	73	46.1	65.8	61.2	32.2	40.8	46.1
P9	68.4	73.7	53.9	58	81.6	75.7	29	63.2	56.6
Average	52.1 ± 8.34	58.3 ± 13.93	58.5 ± 12.2	54 ± 9.98	57.7 ± 13.86	55.7 ± 16.03	42.5 ± 9.88	44.4 ± 11.79	44.2 ± 13.5
Significance level	40	38	37.11	300	28.5	28	20.33	19.6	18.77

Table 5. Results of 3-way ANOVA between the three recalibration schemes. Significant difference was tested for the main factors with recalibration scheme (3 levels: scheme 1, scheme 2, scheme 3), classification problem (3 levels: 3-, 4- and 6-classes), test sessions (3 levels: S2, S3, S4) and interaction factor.

	3-way ANOVA scheme × class × session		
	d*f*	*F*-value	*p*-value
Class	2	43.71	$p < 0.0001$[a]
Scheme	2	11.71	$p < 0.0001$[a]
Session	2	0.72	0.484
Scheme × class	4	0.88	0.475
Scheme × session	4	0.22	0.923
Class × session	4	0.17	0.951
Scheme × class × session	8	0.08	0.999
Error	216		

[a] $p < 0.05$.

training (S1, S2) and tested on session S3; c) three sessions (S1, S2, S3) were used for training and tested on session S4.

For the first recalibration in table 4, the mean classification accuracies (S1 for training; S2 for testing) were 52.1 ± 8.34%, 54 ± 9.98%, and 42.5 ± 9.88% for 3-class, 4-class, and 6-class, respectively (table 4). The maximum classification accuracy was observed for 3-, 4-, and 6-class 68.4% (Participant9), 72.4% (Participant2), and 55.9% (Participant2). The minimum classification accuracy in 3-, 4- and 6-class paradigm was obtained 41.4% (Participant6), 37.5% (Participant6), and 29% (Participant9), respectively.

In the second recalibration in table 4, mean classification accuracies (S1 and S2 for training; S3 for testing) were 58.3 ± 13.93%, 57.7 ± 13.86%, and 44.4 ± 11.79%. The maximum average accuracy was observed for 3-, 4-, and 6-class 77% (Participant8), 81.6% (Participant9), and 63.2% (Participant9), respectively. The minimum classification accuracy in the 3-, 4- and 6-class was obtained for 38.8% (Participant7), 41.4% (Participant3), and 27% (Participant6), respectively.

Table 6. Results of the multiple comparisons for scheme and class. Significant difference was tested for the calibration schemes pair-wise (scheme 1 versus scheme 2, scheme 1 versus scheme 3, and scheme 2 versus scheme 3) and classification problem pair-wise (3-class versus 4-class, 3-class versus 6-class, 4-class versus 6-classes).

Scheme	**Sch1 Sch2**	**Sch1 Sch3**	**Sch2 Sch3**
p-value	0.876	$p < 0.0001$[a]	0.001[a]
Class	**3-class 4-class**	**3-class 6-class**	**4-class 6-class**
p-value	0.130	$p < 0.0001$[a]	$p < 0.0001$[a]

[a] $p < 0.05$, Bonferroni corrected.

In the third recalibration in table 4, mean classification accuracies (S1, S2, S3 for training; S4 for testing) were 58.5 ± 12.2, 55.7 ± 16.03, and 44.2 ± 13.5, respectively. The maximum classification accuracy was observed for 3-, 4- and 6-class 71.7% (Participant7), 75.7% (Participant9), and 68.4% (Participant2). The minimum classification accuracy in the 3-, 4- and 6-class was obtained for 41.4% (Participant1), 32.2% (Participant1), and 25.7% (Participant6). ANOVA analysis to test session effect resulted in not significant results for scheme 3 (see table 4) in the recalibration of the classifier (3-class p-value = 0.43; 4-class p-value = 0.83; 6-class p-value = 0.93).

Comparison of recalibration schemes. A 3-way ANOVA was used to assess the influence of the three calibration schemes (within session, recalibrated between sessions, and between sessions), classification problems (3-, 4-, and 6-classes), testing sessions, and the interaction between factors (see table 5). As can be seen in table 5, the factors scheme and class had a significant effect on the classification accuracy (Scheme, $F = 11.71$; $p < 0.0001$ and class, $F = 43.71$; $p < 0.0001$). The factor sessions, as well as all the interactions between factors were not significant. All the post-hoc comparisons can be seen in table 6. For the factor scheme, significant differences were found between Schemes 1 and 3 (i.e. calibration within session versus between sessions, $p < 0.0001$), and

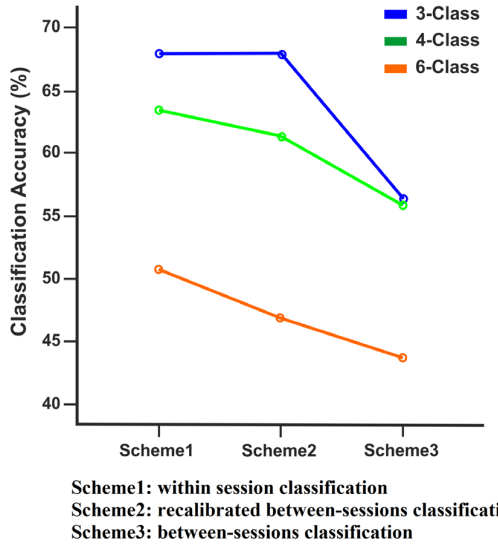

Figure 4. Classification accuracy of three class combination between three schemes. The graph shows the mean classification accuracy for three classification problem (3-, 4- and 6-classes) between three recalibration schemes (scheme 1: within session classification, scheme 2: recalibrated between sessions, and scheme 3: between-sessions classification).

between Schemes 2 and 3 (i.e. recalibrated between sessions versus between sessions, $p = 0.001$). For the factor classification problem, significant differences were found between the 3-class and 6-class problems ($p < 0.0001$), and between the 4-class and 6-class problems ($p < 0.0001$). Figure 4 shows the interaction plot between the two significant factors and the dependent variable (classification accuracy).

Discussion

In this study, we demonstrated multiclass decoding accuracy above significance level of different reaching movements from the same limb using EEG data. Different number of movements (classes) and recalibration strategies were investigated. We consider a performance level to be acceptable if significant above chance level accuracy and the presented results could serve as a starting point in the context of a neurofeedback-based learning process, in which users learn to adapt their brain activity to control a rehabilitative device.

Firstly, we achieved 3-class classification for two targets (Blue and Red) and rest with an overall accuracy above 69% reaching even 91% in one participant (significance level = 36.5%). Then, we explored the possibility of extending the 3-class to a 4-class (including backward movement to starting position) achieving an overall accuracy above 62% reaching even 86% in one participant (significance level = 28%). After that, we extended the classification problem to a 6-class BCI to discriminate four different movements towards 4 targets (Blue, Red, Green, and Brown), rest, and backwards to the starting position achieving an overall accuracy above 50% reaching even 68% in one participant (significance level = 18.77%). With these results we demonstrate that acceptable decoding can be achieved for even 6 movement classes from the same limb using EEG only. We consider these performances to be acceptable as a starting point in the context of a rehabilitative environment, in which subjects perform a learning process and adapt their brain activity to control a rehabilitative device. The link between oscillatory neuroelectric activity and the movement (proprioceptive feedback) will allow the users to learn to control system improving their performance [2]. Furthermore, there is no need of excellent performance level to induce motor learning and recovery using proprioceptive BMIs as rehabilitation tool in chronic severely paralyzed stroke patients [3], which indeed are the patient population benefiting of the here presented developments.

Finally, we demonstrated that for a real scenario application in which previous data is used to classify different functional movements from the same upper limb, classification accuracy can be maintained if the classifier is trained with previous sessions data and can be significantly enhanced when data from the beginning of each session is added to data from previous sessions to recalibrate/retrain the classifier confirming previous results [49]. These results demonstrate the potential online use of the here proposed classification algorithm to decode up to 6 different movements from the same limb to control a multi degree of freedom rehabilitative devices (i.e. provide ecologically valid neurofeedback).

The brain oscillatory signature of different movements from the same limb can be adequately isolated using FBCSP and the commonly known 'session-to-session-transfer' issue in EEG does not affect the classification accuracy results significantly. However, consistent with other studies [50, 51], our results did not show any significant impact of the amount of previous sessions data used for recallibration or re-training of the classifier on the decoding accuracy.

In this study we used the filter bank common spatial pattern (FBCSP) for feature extraction because it uses frequency filtering with multiple frequency bands, which may help isolating oscillatory activity related to different motor tasks as previously proposed [52]. Decoding accuracy was higher using FBCSP compared to previous work using CSP only [34, 53].

Our results argue in favor of using adaptive methods that constantly adapt the decoder with the current session's data. We successfully applied a recalibration of sessions to specifically address the problem of non-stationarities and the session-transfer problem [54].

Although our results are promising and we achieved overall participants and sessions accuracies in the range of 69%, 62%, and 50% for 3-class, 4-class, and 6-class, respectively improving reported work [18], the control of rehabilitative devices (e.g. robotic orthosis, FES, etc) need higher classification accuracies. However the continuous use of the system might produce some learning effects and accuracies could improve significantly.

Motor execution of reaching movements of the same limb activating muscles at different joints activates regions with very close representation on the motor cortex [28]. This spatial proximity, EEG volume conducting effects, spectral limitations and signal to noise ratio and electrical and

neurophysiological artefacts makes classification of such movements more difficult. Furthermore, when attempting to classify very similar movements (reaching neighbor targets green and brown) this problem becomes very challenging, as demonstrated in the confusion matrix of scheme 1 for 6-class being confused for decoding of close targets in the setup.

In the here presented work we report the performance of a BCI using 1 s time windows and 19 EEG electrodes and it has been already shown that the accuracy of classifier increases using longer time window after onset [38] and denser EEG electrodes around the motor cortex [33]. Adding more features such as movement related cortical potential (MRCP) to the proposed system may further improve the performance [30, 32]. Further experimental work is needed to investigate the use of longer time windows, more EEG channels and other new features.

In general, healthy subjects show strong brain activation in the regions contralateral to the moving hand but other areas are being also significantly activated depending on the phase of the movement (planning, onset, execution, cessation) [52]. These cortical activations captured by EEG are affected after any neural lesion (e.g. stroke) and maintaining the classification performance we obtained in healthy participants will be more challenging. Chronic stroke patients show often a more bilateral brain activation when they move their affected hand [3, 55]. These results together with the here presented results in healthy participants suggest the use of bihemispheric EEG activity and FBCSP in order to provide stroke patients with a multi degree of freedom control of rehabilitation or assistive devices.

Further experiments to test the feasibility and efficacy of our approach need to be performed. However, we believe that the here presented results in healthy participants constitute a baseline population, which can be afterwards compared to and used as control group (not age-matched though) for different typologies of patients with different brain alterations, such as stroke and spinal cord injury. From our previous study [2] we know that the link between oscillatory neuroelectric activity and the movement (proprioceptive feedback) allows severely paralyzed stroke patients to learn to control the system improving their performance and inducing motor recovery [3].

In summary, the here presented promising results, constitute the first step towards a multi-directional rehabilitation exoskeleton online control system for severely paralyzed stroke patients

Conclusion

We demonstrated the feasibility of classifying up to 6 functional movements from the same upper limb using EEG data with acceptable levels of accuracy and demonstrated how a classifier trained on previous sessions' data can maintain the classification accuracy demonstrating robustness against session-to-session transfer issues. Furthermore, we demonstrated how retraining the classifier with some data of the current session could significantly increase the classification accuracy.

We demonstrated how FBCSP could help isolate brain oscillatory signatures of different movements of the same limb using their spatiotemporal filters at multiple frequencies and therefore create good features to allow acceptable classification rates to link several DoFs of robotic rehabilitation exoskeletons with brain neuroelectric oscillatory activity.

Acknowledgments

This study was funded by the *Baden-Württemberg Stiftung* (GRUENS), the *Deutsche Forschungsgemeinschaft* (DFG, Koselleck and SP-1533/2-1), *Bundes Ministerium für Bildung und Forschung* BMBF MOTORBIC (FKZ 13GW0053), the *fortune*-Program of the University of Tübingen (2422-0-0), and AMORSA (FKZ 16SV7754). A Sarasola-Sanz's work is supported by the *La Caixa-DAAD* scholarship, and N Irastorza-Landa's work by the *Basque Government and IKERBASQUE*, Basque Foundation for Science.

References

[1] Wolpaw J R, Birbaumer N, McFarland D J, Pfurtscheller G and Vaughan T M 2002 Brain–computer interfaces for communication and control *Clin. Neurophysiol.* **113** 767–91

[2] Ramos-Murguialday A, Schürholz M, Caggiano V, Wildgruber M, Caria A, Hammer E M, Halder S and Birbaumer N 2012 Proprioceptive feedback and brain computer interface (BCI) based neuroprostheses *PLoS One* **7** e47048

[3] Ramos-Murguialday A *et al* 2013 Brain–machine interface in chronic stroke rehabilitation: a controlled study *Ann. Neurol.* **74** 100–8

[4] Ang K K, Guan C, Phua K S, Wang C, Zhou L, Tang K Y, Joseph G J E, Kuah C W K and Chua K S G 2014 Brain–computer interface-based robotic end effector system for wrist and hand rehabilitation: results of a three-armed randomized controlled trial for chronic stroke *Frontiers Neuroeng.* **7** 30

[5] Ono T *et al* 2014 Brain–computer interface with somatosensory feedback improves functional recovery from severe hemiplegia due to chronic stroke *Frontiers Neuroeng.* **7** 19

[6] Pichiorri F, Morone G, Petti M, Toppi J, Pisotta I, Molinari M, Paolucci S, Inghilleri M, Astolfi L and Cincotti F 2015 Brain–computer interface boosts motor imagery practice during stroke recovery *Ann. Neurol.* **77** 851–65

[7] Turner D L, Ramos-Murguialday A, Birbaumer N, Hoffmann U and Luft A 2013 Neurophysiology of robot-mediated training and therapy: a perspective for future use in clinical populations *Frontiers Neurol.* **4** 184

[8] Oweiss K G and Badreldin I S 2015 Neuroplasticity subserving the operation of brain–machine interfaces *Neurobiol. Dis.* **83** 161–71

[9] Wolpaw J R and McFarland D J 2004 Control of a two-dimensional movement signal by a noninvasive brain–computer interface in humans *Proc. Natl Acad. Sci. USA* **101** 17849–54

[10] McFarland D J, Sarnacki W A and Wolpaw J R 2010 Electroencephalographic (EEG) control of three-dimensional movement *J. Neural Eng.* **7** 036007

[11] Iturrate I, Chavarriaga R, Montesano L, Minguez J and Millán J D R 2015 Teaching brain–machine interfaces as an alternative paradigm to neuroprosthetics control *Sci. Rep.* **5** 13893

[12] Ortner R, Allison B Z, Korisek G, Gaggl H and Pfurtscheller G 2011 An SSVEP BCI to control a hand orthosis for persons with tetraplegia *IEEE Trans. Neural Systems Rehabil. Eng.* **19** 1–5

[13] McCane L M *et al* 2015 P300-based brain–computer interface (BCI) event-related potentials (ERPs): people with amyotrophic lateral sclerosis (ALS) versus age-matched controls *Clin. Neurophysiol.* **126** 2124–31

[14] Sellers E W and Donchin E 2006 A P300-based brain–computer interface: initial tests by ALS patients *Clin. Neurophysiol.* **117** 538–48

[15] Escolano C, Murguialday A R, Matuz T, Birbaumer N and Minguez J 2010 A telepresence robotic system operated with a P300-based brain–computer interface: initial tests with ALS patients *Engineering in Medicine and Biology Society (EMBC), 2010 Annual Int. Conf. of the IEEE* pp 4476–80

[16] Bradberry T J, Gentili R J and Contreras-Vidal J L 2010 Reconstructing three-dimensional hand movements from noninvasive electroencephalographic signals *J. Neurosci.* **30** 3432–7

[17] Antelis J M, Montesano L, Ramos-Murguialday A, Birbaumer N and Minguez J 2013 On the usage of linear regression models to reconstruct limb kinematics from low frequency EEG signals *PLoS One* **8** e61976

[18] Waldert S, Preissl H, Demandt E, Braun C, Birbaumer N, Aertsen A and Mehring C 2008 Hand movement direction decoded from MEG and EEG *J. Neurosci.* **28** 1000–8

[19] Georgopoulos A P, Schwartz A B and Kettner R E 1986 Neuronal population coding of movement direction *Science* **233** 1416–9

[20] Carmena J M, Lebedev M A, Crist R E, O'Doherty J E, Santucci D M, Dimitrov D F, Patil P G, Henriquez C S and Nicolelis M A 2003 Learning to control a brain–machine interface for reaching and grasping by primates *PLoS Biol.* **1** e42

[21] Schwartz A B, Cui X T, Weber D J and Moran D W 2006 Brain-controlled interfaces: movement restoration with neural prosthetics *Neuron* **52** 205–20

[22] Hochberg L R, Bacher D, Jarosiewicz B, Masse N Y, Simeral J D, Vogel J, Haddadin S, Liu J, Cash S S and van der Smagt P 2012 Reach and grasp by people with tetraplegia using a neurally controlled robotic arm *Nature* **485** 372–5

[23] Collinger J L, Wodlinger B, Downey J E, Wang W, Tyler-Kabara E C, Weber D J, McMorland A J, Velliste M, Boninger M L and Schwartz A B 2013 High-performance neuroprosthetic control by an individual with tetraplegia *Lancet* **381** 557–64

[24] Bouton C E, Shaikhouni A, Annetta N V, Bockbrader M A, Friedenberg D A, Nielson D M, Sharma G, Sederberg P B, Glenn B C and Mysiw W J 2016 Restoring cortical control of functional movement in a human with quadriplegia *Nature* **12** 533

[25] Pistohl T, Ball T, Schulze-Bonhage A, Aertsen A and Mehring C 2008 Prediction of arm movement trajectories from ECoG-recordings in humans *J. Neurosci. Methods* **167** 105–14

[26] Spüler M, Rosenstiel W and Bogdan M 2014 Predicting wrist movement trajectory from ipsilesional ECoG in chronic stroke patients *Proc. of 2nd Int. Congress on Neurotechnology, Electronics and Informatics (NEUROTECHNIX)* pp 38–45

[27] Spüler M, Walter A, Ramos-Murguialday A, Naros G, Birbaumer N, Gharabaghi A, Rosenstiel W and Bogdan M 2014 Decoding of motor intentions from epidural ECoG recordings in severely paralyzed chronic stroke patients *J. Neural Eng.* **11** 066008

[28] Sanes J N, Donoghue J P, Thangaraj V, Edelman R R and Warach S 1995 Shared neural substrates controlling hand movements in human motor cortex *Science* **268** 1775

[29] Shindo K, Kawashima K, Ushiba J, Ota N, Ito M, Ota T, Kimura A and Liu M 2011 Effects of neurofeedback training with an electroencephalogram-based brain–computer interface for hand paralysis in patients with chronic stroke: a preliminary case series study *J. Rehabil. Med.* **43** 951–7

[30] López-Larraz E, Montesano L, Gil-Agudo Á and Minguez J 2014 Continuous decoding of movement intention of upper limb self-initiated analytic movements from pre-movement EEG correlates *J. Neuroeng. Rehabil.* **11** 1

[31] Buch E, Weber C, Cohen L G, Braun C, Dimyan M A, Ard T, Mellinger J, Caria A, Soekadar S and Fourkas A 2008 Think to move: a neuromagnetic brain–computer interface (BCI) system for chronic stroke *Stroke* **39** 910–7

[32] López-Larraz E, Trincado-Alonso F, Rajasekaran V, Perez-Nombela S, Del-Ama A J, Aranda J, Minguez J, Gil-Agudo Á and Montesano L 2016 Control of an ambulatory exoskeleton with a brain-machine interface for spinal cord injury gait rehabilitation *Frontiers Neurosci.* **10** 359

[33] Yong X and Menon C 2015 EEG classification of different imaginary movements within the same limb *PLoS One* **10** e0121896

[34] Shiman F, Irastorza-Landa N, Sarasola-Sanz A, Spuler M, Birbaumer N and Ramos-Murguialday A 2015 Towards decoding of functional movements from the same limb using EEG *Engineering in Medicine and Biology Society (EMBC), 2015 37th Annual Int. Conf. of the IEEE* pp 1922–5

[35] Liao K, Xiao R, Gonzalez J and Ding L 2014 Decoding individual finger movements from one hand using human EEG signals *PLoS One* **9** e85192

[36] Vuckovic A and Sepulveda F 2008 Delta band contribution in cue based single trial classification of real and imaginary wrist movements *Med. Biol. Eng. Comput.* **46** 529–39

[37] Sarasola-Sanz A, Irastorza-Landa N, Shiman F, Lopez-Larraz E, Spuler M, Birbaumer N and Ramos-Murguialday A 2015 EMG-based multi-joint kinematics decoding for robot-aided rehabilitation therapies *2015 IEEE Int. Conf. on Rehabilitation Robotics (ICORR)* pp 229–34

[38] Ibáñez J, Serrano J, Del Castillo M, Minguez J and Pons J 2015 Predictive classification of self-paced upper-limb analytical movements with EEG *Med. Biol. Eng. Comput.* **53** 1201–10

[39] Cirstea M and Levin M F 2000 Compensatory strategies for reaching in stroke *Brain* **123** 940–53

[40] Zabaleta H, Valencia D, Perry J, Veneman J and Keller T 2011 Absolute position calculation for a desktop mobile rehabilitation robot based on three optical mouse sensors *2011 Annual Int. Conf. of the IEEE Engineering in Medicine and Biology Society* pp 2069–72

[41] Schalk G, McFarland D J, Hinterberger T, Birbaumer N and Wolpaw J R 2004 BCI2000: a general-purpose brain–computer interface (BCI) system *IEEE Trans. Biomed. Eng.* **51** 1034–43

[42] Yeredor A 2000 Blind separation of Gaussian sources via second-order statistics with asymptotically optimal weighting *IEEE Signal Process. Lett.* **7** 197–200

[43] Gómez-Herrero G 2007 Automatic artifact removal (AAR) toolbox v1. 3 (Release 09.12. 2007) for MATLAB Tampere University of Technology

[44] Delorme A, Mullen T, Kothe C, Acar Z A, Bigdely-Shamlo N, Vankov A and Makeig S 2011 EEGLAB, SIFT, NFT, BCILAB, and ERICA: new tools for advanced EEG processing *Comput. Intell. Neurosci.* **2011** 10

[45] Ang K K, Chin Z Y, Zhang H and Guan C 2008 Filter bank common spatial pattern (FBCSP) in brain–computer interface *2008 IEEE Int. Joint Conf. on Neural Networks (IEEE World Congress on Computational Intelligence)* pp 2390–7

[46] Ramoser H, Muller-Gerking J and Pfurtscheller G 2000 Optimal spatial filtering of single trial EEG during imagined hand movement *IEEE Trans. Rehabil. Eng.* **8** 441–6
[47] Bishop C M 2006 *Pattern Recognition* (New York: Springer) pp 1–58
[48] Combrisson E and Jerbi K 2015 Exceeding chance level by chance: the caveat of theoretical chance levels in brain signal classification and statistical assessment of decoding accuracy *J. Neurosci. Methods* **250** 126–36
[49] López-Larraz E, Trincado-Alonso F and Montesano L 2015 Brain-machine interfaces for motor rehabilitation: Is recalibration important? *2015 IEEE Int. Conf. on Rehabilitation Robotics (ICORR)* pp 223–8
[50] Rohm M, Schneiders M, Müller C, Kreilinger A, Kaiser V, Müller-Putz G R and Rupp R 2013 Hybrid brain–computer interfaces and hybrid neuroprostheses for restoration of upper limb functions in individuals with high-level spinal cord injury *Artif. Intell. Med.* **59** 133–42
[51] Arvaneh M, Guan C, Ang K K and Quek C 2012 Omitting the intra-session calibration in EEG-based brain computer interface used for stroke rehabilitation *Engineering in Medicine and Biology Society (EMBC), 2012 Annual Int. Conf. of the IEEE* pp 4124–7
[52] Ramos-Murguialday A and Birbaumer N 2015 Brain oscillatory signatures of motor tasks *J. Neurophysiol.* **113** 3663–82
[53] Robinson N, Guan C, Vinod A, Ang K K and Tee K P 2013 Multi-class EEG classification of voluntary hand movement directions *J. Neural Eng.* **10** 056018
[54] Spüler M, Rosenstiel W and Bogdan M 2012 Adaptive SVM-based classification increases performance of a MEG-based brain–computer interface (BCI) *Int. Conf. on Artificial Neural Networks* pp 669–76
[55] Dimyan M A and Cohen L G 2011 Neuroplasticity in the context of motor rehabilitation after stroke *Nat. Rev. Neurol.* **7** 76–85

Towards decoding of functional movements from the same limb using EEG

Farid Shiman, Nerea Irastorza-Landa, Andrea Sarasola-Sanz, Martin Spüler, Niels Birbaumer, and Ander Ramos-Murguialday

Abstract— **In recent years, there has been an increasing interest in using electroencephalographic (EEG) activity to close the loop between brain oscillations and movement to induce functional motor rehabilitation. Rehabilitation robots or exoskeletons have been controlled using EEG activity. However, all studies have used a 2-class or one-dimensional decoding scheme. In this study we investigated EEG decoding of 5 functional movements of the same limb towards an online scenario. Six healthy participants performed a three-dimensional center-out reaching task based on direction movements (four directions and rest) wearing a 32-channel EEG cap. A BCI design based on multiclass extensions of Spectrally Weighted Common Spatial Patterns (Spec-CSP) and a linear discriminant analysis (LDA) classifier was developed and tested offline. The decoding accuracy was 5-fold cross-validated. A decoding accuracy of 39.5% on average for all the six subjects was obtained (chance level being 20%). The results of the current study demonstrate multiple functional movements decoding (significantly higher than chance level) from the same limb using EEG data. This study represents first steps towards a same limb multi degree of freedom (DOF) online EEG based BCI for motor restoration.**

I. Introduction

In the past years, sensorimotor rhythm based Brain-Computer Interface (BCI) technologies [1-4] have been developed to decode brain states into commands to control rehabilitation robots. Furthermore, BCIs have proved their efficacy in restoring motor function in severely paralyzed stroke patients [5].

Different studies have proved the possibility of decoding movement parameters from neurophysiological signals, including EEG [6, 7], electrocorticography (ECoG) [8-10], functional magnetic resonance imaging (fMRI) [11, 12], magnetoencephalography (MEG) [13], near-infrared spectroscopy (NIRS) [14], and electromyography (EMG) [15, 16]. In particular, EEG-based decoding is of great interest for non-invasive decoding in completely paralyzed patients for reaching directions [17] and continuous trajectories [7, 18] which have been already decoded.

F. S, N. I, A. SS, N. B, and A. RM are with the Institute of Medical Psychology and Behavioral Neurobiology, University of Tübingen, Tübingen, Germany.

F. S, N.I, and A.SS are with IMPRS for Cognitive and Systems Neuroscience, Tübingen, Germany.

N. B is also with Ospedale San Camillo, Istituto di Ricovero e Cura a Carattere Scientifico, Venezia, Italy

A. RM is also with TECNALIA, San Sebastian, Spain

M. S is with Computer Science Department, Wilhelm-Schickard-Institute, University of Tübingen, Tübingen, Germany.

While in [7], 2-D movement control was achieved with EEG the BCI control was achieved using imagery of two different limbs. Bradberry et al. [6] demonstrated for the first time 3-D hand trajectories decoding during center-out tasks offline using EEG temporal information. However, one should be careful with the interpretation and use of linear methods for decoding trajectories using EEG [19]. Using Independent Component Analysis (ICA) as feature extraction method, has been used combined with a support vector machine (SVM) classifier to decode right versus left intended movement direction using EEG [20].

In another study wavelet transform was applied to time-frequency representations to decode slow and fast movement using EEG signals [21] and Robinson et al. [22] proposed a regularized wavelet-common spatial pattern algorithm for multi-class EEG classification of voluntary hand movement directions. Furthermore, normalized variance of CSP-spatial filtering of EEG signal has been applied for decoding 1-dimensional hand directional tasks in [23].

All these studies have indicated that it is possible to decode hand movements direction from EEG. However, in the above mentioned studies there are some limitations regarding various parameters that should be optimized for selecting the type of wavelets and the number of features. In the interest of using a real-time BCI in stroke patients, these factors are important. For this reason, we propose in the current study to apply a modified spectrally weighted CSP because it can optimize simultaneous spatiotemporal filtering of motor-related EEG activity. Furthermore, CSP has been very useful in obtaining spatial filters for detecting event-related de-synchronization (ERD) and event-related synchronization (ERS)[7].

The objective of the current study is to decode 5 different movements of the same limb using EEG data towards an online BCI for motor rehabilitation.

II. Materials and Methods

A. Subjects

Six healthy right-handed subjects without any neurologic disease history (three males and three females, mean age 24 years) participated in four recording sessions. Subjects were informed about the experimental procedure and signed a written consent form. This study was approved by the ethical committee of the Faculty of Medicine, University of Tübingen, Germany.

978-1-4244-9270-1/15/$31.00 ©2015 IEEE

B. Experimental Setup

Subjects performed a center-out reaching task (see figure 1) using their right arm and hand wearing a 7-DOF Exoskeleton (Tecnalia, San Sebastian, Spain).

The task involved four different movement directions from a starting position (rest position) towards one of four different target colors (see figure 1). Upon the presentation of an imperative auditory cue specifying the target, participants were asked to perform the movement and return to the starting position at a comfortable pace but within 4 seconds. The auditory cues and the EEG data were presented and acquired using BCI2000 software respectively [www.bci2000.org].

The experiment was divided in 5 runs of 40 trials each for each session, which gave 50 trials per class. A resting interval was inserted between the trials for random length between 2-3 seconds. Four sessions on the right hand were recorded for each subject on different days.

C. EEG data acquisition

EEG was recorded using a 32-channel ActiCap and a 32-channel BrainAmp amplifier (Brain Products GmbH, Germany) at a sampling frequency of 2500Hz. Electrode impedances were kept below 5 kΩ. The cap contained the electrodes FP1, FP2, F7, F3, Fz, F4, F8, FC5, FC1, FC2, FC6, T7, C3, Cz, C4, T8, TP9, CP5, CP1, CP2, CP6, TP10, P7, P3, Pz, P4, P8, PO9, O1, Oz, O2, PO10 and was fixed by a chinstrap to avoid electrode shifts, using AFz as ground and FCz as the reference.

III. EEG DATA ANALYSIS

A. Preprocessing

Data analysis was performed offline. After visual inspection, noisy channels (TP9, TP10, PO9, and PO10) were removed and the Blind Source Separation (BBS) algorithm [24] from the Automatic Artifact Removal (AAR) toolbox as an EEGLAB plug-in [25] was used to remove artifacts caused by eye-blinks and eye movements, and muscle activity from face, neck and shoulder movements. Data was downsampled to 250 Hz.

B. Feature extraction and classification

EEG data were band-pass filtered (0.5-70 Hz) and power line noise was removed using a 50 Hz notch filter. EEG signals were then divided into trial epochs from 0 s to +2.5s with respect to movement onset triggers (t = 0s). A band pass filter between 7 – 30 Hz was then applied to extract mu and beta frequency band data and a Spectrally weighted Common Spatial Pattern (Spec-CSP) [26] was applied to the data. Spec-CSP is an algorithm based on simultaneous optimization of spatiotemporal filters that helps to solve the limitation of single trial EEG classification. Spec-CSP computes discriminative features, whose variances are optimal between two classes with respect to their patterns.

The algorithm is based on the simultaneous diagonalization of two covariance matrices and weights of the EEG channels given rows of the weight matrix. In this study, the algorithm normally used for a 2-class CSP was also applied to five classes of EEG signals on all possible

Fig. 1. Subject perfoms a reaching task to wards one of the four targets (colored panels). The semicircular mechanical stop at the top of the picture serves as starting point position.

combination pairs as only binary classifiers were trained.

Let $X \in R^{d \times T}$ be a CSP-filtered EEG signal of a single trial; d is the number of channels and T is the number of samples in time by which the class label for a single trial X is predicted. Predicting the Log-variance feature vector is given as:

$$\varphi_j\left(X;\ \omega_j\ , \alpha^{(j)}\right) = \log \sum_{k=1}^{T} \alpha_k^{(j)}\ \omega_j^T\ V_k\ \omega_j \qquad (1)$$

$$(j = 1, \dots, J),$$

In this case, $w_j \in R^d$ is a spatial projection that projects the signal into a single dimension, $\alpha^{(j)}$ is the spectrum of the temporal filter, and V_k are the cross-spectrum matrices [26]. The resulting feature vector was then fed to the LDA classifier as multi class classifier. It is basically for two classes extended to more classes by 1-vs-1 voting to determine the class label, where the data in each class is distributed in the feature space according to a normal distribution. In the 1-vs-1 voting, the classifier is applied to an unseen sample and the class obtaining the highest number of votes is selected as classifier output. The classifier is trained in two steps. The first step includes the optimization of the coefficients w_j and $\alpha^{(j)}$ and second the training of the Linear Discriminant Analysis (LDA) classifier.

For evaluation of the decoding model, a 5-fold blockwise cross-validation process with 5 trials safety margin was performed. The data of one session was divided in 5 blocks and in every fold the model was trained on four blocks and tested on the remaining one. Decoding accuracy was estimated according to the average over all folds for each session.

IV. RESULTS AND DISCUSSION

In this work we developed and tested a multi-class classification model aiming at decoding movements of the same upper limb in four directions and ‘’rest’’ using EEG data.

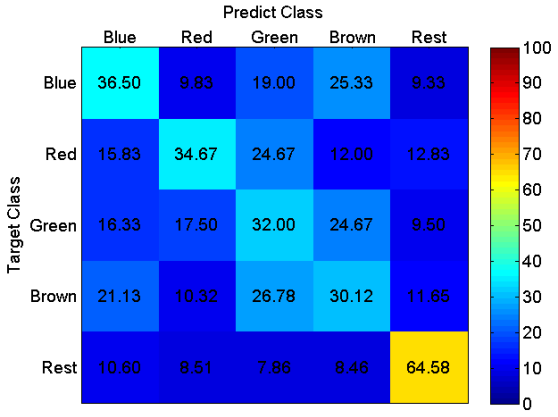

Fig. 2. Confusion Matrix of all subjects for 5 classes

The average accuracy for all subjects when using one session (50 trials per class) to decode 5 movement classes from the same limb was 39.5% (See Table I).

As the theoretical chance level (100/5 = 20%) is defined for an infinite number of data, we used the binomial cumulative distribution [27] to calculate the statistical significance thresholds for the decoding accuracy which resulted to be at 24.4% (n=250, 5-class and $p<0.05$).

The grand average classification accuracy results for all classes and participants are summarized in form of a confusion matrix in Figure 2, being "rest" the class with the best decoding accuracy as expected (64.58%), followed by the other classes (all above chance level). Decoding performance for the blue and red target were better, as expected, because they only have one other target next by. Our decoder confused neighbor targets for the limitation of space resolution. We will be applied a combination of less confused functional movements and a probabilistic output to improve the upper limb movements classification.

The topographical pattern of Spec-CSP of subject 1 for four pairs shows that Blue versus Red has clear discrimination rather than Green versus Brown in Figure 3.

Subject specific decoding results showed a slight variation in performance during different sessions (See Table 1). The subject performance is directly related to the Spec-CSP filter used, which resulted in distinguishable features for different directions.

TABLE I. MEAN CLASSIFICATION ACCURACY (%) OF SIX SUBJECTS FOR EACH SESSIONS.

Subjects	*Sess01*	*Sess02*	*Sess03*	*Sess04*	Average
S1	26%	40%	41%	38%	36.25%
S2	48%	56%	31%	42%	44.25%
S3	47%	42%	39%	48%	44%
S4	32%	33%	34%	33%	33%
S5	39%	39%	36%	37%	37.75%
S6	41%	37%	43%	39%	40%
					39.5%

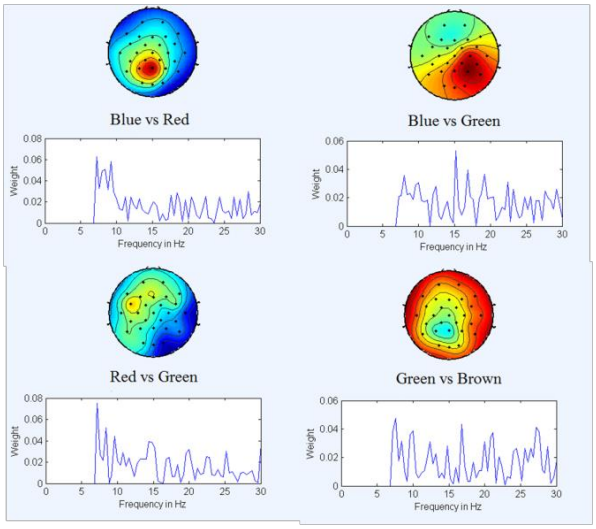

Fig. 3. Spec-CSP topographical patterns and the spectrum of the filter of subject 1 for four class pairs (Blue vs Red, Blue vs Green, Red vs Green and Green vs Brown).

V. CONCLUSION

This study evaluated offline the decoding accuracy in a 5-class hand movement task (actual direction of hand movement) using an optimized spatio-spectral filter as feature extraction method. The obtained results show that directional hand movement decoding is possible using untrained healthy subjects EEG data. The decoding of several movements on the same limb reached significance levels. This work represents first steps towards the development of a high-dimensional EEG based BCI, that decodes movements from the same limb.

In our future work, five different functional hand movements (grasp, pinching, pointing, pronation, supination) will be integrated and new feature extraction and classification methods will be used and compared.

Although very preliminary, these results are promising and could help to design more functional BCIs for motor rehabilitation.

ACKNOWLEDGMENT

This study was funded by the Baden-Württemberg Stiftung (GRUENS), the Indian-European collaborative research and technological development projects (INDIGO-DTB2-051), the WissenschaftsCampus Tübingen, the Deutsche Forschungsgemeinschaft (DFG, Grant RO 1030/15-1, KOMEG), the Volkswagen Stiftung, the Natural Science Fundation of China (NSFC 31450110072), EU COST action TD1006, Deutsche Forschungsgemeinschaft (DFG, Koselleck), and Bundes Ministerium für Bildung und Forschung BMBF MOTORBIC (FKZ 13GW0053). A. Sarasola-Sanz's is supported by La Caixa-DAAD scholarship, and N. Irastorza-Landa's work by the Basque Government and IKERBASQUE, Basque Foundation for Science.

REFERENCES

[1] A. Ramos-Murguialday, M. Schürholz, V. Caggiano, M. Wildgruber, A. Caria, E. M. Hammer, S. Halder, and N. Birbaumer, "Proprioceptive feedback and brain computer interface (BCI) based neuroprostheses," *PLoS One,* vol. 7, p. e47048, 2012.

[2] K. K. Ang, C. Guan, K. Sui Geok Chua, B. T. Ang, C. Kuah, C. Wang, K. S. Phua, Z. Y. Chin, and H. Zhang, "Clinical study of neurorehabilitation in stroke using EEG-based motor imagery brain-computer interface with robotic feedback," in *Engineering in Medicine and Biology Society (EMBC), 2010 Annual International Conference of the IEEE*, 2010, pp. 5549-5552.

[3] T. Ono, K. Shindo, K. Kawashima, N. Ota, M. Ito, T. Ota, M. Mukaino, T. Fujiwara, A. Kimura, M. Liu, and J. Ushiba, "Brain-computer interface with somatosensory feedback improves functional recovery from severe hemiplegia due to chronic stroke," *Frontiers in neuroengineering,* vol. 7, 2014.

[4] A. Ramos, S. Halder, and N. Birbaumer, "Proprioceptive feedback in bci," in *Neural Engineering, 2009. NER'09. 4th International IEEE/EMBS Conference on*, 2009, pp. 279-282.

[5] A. Ramos‐Murguialday, D. Broetz, M. Rea, L. Läer, Ö. Yilmaz, F. L. Brasil, G. Liberati, M. R. Curado, E. Garcia‐Cossio, and A. Vyziotis, "Brain‐machine interface in chronic stroke rehabilitation: a controlled study," *Annals of neurology,* vol. 74, pp. 100-108, 2013.

[6] T. J. Bradberry, R. J. Gentili, and J. L. Contreras-Vidal, "Reconstructing three-dimensional hand movements from noninvasive electroencephalographic signals," *The journal of Neuroscience,* vol. 30, pp. 3432-3437, 2010.

[7] J. R. Wolpaw and D. J. McFarland, "Control of a two-dimensional movement signal by a noninvasive brain-computer interface in humans," *Proceedings of the National Academy of Sciences of the United States of America,* vol. 101, pp. 17849-17854, 2004.

[8] M. Spüler, A. Walter, A. Ramos-Murguialday, G. Naros, N. Birbaumer, A. Gharabaghi, W. Rosenstiel, and M. Bogdan, "Decoding of motor intentions from epidural ECoG recordings in severely paralyzed chronic stroke patients," *Journal of neural engineering,* vol. 11, p. 066008, 2014.

[9] K. J. Miller, G. Schalk, E. E. Fetz, M. den Nijs, J. G. Ojemann, and R. P. Rao, "Cortical activity during motor execution, motor imagery, and imagery-based online feedback," *Proceedings of the National Academy of Sciences,* vol. 107, pp. 4430-4435, 2010.

[10] T. Pistohl, A. Schulze-Bonhage, A. Aertsen, C. Mehring, and T. Ball, "Decoding natural grasp types from human ECoG," *Neuroimage,* vol. 59, pp. 248-260, 2012.

[11] R. Sitaram, A. Caria, R. Veit, T. Gaber, G. Rota, A. Kuebler, and N. Birbaumer, "FMRI brain-computer interface: a tool for neuroscientific research and treatment," *Computational intelligence and neuroscience,* vol. 2007, 2007.

[12] S.-S. Yoo, T. Fairneny, N.-K. Chen, S.-E. Choo, L. P. Panych, H. Park, S.-Y. Lee, and F. A. Jolesz, "Brain–computer interface using fMRI: spatial navigation by thoughts," *Neuroreport,* vol. 15, pp. 1591-1595, 2004.

[13] T. J. Bradberry, F. Rong, and J. L. Contreras-Vidal, "Decoding center-out hand velocity from MEG signals during visuomotor adaptation," *Neuroimage,* vol. 47, pp. 1691-1700, 2009.

[14] S. M. Coyle, T. E. Ward, and C. M. Markham, "Brain–computer interface using a simplified functional near-infrared spectroscopy system," *Journal of neural engineering,* vol. 4, p. 219, 2007.

[15] G.-C. Chang, W.-J. Kang, J.-J. Luh, C.-K. Cheng, J.-S. Lai, J.-J. J. Chen, and T.-S. Kuo, "Real-time implementation of electromyogram pattern recognition as a control command of man-machine interface," *Medical engineering & physics,* vol. 18, pp. 529-537, 1996.

[16] R. Boostani and M. H. Moradi, "Evaluation of the forearm EMG signal features for the control of a prosthetic hand," *Physiological measurement,* vol. 24, p. 309, 2003.

[17] S. Waldert, H. Preissl, E. Demandt, C. Braun, N. Birbaumer, A. Aertsen, and C. Mehring, "Hand movement direction decoded from MEG and EEG," *The journal of Neuroscience,* vol. 28, pp. 1000-1008, 2008.

[18] N. Birbaumer, "Breaking the silence: brain–computer interfaces (BCI) for communication and motor control," *Psychophysiology,* vol. 43, pp. 517-532, 2006.

[19] J. M. Antelis, L. Montesano, A. Ramos-Murguialday, N. Birbaumer, and J. Minguez, "On the usage of linear regression models to reconstruct limb kinematics from low frequency EEG signals," *PLoS One,* vol. 8, p. e61976, 2013.

[20] Y. Wang and S. Makeig, "Predicting intended movement direction using EEG from human posterior parietal cortex," in *Foundations of Augmented Cognition. Neuroergonomics and Operational Neuroscience*, ed: Springer, 2009, pp. 437-446.

[21] G. Ofner and G. Müller-Putz, "Decoding of hand movement velocities in three dimensions from the eeg during continuous movement of the arm," in *TOBI Workshop III*, 2012.

[22] N. Robinson, C. Guan, A. Vinod, K. K. Ang, and K. P. Tee, "Multi-class EEG classification of voluntary hand movement directions," *Journal of neural engineering,* vol. 10, p. 056018, 2013.

[23] G. Clauzel, C. Neuper, and G. Müller-Putz, "Offline decoding of hand movement directions from non-invasive EEG," *trials,* vol. 8, p. 6, 2011.

[24] A. Yeredor, "Blind separation of Gaussian sources via second-order statistics with asymptotically optimal weighting," *Signal Processing Letters, IEEE,* vol. 7, pp. 197-200, 2000.

[25] G. Gómez-Herrero, "Automatic Artifact Removal (AAR) toolbox v1. 3 (Release 09.12. 2007) for MATLAB," *Tampere University of Technology,* 2007.

[26] R. Tomioka, G. Dornhege, G. Nolte, B. Blankertz, K. Aihara, and K.-R. Müller, "Spectrally weighted common spatial pattern algorithm for single trial EEG classification," *Dept. Math. Eng., Univ. Tokyo, Tokyo, Japan, Tech. Rep,* vol. 40, 2006.

[27] E. Combrisson and K. Jerbi, "Exceeding chance level by chance: The caveat of theoretical chance levels in brain signal classification and statistical assessment of decoding accuracy," *Journal of neuroscience methods,* 2015.

Exaggerated Phase-amplitude coupling in chronic Stroke during Rehabilitation

Farid Shiman[1,2], Eduardo López -Larraz[1] , Thiago Figueiredo[1,5], Nerea Irastorza-Landa[1,2], Andrea Sarasola-Sanz[1,2], Martin Spüler[5], Niels Birbaumer[1,3], Ander Ramos-Murguialday[1,4]

[1]Institute of Medical Psychology and Behavioral Neurobiology, University of Tübingen, Tübingen, Germany.
[2]International Max Planck Research School (IMPRS) for Cognitive and Systems Neuroscience, Tübingen, Germany.
[3]Wyss Center for Bio-and Neuroengineering, Geneva, Switzerland.
[4]TECNALIA, San Sebastian, Spain.
[5]Computer Science Department, Wilhelm-Schickard-Institute, University of Tübingen, Tübingen, Germany.

Introduction

Neural oscillations show the synchronized activity according to motor and cognitive functions. It has been shown that phase–amplitude coupling (PAC) has a functional role in neural computation and learning [1–4] within and between distinct regions of the brain. Phase-amplitude coupling occurs in several areas of the brain when the phase of the low frequency oscillation modulates the amplitude of the high frequency oscillation during a variety of cognitive, sensory, and motor tasks [1,5,6]. Phase-amplitude coupling was reported between high-γ amplitude and the phase of low-frequency oscillations, especially θ [2,7], α [7–10] and β [11,12] in cortical and subcortical areas [4,13–16]. Although, the amplitude of low frequency bands such as α (8–13 Hz), β (13–30 Hz), and high-γ (80–150 Hz) has demonstrated a substantial role in motor functions [17], the relationship between such oscillations and how it affects encoding of sensorimotor function is not fully understood.

Moreover, changes in cross-frequency coupling in particular PAC have been linked to neurological disorders. This coupling has been observed as pathological neuronal synchronization in schizophrenia [18,19], epilepsy [9,20], dystonia [21], and Parkinson [21,22]. Therefore, understanding of CFC patterns can be crucial for diagnostics, and ultimately help to design new treatments for neurological disorders. In motor cortex, reduction in PAC has

been shown as a critical step in movement execution [9,23]. PAC is proposed to dynamically link in cortical areas that are essential for task performance [2,8,16].

In primary motor cortex, Hemptinne et al. reported that there is an exaggerated coupling between the phase of beta oscillation and the amplitude of high gamma activity in Parkinson patients [21]. They studied patients suffering from Parkinson, primary craniocervical dystonia, and human without movement disorder for medically intractable epilepsy without basal ganglia disease. Their results reported that there is significantly larger PAC in movement disorders than there is in humans with epilepsy without motor disorders. Moreover, a previous study on sensorimotor cortex PAC in epileptic patients, has demonstrated that the coupling between gamma amplitude and alpha phase during rest and movement planning period prior to movement is significantly larger compared to movement period [24]. They concluded that PAC could be applied to improve Brain-Machine-Interfaces (BMIs).

BMIs based on sensorimotor rhythm control have been proposed as a valid tool to study sensorimotor learning [25] and to produce motor recovery in completely paralyzed stroke patients circumventing the lesion [26]. An artificial output of the brain can be used to control brain oscillations closing the loop between volitional top-brain signals and sensory input (normally visual feedback). The feedback modality plays an important role because it determines the type of sensorimotor integration happening during learning or neuroprosthetic skill learning. If proprioceptive feedback is used, visual and afferent haptic and proprioceptive feedback will be used to close the control loop artificially imitating the visuomotor control loop used in normal sensorimotor skill learning with the exception of the top-down motor command in the case of paralyzed stroke patients. As previously reported proprioceptive-BMIs rehabilitation on clinical and physiological pattern [25,27].

The influence of stroke in PAC in the sensorimotor cortex has never been investigated and less has the role of PAC in sensorimotor integration and learning and in a motor recovery process. For this reason, study of cross-frequency coupling (CFC) in stroke patients during BCI rehabilitation can be addressed the problem of understanding of neural changes as pathological sign.

The first objective of our study is to characterize PAC in the sensorimotor cortex in stroke patients. We hypothesized that stroke patients, similar to other neurological disorders affecting corticothalamic and corticospinal pathways like Parkinson and dystonia, present abnormal synchronization between the phase of low-frequency and the amplitude of high-frequency. Parkinson's disease is related to pathological high-amplitude beta band (13-30 Hz) within the cortico-basal gangalia [22,28]. However, this high beta synchronisation is not understood how lead to motor impairments. Hemptinne et al. reported the coupling between the phase of beta band oscillations recorded from the subthalamic nucleus (STN) and the amplitude of broad band gamma activity in the primary motor cortex (M1) [21]. Interestingly, they revealed a similar phase-amplitude coupling in primary motor cortex. Furthermore, this pathological coupling has been shown to be abolished during deep brain stimulation (DBS) [12,21]. Although they mentioned that this abnormal coupling in motor controlling cortical areas was produced by basal ganglia disease, this coupling also presented in sensorimotor cortex of human without basal ganglia diseases like epilepsy in another studies [24,29] . For this reason, we hypothesized that, in stroke with cortical and subcortical lesion, there is abnormal phase-amplitude coupling in sensorimotor cortex. In addition, we investigated if the coupling is produced by basal ganglia disease in stroke patients because we investigated two chronic stroke patients with basal ganglia disease and one without this disease.

To test this hypothesis, we studied phase-amplitude coupling in three chronic stroke patients implanted with an epidural electrocorticography (ECoG) array. We found exaggerated alpha-phase broadband-gamma amplitude coupling in the sensorimotor cortex of stroke patients with and without basal ganglia disease. Moreover, abnormal cortical coupling was reduced by BCI-rehabilitation, both at rest and during movement. These findings of cross-frequency coupling in sensorimotor cortex of stroke patients and decoupling of high-frequency rhythms from low-frequency caused by BCI-rehabilitation therapy present a fundamental network abnormality in stroke patients.

Methods:

We studied three chronic stroke patients (details are shown in Table 1.) with paresis of the left hand undergoing a long-term investigational study for motor cortex stimulation using epidural electrocorticography (ECoG) implants. In addition, they were receiving rehabilitation training to improve upper limb motor function after stroke. Patients were not able to produce voluntary finger movements with the left hand. The study was approved by the local ethics committee (Faculty of Medicine, University Hospital Tübingen).

Each patient was implanted with 16 platinum-iridium disk electrodes (Resume II, Medtronic, Fridley, USA) with a diameter of 4 mm placed over the hand area of iplesional S1, M, and pre-motor cortex on four strips with four electrodes each with a center-to-center distance of 1 cm. Placement of grids was guided by an image-guidance approach [30] including the representation of cortical hand via intraoperative functional localization [31]. The location of a 4 × 4 grid-like pattern is shown in Figure1. A. We also removed noisy ECoG channels (11 channels in total) resulted n=85 of 96 across all patients (more information can be seen in supplementary file).

Table 1. Demographic characteristics of three stroke patients.

Patient	**P1**	**P2**	**P3**
Age (y)	63	56	52
Sex	Female	Male	Male
Months since insult	71	80	159
Paralysis	Left	Left	Left
lesioned hemisphere and location	Right subcortical and cortical	Right subcortical and cortical	Right subcortical and cortical
Lesion	Basal ganglia hemorrhage	Basal ganglia hemorrhage	MCA territory infarct (frontal)
Affected area	Head of striate body, lentiform nucleus, thalamus, whole internal capsule, insula, frontal lobe	Putamen, internal capsule, insula, opercular part of inferior frontal gyrus	Frontal lobe including motor cortex (M1), parietal lobe including somatosensory cortex (S1)

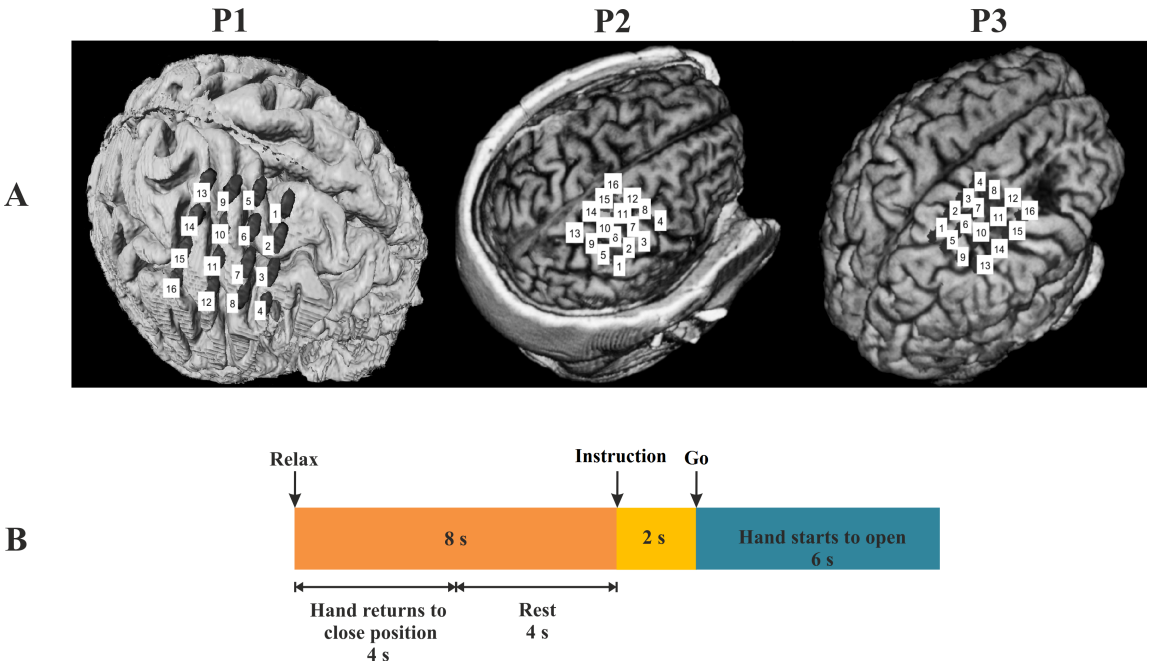

Figure 1. Location of the ECoG electrodes and experimental paradigm. A: Location of the epidurally implanted ECoG electrodes is indicated by the numbers 1-16 (A0, A1, A2, A3, B0, B1, B2, B3, C0, C1, C2, C3, D0, D1, D2, D3) for three patients. The MRI volume of patients was used with permission from [32] B: Motor task timing diagram. The patients were presented with visual and auditory cues indicating "Relax'', Pre-Feedback or "Instruction'', and Feedback or "Go'' periods. Patients were asked to perform a task specified with the Pre-Feedback cue once the Feedback cue was presented.

Task:

The paretic upper limb of the patient was fixed to a mechatronic hand orthosis (Tyromotion Amadeo HTS, Graz, Austria) using two straps, one placed at the forearm and one around the wrist. Patients were asked to open and close the hand (e.g. extend or flex the fingers). Magnets fixed the finger tips to the actuators of the orthosis. Imperative stimuli were presented visually (19'' monitor) and auditory to help patients with the timing (Fig1. B).

Movement of the fingers in the paralyzed hand between hand "open" and "close" positions was guided by sensorimotor rhythm (SMR)-based BCI controlled hand orthosis. Based on the spasticity of the patients, the movement range was individually adjusted in each session [33]. In this study for further analysis, we used the data from two sessions during BCI

rehabilitation. Moreover, patients performed similar BCI rehabilitation undergoing electrical epidural stimulation between these two sessions.

Each trial started with the hand closed and in a resting position and consisted of three phases: 1) preparation (2sec), in which patients were presented with the auditory cue “Left Hand’’ and were instructed to wait until the next auditory cue. 2) feedback (6sec), a “Go” cue was presented and patients were asked to open the their paretic hand until the end of the feedback phase; 3) Relax (8sec), an auditory cue “Relax” was presented to the patients, who were instructed to rest, while the fingers were moved by the robot returning to the starting closed position (2-3sec) and the patients were instructed to relax for the rest of the time. For the analysis, we consider the rest interval to be the last 4 seconds of the relax phase. Each experimental session was divided in 12 runs, each consisting of 11 trials resulting in 131 trials. The experimental paradigm for each trial is shown in Figure 1. B.

Recording and pre-processing:

ECoG signals were recorded using BrainAmp DC amplifiers (Brain Products GmbH, Munich, Germany) with a sampling rate of 1000 Hz. A high-pass filter at 0.16 Hz and a notch filter to remove the 50 Hz noise were applied.

BCI2000 (Schalk et al., 2004) was used for data acquisition, processing and control of the robotic orthosis. Channels with low signal-to-noise ratio were excluded from the analysis, and ECoG signals were re-referenced to the common average.

Analysis of Phase–Amplitude Cross-Frequency coupling

Phase-amplitude coupling (PAC) was quantified using the modulation index (MI) introduced by Tort et al.[34]. Previous studies [35,36] were used as the reference to guide the methodological steps. The MI method reflects the strength of coupling between the phase variations of low-frequency oscillation and amplitude variations of high-frequency oscillation.

The MI method has been developed based on the Kullbeck–Leiber distance and shows a close relationship to Shannon entropy demonstrating a nonuniform distribution when amplitude of high-frequency is modulated by the phase of low-frequency.

The Tort's MI was calculated as described below:

First, ECoG signals were bandpass filtered at low frequency (f_p) from 4 to 29 Hz (with 1.5-Hz steps) and high frequency (f_A) from 30 to 250 Hz (with 3-Hz steps) with a fourth-order, two-pass Butterworth filter. A variable bandpass filter was used as ±1/3 of the center frequency (e.g., 10 ± 3.3 Hz as [6.3 13.3] Hz) to improve detection of cross-frequency coupling [35]. Secondly, the phase of low-frequency $x_{fp}(t)$ and the amplitude of high-frequency $x_{fA}(t)$ were extracted from filtered signal after Hilbert transformed. For each single channel, all recorded trials were concatenated to generate these signals. Afterwards, the phases of signal $x_{fp}(t)$ are equally divided into bins of 20° (N = 18 bins; see [34]).

The average amplitude $M(k)_{mean}$ of $x_{fA}(t)$ corresponding to each phase bin k can be calculated and then normalized by the sum of all averages over all bins N as follows:

$$P(k) = \frac{M(k)}{\sum_{k=1}^{N} M(k)}$$

The uniformity of the normalized amplitude distribution across phases will not be present if the amplitude is modulated by phase. The method hypothesizes the expected amplitude to have a uniform distribution. Moreover, we applied Kullbeck-Leiber distance (D_{KL}) for calculating the deviation of P(k) from uniform distribution $Q(k)$ in order to quantify the phase-amplitide coupling.

$$D_{KL}(P, Q) = \sum_{k=1}^{N} P(k).\ \log\ (\frac{P(k)}{Q(k)})$$

The MI can be calculated from normalized D_{KL} :

$$MI = \frac{D_{KL}(P, Q)}{\log(N)}$$

Testing the significant Changes in Cross-Frequency Coupling across all ECoG channels.

We compared the cross frequency coupling during movement to the one during rest period across all ECoG channels normalizing the PAC as follows:

$$CFC_{Norm} = \frac{CFC_{Movement} - CFC_{Rest}}{CFC_{Movement} + CFC_{Rest}}$$

For each phase-to-amplitude frequency combination, a Wilcoxon sign-rank test (α =0.05) was used to estimate the significance of Phase-amplitude coupling change across all the ECoG channels. Bonferroni-Holm method was subsequently applied to correct for false discovery rate (FDR).

Statistical Surrogate Analysis:

We applied a statistical control analysis for each ECoG channel cross frequency coupling to verify if the observed value differs from chance. In this way, significant channels determined by a surrogate shuffling method suggested by Aru et al. [35]. The surrogate method is verified with a non-parametric block-resampling techniques. It has been shown that distortion is minimized from the original phase dynamics which can reduce the number of false-positives detections. A time-series of the high-frequency signal $x_{fA}(t)$ were split into two blocks and the resulting blocks permuted randomly. A p-value was derived by repeating this procedure 200 times[4,15].

Results

In this study we characterize PAC on the sensorimotor cortex in stroke patients during a motor task (see Fig. 1).

Phase-amplitude coupling across all patients.

We investigated whether the cross-frequency was functionally coupled by calculating the change in Tort's modulation index (MI) in Movement vs. Rest. Across all the ECoG channels (n=85), we found a significant increase in cross-frequency coupling (average normalized change in MI) between the phase of alpha frequency (8 Hz), and the amplitude of gamma-frequency (45 Hz) (Wilcoxon sign-rank test, $P = 1.07*10^{-5}$, corrected for the false discovery rate (FDR) as shown in Fig 2. *Left*).

For alpha-gamma frequency coupling, 14 ECoG channels detected a statistically significant increase in phase-amplitude coupling in the rest and significant decrease in movement cue (Monte Carlo surrogate test, $P < 0.05$) as can be seen in Fig. 2. *Right*. Table 2. Shows the *P* values of significant channels between the phase of the 8-Hz alpha frequency, and the amplitude of 45-Hz gamma frequency in both sessions for each patient.

Table 2. *P* values of significant channels (for alpha-gamma coupling) from surrogate test for all patients. B2, B3, C0, C1, and C2 are ECoG channels. For more information regarding the location and/or other channels check Fig. 1. *A* and supplementary files, respectively. 'S1' and 'S2' indicate session1 and session2, respectively. 'P' indicates patients.

Patients		P1				P2		P3		
ECoG Channels		B2	B3	C1	C2	B2	B3	B2	B3	C0
S1	Rest	0.005	0.0047	0.005	0.004	0.0149	0.005	0.602	0.3134	0.005
	Movement	0.0149	0.005	0.003	0.005	0.005	0.0199	0.0149	0.01	0.005
S2	Rest	0.5473	0.1493	0.0249	0.0299	0.005	0.011	0.2637	0.1443	0.004
	Movement	0.005	0.0348	0.1294	0.005	0.014	0.005	0.1493	0.0249	0.005

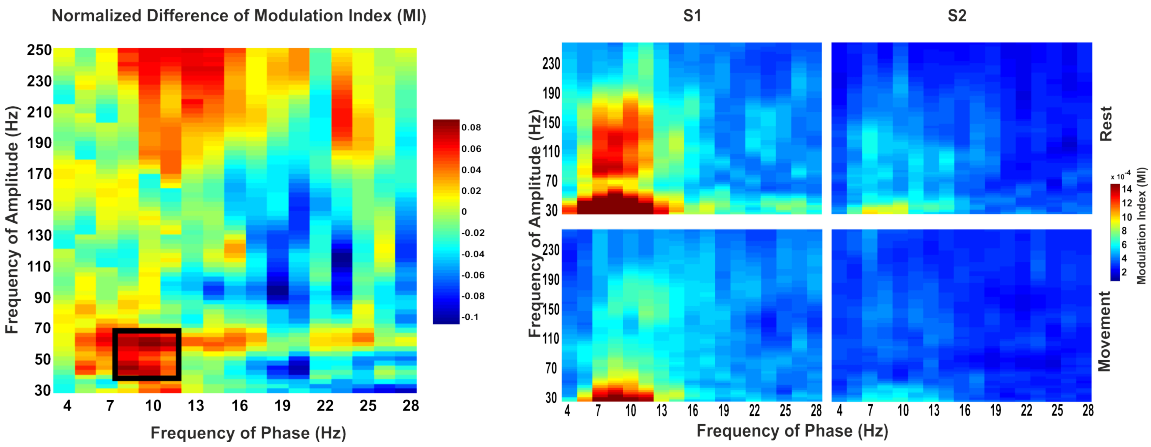

Figure 2 . Results across all patients. *Left:* Normalized difference of MI (Movement vs Rest) across all channels. *Right:* Significant channels in each session during rest and movement.

Phase-amplitude coupling of significant channels for each patient in two sessions.

In patient 1, 8 of 27 ECoG channels show significant alpha-gamma coupling during rest and movement in session1 (S1). Average of restricted channels can be seen in Fig 3 for two sessions, which clearly shows that phase-amplitude coupling decreases in session2.

In patient 2, 4 of 29 ECoG channels show significant alpha-gamma coupling between the phase of a ~8-Hz alpha frequency, and the amplitude of ~45-Hz gamma frequency in both sessions for rest and movement. As can be seen in Fig 4, there is also significant coupling between phase of beta frequency (13-18 Hz) and amplitude of gamma frequency. Like patient 1, average of significant channels can be seen in Fig 4, which clearly shows phase-amplitude coupling decreases in session2.

In patients 3, 6 of 26 ECoG channels show significant coupling in two sessions but only one of the channels is consistent with the results across patients for alpha-gamma coupling (see Fig. 2. *Left*). As can be seen in Fig 5, the average of significant channels shows a decreased coupling in session two consistent with other patients. Time-frequency analysis and power can be also seen in the middle and bottom of the figures, respectively, for each patient.

Average of time-frequency for significant channels (Fig 5. Middle) shows how the lower frequency decreases during hand movement.

Phase-amplitude coupling of each significant channels and time-frequency of all ECoG channel can be seen in supplementary files. The overall significant increase in alpha-gamma coupling across significant ECoG channels for individual patients was not statistically significant (P = 1, FDR corrected).

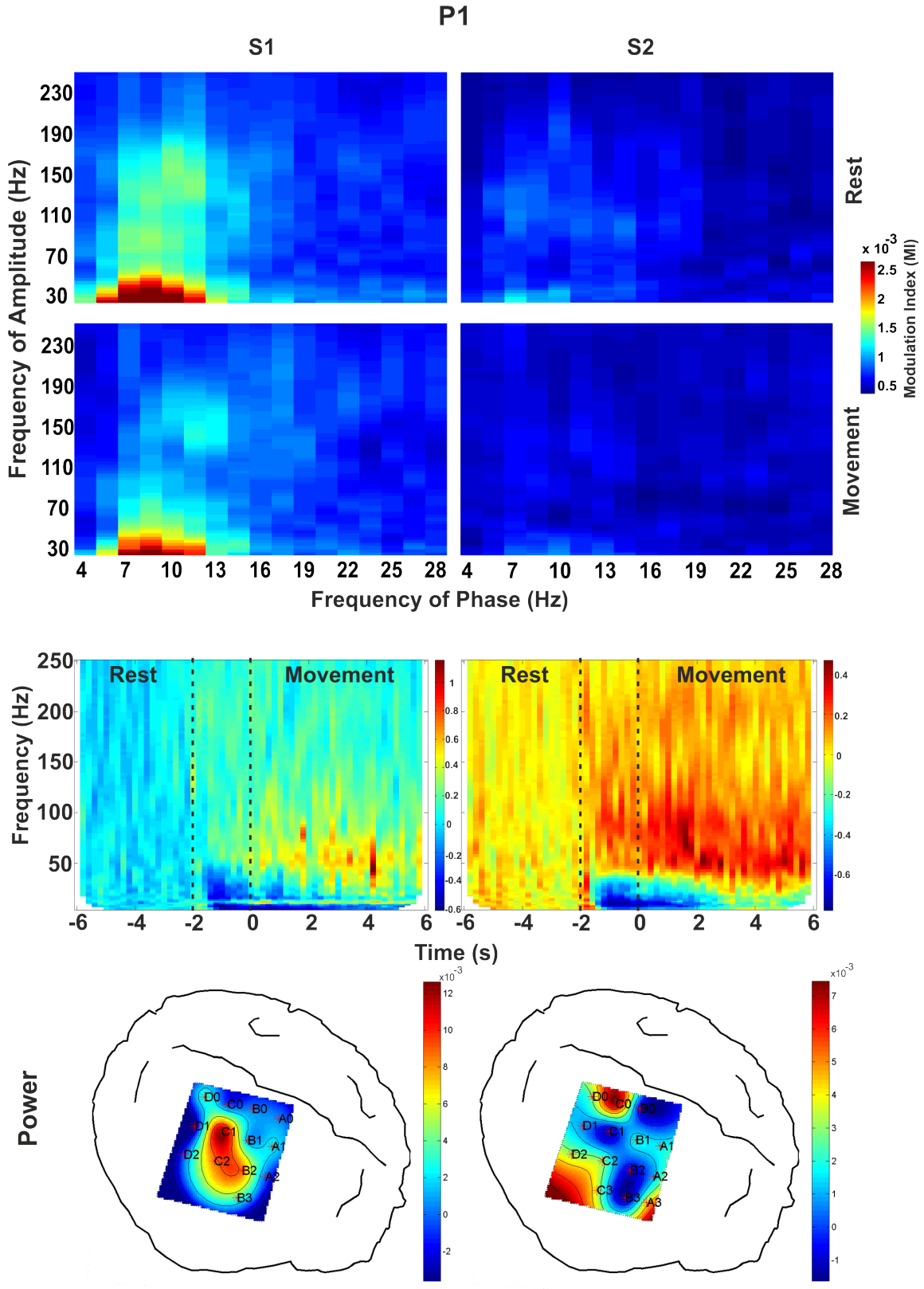

Figure 3. Phase amplitude coupling, time frequency, and average of higher gamma power for P1. ***Upper:*** **average of significant channels for movement and rest for both sessions.** ***Middle:*** **average of time-frequency analysis for significant channels.** ***Bottom:*** **average of higher gamma (35-150 Hz) amplitude during rest for all channel placed on head shape of P1.**

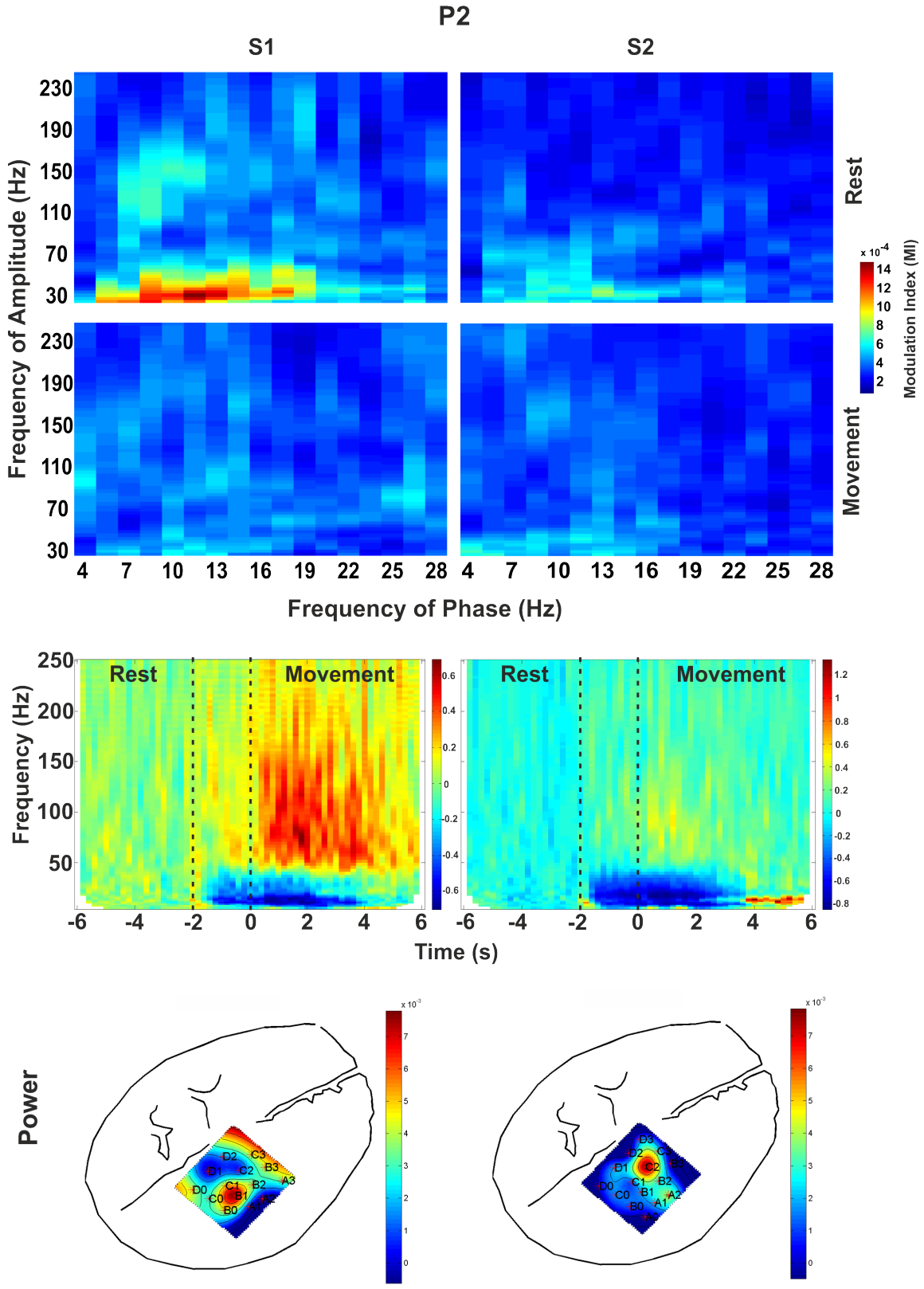

Figure 4. Phase amplitude coupling, time frequency, and average of higher gamma power for P2. ***Upper:*** average of significant channels for movement and rest for both sessions. ***Middle:*** average of time-frequency analysis for significant channels. ***Bottom:*** average of higher gamma (35-150 Hz) amplitude during rest for all channel placed on head shape of P2.

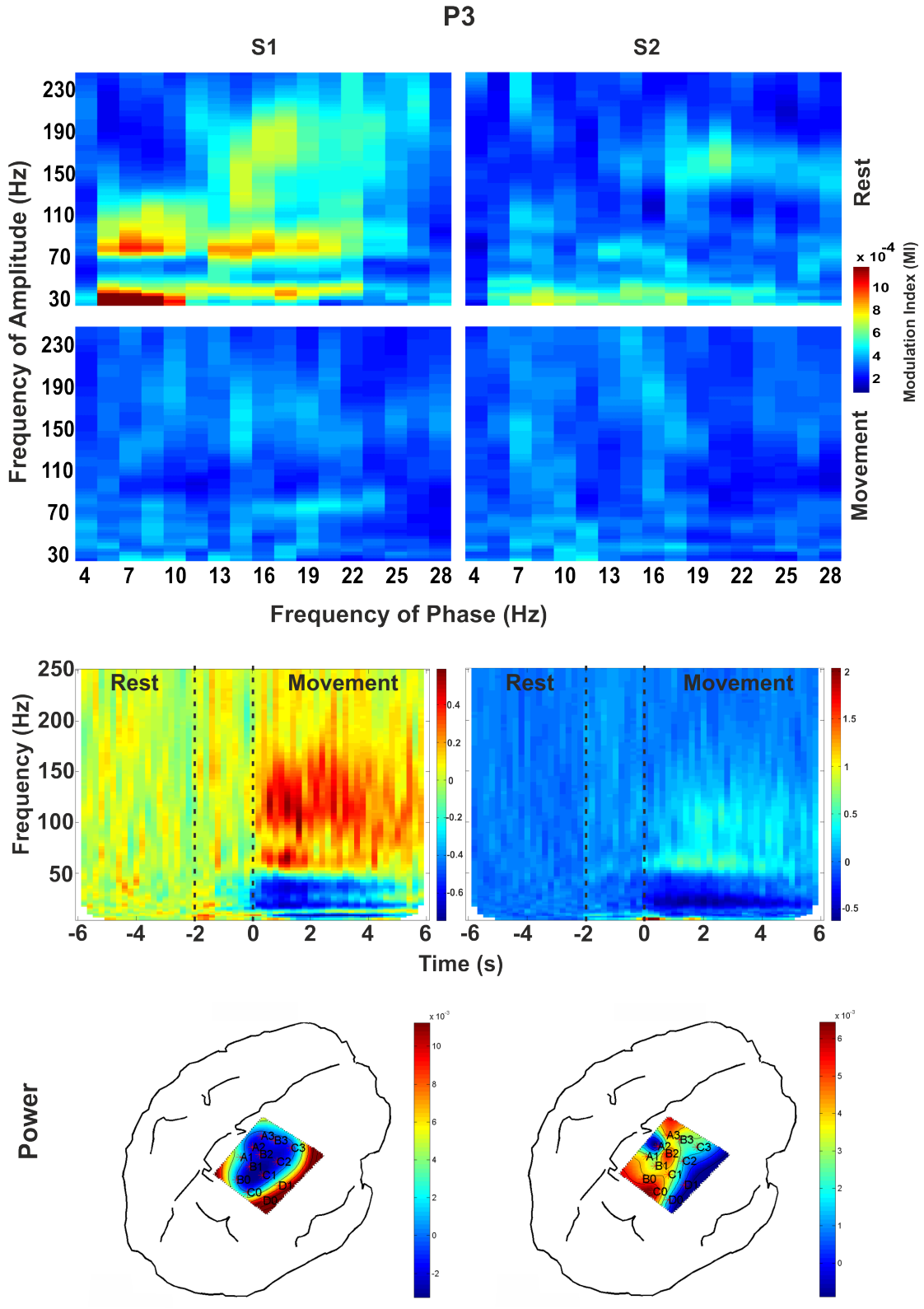

Figure 5. Phase amplitude coupling, time frequency, and average of higher gamma power for P3. ***Upper:*** **average of significant channels for movement and rest for both sessions.** ***Middle:*** **average of time-frequency analysis for significant channels.** ***Bottom:*** **average of higher gamma (35-150 Hz) amplitude at each channels during rest for all channel placed on head shape of P3.**

Statistical analysis between session1 and session2.

To check whether the phase-amplitude coupling carried information about the BCI performance, we tested two types of statistical analysis between two sessions across all patients performed BCI rehabilitation.

We first conducted a test across all ECoG channels, and then only between significant channels.

a) Across all channels, we found a trend for higher increase in phase-amplitude when movement was cued for session1 vs. session2 (Fig 6. *Left*; Wilcoxon sign-rank test, P=0.0004). This statistical trend suggests that these channels may carry significant movement information in alpha-gamma coupling.

b) For the restricted ECoG channels (n=14) that showed significant coupling, there is a statistically significant effect for average difference in coupling between two sessions (Fig 6. *Right*; Wilcoxon sign rank, P=0.001). As can be seen in Fig 6. *Right*, the coupling significantly decreased in session2, which can be the effect of rehabilitation compared to the session1.

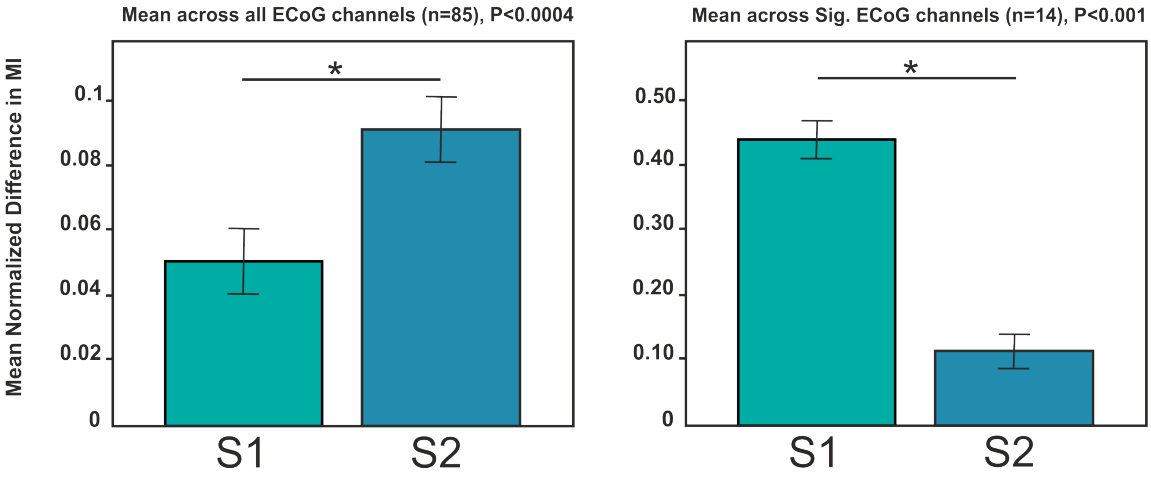

Figure 6. Mean normalized difference for alpha-gamma coupling between two sessions across all patients. *Left*: Mean across all ECoG channels between session1 (S1) and Session2 (S2). *Right*: Mean across significant channels between two sessions.

Discussion

The activity of cortical regions has been investigated in terms of single frequency in chronic stroke [25,27,37] but cross-frequency interaction have not been reported. This study investigated phase-amplitude coupling with ECoG recording in sensorimotor cortex of stroke patients during hand movement and rest. The high gamma amplitudes were shown to be strongly coupled with alpha phase during hand movement across all ECoG channels in stroke during BCI rehabilitation. These findings extend the knowledge of cross-frequency coupling which tends to show exaggerated phase-amplitude coupling on sensorimotor cortex in motor diseases [9,12,21]. Coupling between the phase of low-frequency oscillations and the amplitude of high-frequency activity are shown to play an important role in motor functions as a pathological sign [9,12,21] as well as cognitive functions such as memory, learning and attention [1,4,16]. Furthermore, in this study the coupling was attenuated in the significant channels (n=14) during hand movement which is consistent with previous studies in epilepsy [9] and Parkinson [11,12]. They have shown that high gamma amplitude released from the phase-dependent status during movement. The preliminary study on sensorimotor cortex of epilepsy patients demonstrate that the PAC between the high gamma amplitude and the alpha phase might reflect a local mechanism, in which neuronal firing is modulated by the ongoing alpha oscillation [38]. Hemptinne et al. mentioned that the abnormal phase-amplitude coupling between subthalamic nucleus (STN) and primary motor cortex in Parkinson was produced by basal ganglia disease [21]. However, they also reported a similar phase-amplitude coupling only from primary motor cortex [12,21] which proved in our study showing exaggerated PAC on sensorimotor cortex of chronic stroke not only in patients with basal ganglia disease (P1 and P2) but also without this disease (P3).

This exaggerated phase-amplitude coupling in stroke may reflect a pathological sign, in which the cortex is restricted to a repetitive pattern of coupling. This has also been reported in Parkinson [12] and specially in epilepsy as function for contributing to control muscle contraction during task performance [9]. Because it was shown that low-frequency activity is related to the performance of movement tasks [39,40].

Moreover, our results are consistent with previous studies [24,41] showing the strong coupling suppresses cortical processing by the high-gamma amplitudes modulated with larger alpha oscillation during rest period and the reduction of the coupling with decreasing alpha oscillation during movement facilitates motor representation. Interestingly, we found that the abnormal coupling disappeared in session2 which we can still see the decreasing of alpha power. For this reason, PAC can be used as a feature in the future research of closed-loop BCI rehabilitation or even as prediction of motor recovery in stroke patients.

Testing the effect of BCI on Phase-amplitude coupling in stroke rehabilitation:

To test the effect of BCI rehabilitation on PAC, we tested the significant differences between two sessions and have shown that BCI rehabilitation can reduce the strength of the phase-amplitude coupling. This result is consistent with previous study on Parkinson showing the reduced PAC by therapeutic DBS [12]. A recent study revealed that there is stronger PAC between the gamma amplitude and lower-frequency phase during epileptic seizures [29]. This seizure detection using PAC contributed to improve treatment of epilepsy patients. This findings of phase-amplitude coupling in sensorimotor cortex of stroke patients, and decoupling of the high-frequency activity from the low-frequency produced by BCI-rehabilitation therapy present an abnormal fundamental network in stroke patients.

Limitations

In this study, there are several limitations that may affect the findings in this paper. The number of patients was limited by the available patients undergoing ECoG-based BCI rehabilitation. The dataset was only used from two sessions because other sessions were affected by different stimulations. Also, we did not have the possibility to check the results over a long period of rehabilitation. Furthermore, ECoG signals are only recorded from ipsilesional hemisphere of chronic stroke as it is not possible to implant and to record activities from different areas of brain in normal subjects. Otherwise, we can check the

feasibility of phase-amplitude coupling across different channels in subcortical and cortical area.

Lack of control subjects is also another limitation of our study. However, our findings are likely to be physiological rather than specific to a particular stroke condition considering that the literature have demonstrated similar findings for Parkinson, dystonia, and epilepsy patients. For this reason, a prospective study with a larger data set on stroke can be more specific on the results of phase-amplitude coupling.

References:

1. Canolty, R. T. & Knight, R. T. The functional role of cross-frequency coupling. *Trends Cogn. Sci.* **14,** 506–515 (2010).
2. Canolty, R. T. *et al.* High Gamma Power is Phase-Locked to Theta Oscillations in Human Neocortex. *Science* **313,** 1626–1628 (2006).
3. Jensen, O. & Colgin, L. L. Cross-frequency coupling between neuronal oscillations. *Trends Cogn. Sci.* **11,** 267–269 (2007).
4. Tort, A. B. L., Komorowski, R. W., Manns, J. R., Kopell, N. J. & Eichenbaum, H. Theta-gamma coupling increases during the learning of item-context associations. *Proc. Natl. Acad. Sci.* **106,** 20942–20947 (2009).
5. Hyafil, A., Giraud, A. L., Fontolan, L. & Gutkin, B. Neural Cross-Frequency Coupling: Connecting Architectures, Mechanisms, and Functions. *Trends Neurosci.* **38,** 725–740 (2015).
6. Aru, J. *et al.* Untangling cross-frequency coupling in neuroscience. *Curr. Opin. Neurobiol.* **31,** 51–61 (2015).
7. Voytek, B. *et al.* Shifts in gamma phase-amplitude coupling frequency from theta to alpha over posterior cortex during visual tasks. *Front Hum Neurosci* **4,** 191 (2010).
8. Cohen, M. X., Elger, C. E. & Fell, J. Oscillatory activity and phase-amplitude coupling in the human medial frontal cortex during decision making. *J. Cogn. Neurosci.* **21,** 390–402 (2009).
9. Yanagisawa, T. *et al.* Regulation of motor representation by phase-amplitude coupling in the sensorimotor cortex. *J. Neurosci.* **32,** 15467–75 (2012).
10. Osipova, D., Hermes, D. & Jensen, O. Gamma power is phase-locked to posterior alpha activity. *PLoS One* **3,** 1–7 (2008).
11. de Hemptinne, C. *et al.* Exaggerated phase-amplitude coupling in the primary

motor cortex in Parkinson disease. *Proc. Natl. Acad. Sci. U. S. A.* **110,** 4780–5 (2013).

12. de Hemptinne, C. *et al.* Therapeutic deep brain stimulation reduces cortical phase-amplitude coupling in Parkinson's disease. *Nat. Neurosci.* **18,** 779–786 (2015).

13. Cohen, M. X. *et al.* Good vibrations: cross-frequency coupling in the human nucleus accumbens during reward processing. *J. Cogn. Neurosci.* **21,** 875–889 (2009).

14. Buzsáki, G. *et al.* Hippocampal network patterns of activity in the mouse. *Neuroscience* **116,** 201–211 (2003).

15. Tort, A. B. L. *et al.* Dynamic cross-frequency couplings of local field potential oscillations in rat striatum and hippocampus during performance of a T-maze task. *Proc. Natl. Acad. Sci. U. S. A.* **105,** 20517–20522 (2008).

16. Axmacher, N. *et al.* Cross-frequency coupling supports multi-item working memory in the human hippocampus. *Proc. Natl. Acad. Sci. U. S. A.* **107,** 3228–33 (2010).

17. Canolty, R. T. *et al.* High gamma power is phase-locked to theta oscillations in human n eocortex. *Science (80-.).* **313,** 1626–1628 (2009).

18. Uhlhaas, P. J. & Singer, W. Abnormal neural oscillations and synchrony in schizophrenia. *Nat. Rev. Neurosci.* **11,** 100–13 (2010).

19. Moran, L. V. & Hong, L. E. High vs low frequency neural oscillations in schizophrenia. *Schizophr. Bull.* **37,** 659–663 (2011).

20. Presto, J. S. T. Detection of Epileptic Seizures Using Phase – Amplitude Coupling in Intracranial Electroencephalography.

21. de Hemptinne, C. *et al.* Exaggerated phase-amplitude coupling in the primary motor cortex in Parkinson disease. *Proc. Natl. Acad. Sci. U. S. A.* **110,** 4780–5 (2013).

22. Hammond, C., Bergman, H. & Brown, P. Pathological synchronization in Parkinson's disease: networks, models and treatments. *Trends Neurosci.* **30,** 357–364 (2007).

23. Miller, K. J. *et al.* Human Motor Cortical Activity Is Selectively Phase- Entrained on Underlying Rhythms. **8,** (2012).

24. Yanagisawa, T. *et al.* Regulation of Motor Representation by Phase – Amplitude Coupling in the Sensorimotor Cortex. **32,** 15467–15475 (2012).

25. Ramos-Murguialday, A. & Birbaumer, N. Brain oscillatory signatures of motor tasks. *J. Neurophysiol.* **7,** jn.00467.2013 (2015).

26. Ramos-Murguialday, A. *et al.* Brain–machine interface in chronic stroke rehabilitation: a controlled study. *Ann. Neurol.* **74,** 100–108 (2013).

27. Ramos-Murguialday, A. *et al.* Brain–machine interface in chronic stroke rehabilitation: A controlled study. *Ann. Neurol.* **74,** 100–108 (2013).

28. Gatev, P., Darbin, O. & Wichmann, T. Oscillations in the basal ganglia under normal conditions and in movement disorders. *Mov. Disord.* **21,** 1566–1577 (2006).

29. Edakawa, K. *et al.* Detection of Epileptic Seizures Using Phase-Amplitude Coupling in Intracranial Electroencephalography. *Sci. Rep.* **6,** 25422 (2016).

30. Gharabaghi, A. *et al.* Volumetric image guidance for motor cortex stimulation: integration of three-dimensional cortical anatomy and functional imaging. *Neurosurgery* **57,** 114–120 (2005).

31. Gharabaghi, A. *et al.* Epidural electrocorticography of phantom hand movement following long-term upper-limb amputation. *Front. Hum. Neurosci.* **8,** 285 (2014).

32. Walter, A. *et al.* Coupling BCI and cortical stimulation for brain-state-dependent stimulation: methods for spectral estimation in the presence of stimulation after-effects. *Front. Neural Circuits* **6,** 87 (2012).

33. Ramos-Murguialday, A. *et al.* Proprioceptive Feedback and Brain Computer Interface (BCI) Based Neuroprostheses. *PLoS One* **7,** (2012).

34. Tort, A. B. L., Komorowski, R., Eichenbaum, H. & Kopell, N. Measuring Phase-Amplitude Coupling Between Neuronal Oscillations of Different Frequencies. 1195–1210 (2010). doi:10.1152/jn.00106.2010.

35. Aru, J. *et al.* Untangling cross-frequency coupling in neuroscience. *Curr. Opin. Neurobiol.* **31,** 51–61 (2015).

36. Voloh, B., Valiante, T. a, Everling, S. & Womelsdorf, T. Theta-gamma coordination between anterior cingulate and prefrontal cortex indexes correct attention shifts. *Proc. Natl. Acad. Sci. U. S. A.* **112,** 8457–62 (2015).

37. Hsu, C. *et al.* Study of Repetitive Movements Induced Oscillatory Activities in Healthy Subjects and Chronic Stroke Patients. *Nat. Publ. Gr.* 4–13 (2016). doi:10.1038/srep39046

38. Klimesch, W., Sauseng, P. & Hanslmayr, S. EEG alpha oscillations : The inhibition – timing hypothesis. **3,** (2007).

39. Gilbertson, T. *et al.* Existing Motor State Is Favored at the Expense of New Movement during 13 – 35 Hz Oscillatory Synchrony in the Human Corticospinal System. **25,** 7771–7779 (2005).

40. Engel, A. K. & Fries, P. Beta-band oscillations — signalling the status quo ? 156–165 (2010). doi:10.1016/j.conb.2010.02.015

41. Haegens, S., Nácher, V., Luna, R., Romo, R. & Jensen, O. α-Oscillations in the monkey sensorimotor network influence discrimination performance by rhythmical inhibition of neuronal spiking. *Proc. Natl. Acad. Sci. U. S. A.* **108,** 19377–82 (2011).

Supplementary files:

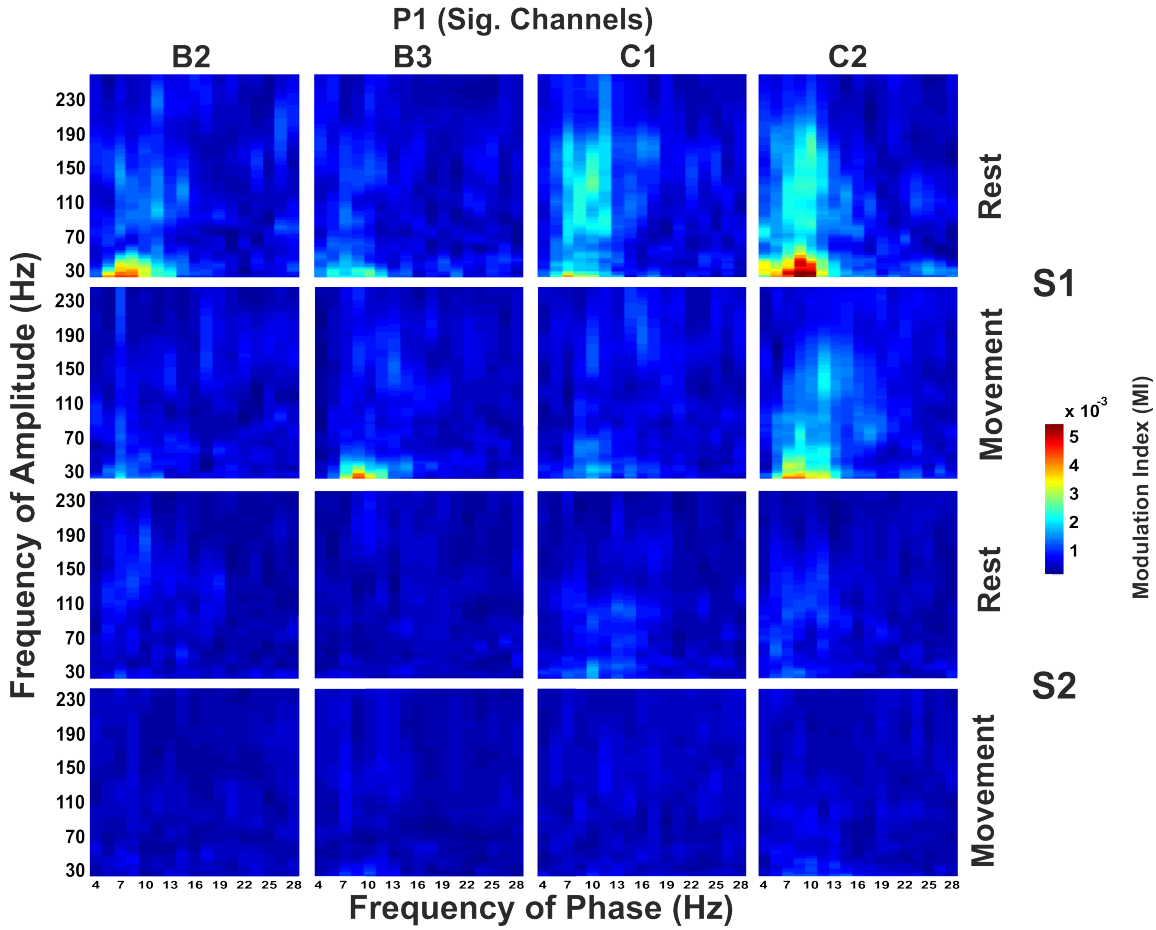

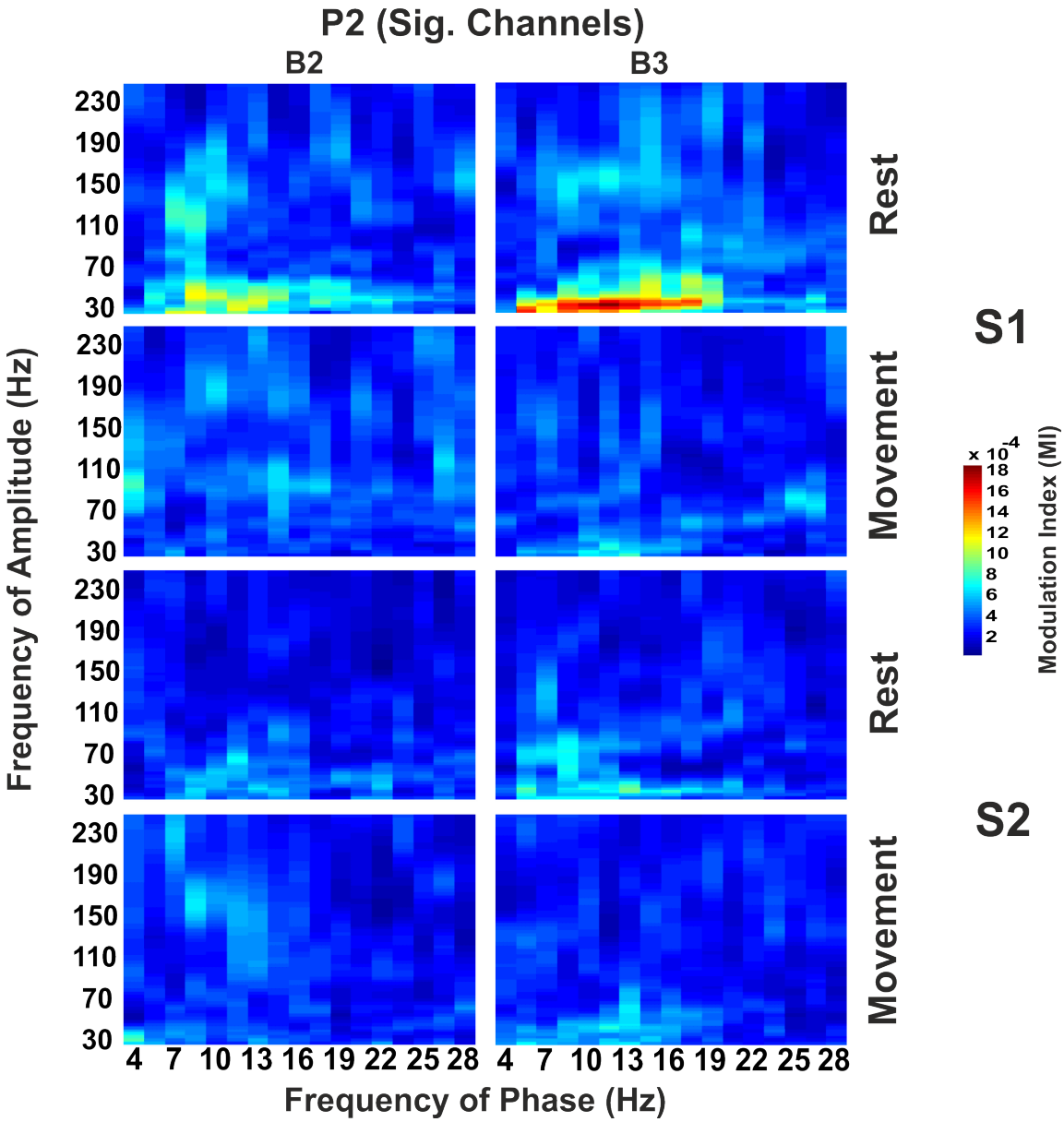
P2 (Sig. Channels)
B2
B3
Rest
Movement
Rest
Movement
S1
S2
Frequency of Amplitude (Hz)
230
190
150
110
70
30
4 7 10 13 16 19 22 25 28
Frequency of Phase (Hz)
x 10^-4
18
16
14
12
10
8
6
4
2
Modulation Index (MI)

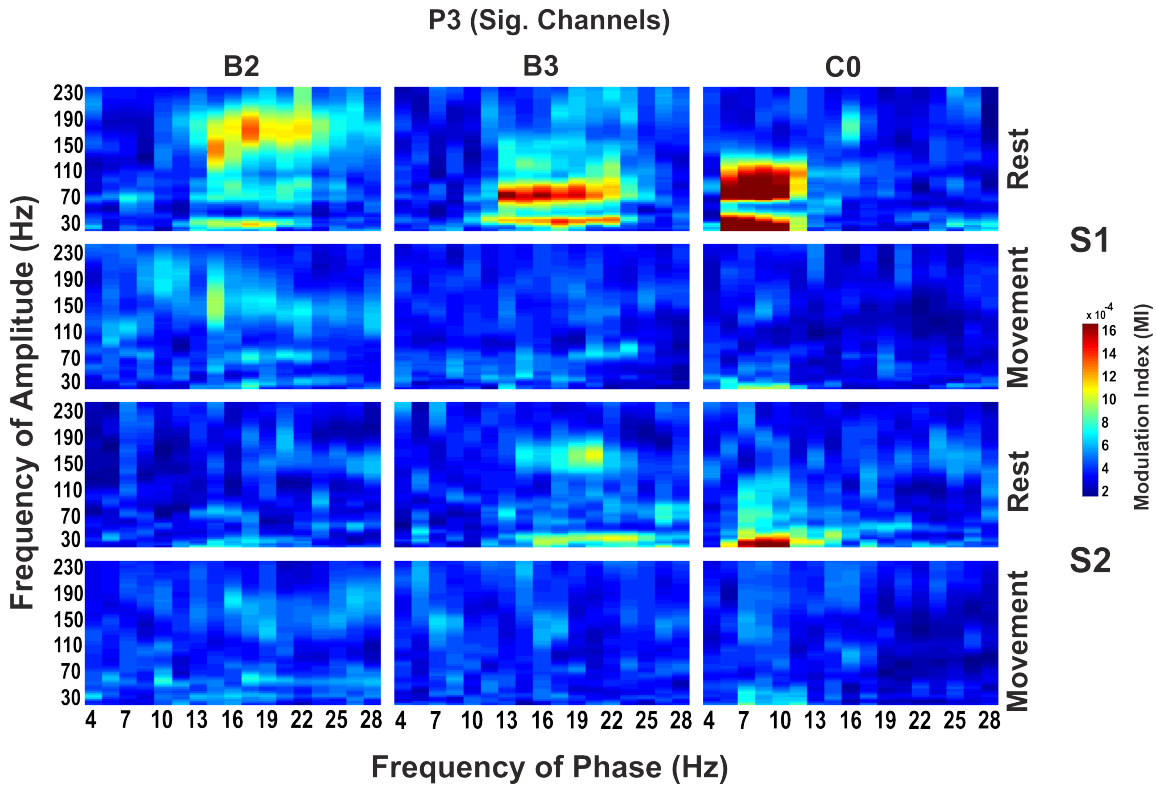
P3 (Sig. Channels)
B2
B3
C0
Rest
Movement
Rest
Movement
S1
S2
Frequency of Amplitude (Hz)
Frequency of Phase (Hz)
230
190
150
110
70
30
4 7 10 13 16 19 22 25 28
x 10^-4
16
14
12
10
8
6
4
2
Modulation Index (MI)

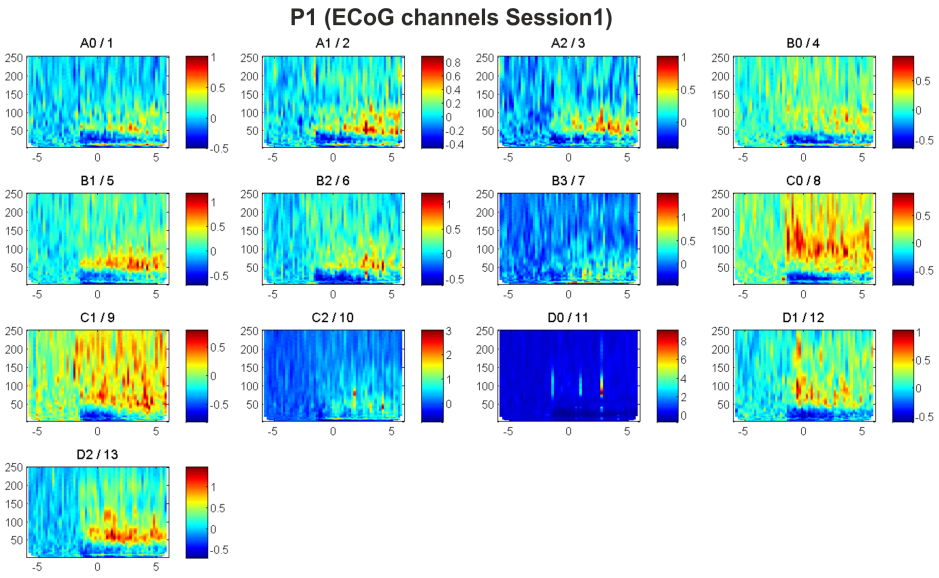
P1 (ECoG channels Session1)
A0 / 1
A1 / 2
A2 / 3
B0 / 4
B1 / 5
B2 / 6
B3 / 7
C0 / 8
C1 / 9
C2 / 10
D0 / 11
D1 / 12
D2 / 13

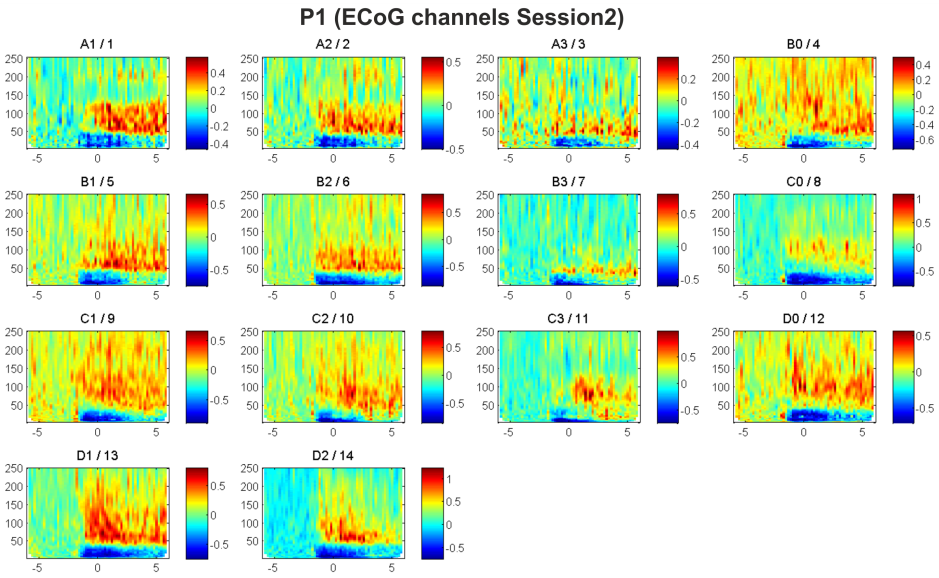
P1 (ECoG channels Session2)
A1 / 1
A2 / 2
A3 / 3
B0 / 4
B1 / 5
B2 / 6
B3 / 7
C0 / 8
C1 / 9
C2 / 10
C3 / 11
D0 / 12
D1 / 13
D2 / 14

P2 (ECoG channels Session1)

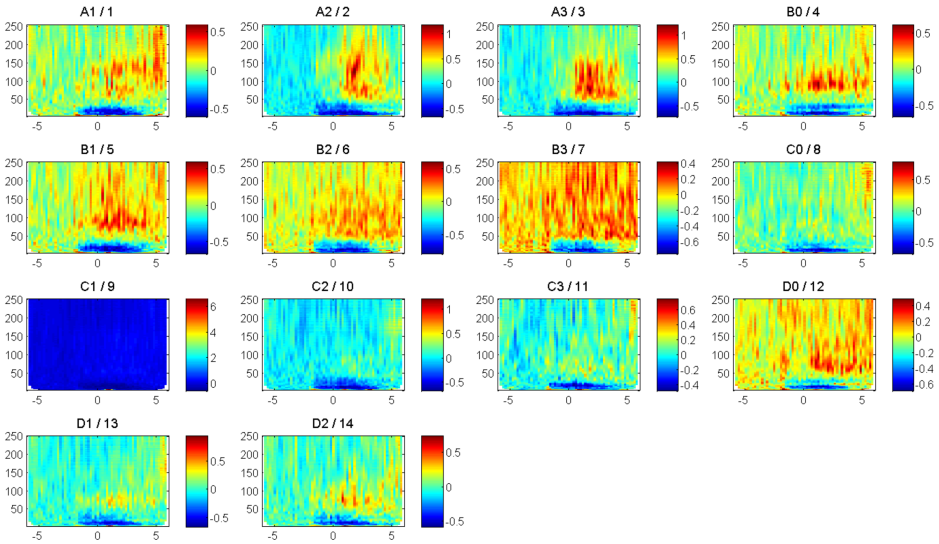

P2 (ECoG channels Session2)

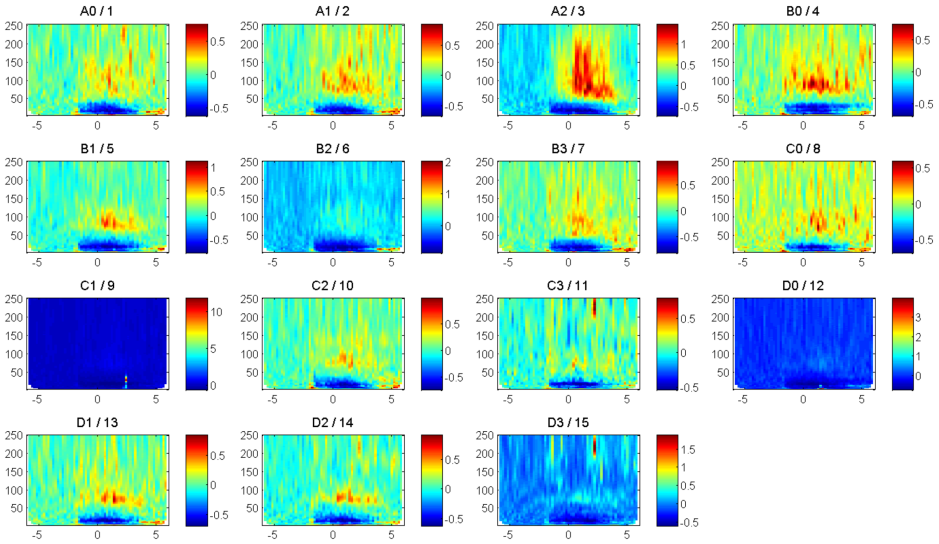

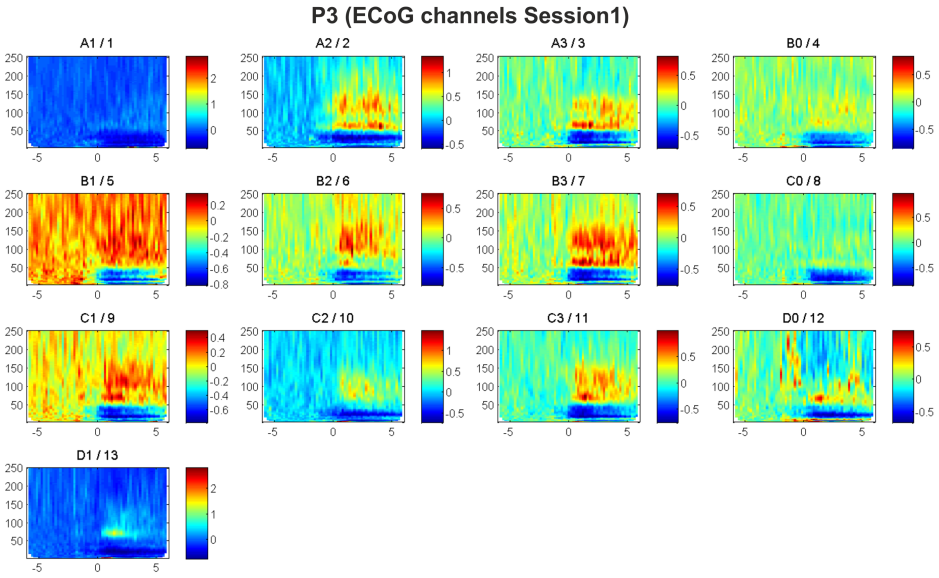
P3 (ECoG channels Session1)
A1 / 1
A2 / 2
A3 / 3
B0 / 4
B1 / 5
B2 / 6
B3 / 7
C0 / 8
C1 / 9
C2 / 10
C3 / 11
D0 / 12
D1 / 13

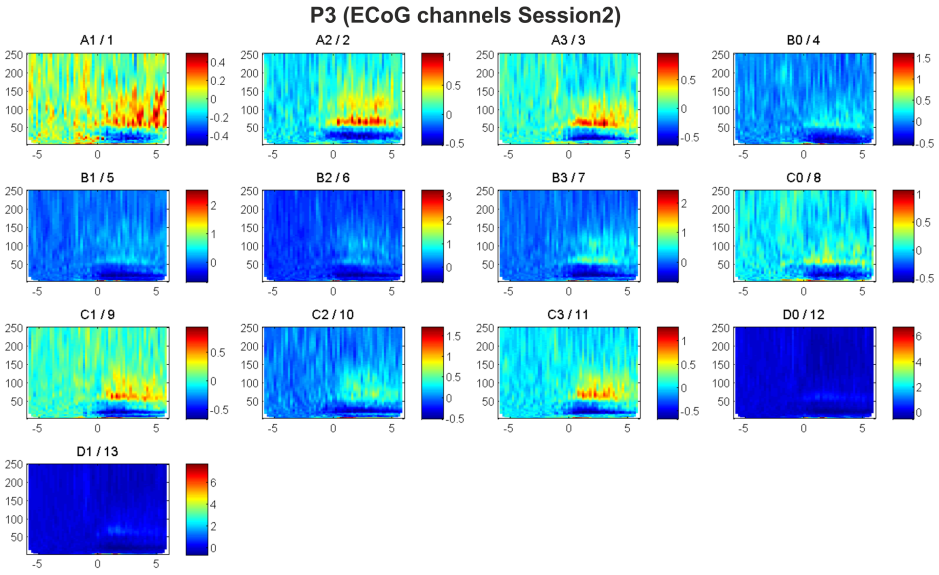
P3 (ECoG channels Session2)
A1 / 1
A2 / 2
A3 / 3
B0 / 4
B1 / 5
B2 / 6
B3 / 7
C0 / 8
C1 / 9
C2 / 10
C3 / 11
D0 / 12
D1 / 13

EMG-based multi-joint kinematics decoding for robot-aided rehabilitation therapies

Andrea Sarasola-Sanz*†, Nerea Irastorza-Landa*†, Farid Shiman*†, Eduardo López-Larraz‡, Martin Spüler§, Niels Birbaumer*¶, Ander Ramos-Murguialday*‖
*Institute of Medical Psychology and Behavioral Neurobiology, University of Tübingen, Germany
†IMPRS for Cognitive and Systems Neuroscience, Tübingen, Germany
‡I3A and Departamento de Informática e Ingeniería de Sistemas, University of Zaragoza, Spain
§Department of Computer Engineering, Wilhelm-Schickard-Institute, University of Tübingen, Germany
¶Ospedale San Camillo, Istituto di Ricovero e Cura a Carattere Scientifico, Venezia, Italy
‖TECNALIA, San Sebastian, Spain

***Abstract*—In recent years, a significant effort has been invested in the development of kinematics-decoding models from electromyographic (EMG) signals to achieve more natural control interfaces for rehabilitation therapies. However, the development of a dexterous EMG-based control interface including multiple degrees of freedom (DOFs) of the upper limb still remains a challenge. Another persistent issue in surface myoelectric control is the non-stationarity of EMG signals across sessions. In this work, the decoding of 7 distal and proximal DOFs' kinematics during coordinated upper-arm, fore-arm and hand movements was performed. The influence of the EMG non-stationarity was tested by training a continuous EMG decoder in three different scenarios. Moreover, the generalization characteristics of two algorithms (ridge regression and Kalman filter) were compared in the aforementioned scenarios. Eight healthy participants underwent EMG and kinematics recordings while performing three functional tasks. We demonstrated that ridge regression significantly outperformed the Kalman filter, indicating a superior generalization ability. Furthermore, we proved that the performance drop caused by the session-to-session non-stationarities could be significantly mitigated by including a short re-calibration phase. Although further tests should be performed, these preliminary findings constitute a step forward towards the non-invasive control of the next generation of upper limb rehabilitation robotics.**

I. Introduction

In recent years, several studies have been carried out in the field of myoelectric control for applications such as teleoperation of robots, prosthesis for amputees and rehabilitation of patients with paralyzed limbs [1], [2], [3], [4], [5], [6], [7], [8], [9], [10]. However, the development of dexterous and natural myoelectric control interfaces with multiple degrees of freedom still remains a challenge.

Most of the studies in this field have emphasized the use of EMG signals for the classification of different movement classes [1], [2]. However, these approaches have limited success when natural and smooth control of the trajectory is necessary. A decoder that maps EMG signals into a continuous profile of upper limb kinematics could overcome this limitation. Studies developing such decoders have already been performed, although most of them are limited to simple movements of either distal [3], [4], [5] or proximal [6], [7], [8] degrees of freedom (DOFs) of the upper limb. To the best of our knowledge, the only study that reported decoding of several distal and proximal DOFs of the upper limb [9] was not focused on rehabilitation approaches. Moreover, in that study target-specific and object-specific models were built for the decoding of reach-to-grasp movements, which led to high error values.

A ubiquitous issue in the field of EMG control interfaces is the non-stationarity of EMG signals that occurs across multiple sessions. Factors such as sweat, fatigue, varying upper limb configurations, electrode shift and impedance changes, could change the EMG signal distribution. This change is referred to as covariate shift and could notably affect the performance of the decoder.

In this study we aimed to decode the motion of seven DOFs (distal and proximal) of the upper limb from surface EMG signals, while participants performed different functional tasks of increasing complexity. Three different decoding schemes were implemented: within-session decoder (WS), session-to-session decoder (SS) and re-calibrated session-to-session decoder (RSS). As re-calibration was shown to improve decoding performance (e.g. by classifier adaptation [11]), a re-calibration phase using data from the beginning of the subsequent session was used to compensate for the negative effects of the session-to-session covariate shift. The performance of these three decoders was compared in order to assess the influence of the EMG non-stationarity on the decoding accuracy. Furthermore, this analysis was performed using two different algorithms, namely, ridge regression [12] and Kalman filter (KF) [13]. Up to this point, Kalman filter has been the most widely used algorithm for these applications [3], [6], [8]. However, the ridge regression technique is often underestimated and has been included in very few recent studies [4] for the decoding of EMG signals. Nevertheless, we hypothesized that, due to regularization (i.e. penalizing model complexity by imposing a constraint to the coefficients to prevent overfitting), the ridge regression technique could have a better generalization ability than the KF (i.e. predict kinematics under variable conditions more accurately).

978-1-4799-1808-9/15/$31.00

II. METHODS

A. Experimental Protocol

Eight healthy participants (3 females, 5 males, age 20-28, all right-handed) participated in this study. None of them had any neuromuscular disorder and all of them gave written consent to the procedures as approved by the ethics committee of the Faculty of Medicine of the University of Tübingen, Germany. Participants performed three different tasks while sitting and wearing a 7-DOF exoskeleton (Tecnalia, San Sebastian, Spain) on their right upper limb placed over a 70×50 cm mat. The exoskeleton allowed movements in 7 DOFs (see Fig. 1): displacement and rotation of the forearm in a 2D horizontal plane parallel to the mat's plane (3 proximal DOFs: (i) p_x position; (ii) p_y position; (iii) θ_{xy} orientation angle), pronation and supination of the wrist (1 distal DOF: (iv) ϕ_{wrist} angle) flexion and extension of the thumb, index and the group of middle, ring and pinky fingers measured as the angle of rotation with respect to the metacarpophalangeal joints (3 distal DOFs: (v) δ_{thumb}; (vi) ψ_{index}; (vii) $\alpha_{3fingers}$).

All the participants underwent two sessions that were separated by 2-9 days. During these sessions they were instructed, by means of imperative auditory cues, to perform three different tasks that always started and ended at a predefined rest position.

1) The first task consisted of reaching movements (hand relaxed) towards one of the four different targets around the mat.

2) In the second task, participants were asked to reach and point to two different targets with his/her index finger, moving towards the first target from the rest position and towards the second target immediately after reaching the first target.

3) In the third task, three objects of different shapes and sizes were located in one of the four target positions. Participants had to reach a target, grab the object placed in that position, move it to another target and then come back to the rest position. It should be noted that each of the objects required a different grasp type, which were: pinch grip, key grasp and cylindrical grasp.

Each of the tasks was divided in 5 blocks, which consisted of a set of 10-40 trials depending on the task type (40 for task 1; 10 for task 2; 22 for task 3). Resting intervals of 1-5 minutes were included between blocks in order to avoid fatigue. Participants were asked to perform the movements at their own pace and were given 4 seconds to complete task 1 trials and 6 seconds for task 2 and task 3 trials. This makes a total of approximately 30 min (task 1), 7 min (task 2) and 15 min (task 3) of recorded data per participant in each of the two sessions. It should be pointed out that, although participants performed the trials at their own pace, the aforementioned trial durations (task 1: 4 sec; task 2 and task 3: 6 sec) implied that they had to keep a rapid pace in order to accomplish the trials within the given time limits.

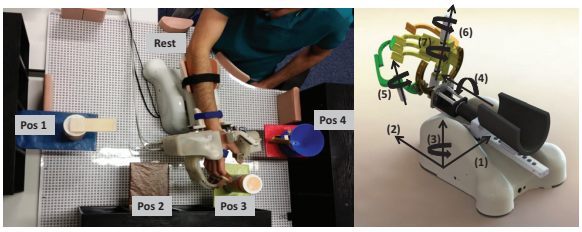

Fig. 1. (Left): Workspace where the experiments were performed. Pos1, Pos2, Pos3 and Pos4 correspond to the four targets and Rest was the predefined rest position where all the trials started and ended. (Right): Schematic of the 7 DOFs of the exoskeleton: (1) p_x; (2) p_y; (3) θ_{xy}; (4) ϕ_{wrist}; (5) δ_{thumb}; (6) ψ_{index}; (7) $\alpha_{3fingers}$

B. Data Collection

Surface EMG activity from 10 disposable bipolar electrodes (Myotronics-Noromed, Tukwila, WA, USA) over the upper-arm and fore-arm was acquired at 2500Hz using a bipolar amplifier (Brain Products GmbH, Gilching, Germany). The electrodes were placed over: 1) the abductor pollicis longus, 2) the extensor carpi ulnaris, 3) the extensor digitorium, 4) the flexor carpi radialis, palmaris longus and flexor carpi ulnaris, 5) the pronator teres, 6) the long head of biceps, 7) the external head of triceps, 8) the anterior portion of deltoid, 9) the lateral portion of deltoid and 10) the posterior portion of deltoid over the teres minor and infraespinatus muscles. The ground monopolar electrode was placed over the right clavicle. Kinematic activity of the above mentioned DOFs was recorded at 18Hz and synchronized offline with the EMG signals. The kinematics of the fore-arm DOFs, namely, p_x, p_y and θ_{xy}, were collected with a camera attached to the bottom of the exoskeleton, which tracked the movements by using an optical symbol recognition system (more details in [14]). The prono-supination angle ϕ_{wrist} was captured from a motor encoder and the fingers' angles δ_{thumb}, ψ_{index} and $\alpha_{3fingers}$ were acquired using potentiometers. Nevertheless, all the kinematic data was acquired with the same software and at the same frequency. Therefore, only the synchronization of the kinematics with the EMG signal had to be done. For this purpose, the EMG recording was initiated first. At the beginning of each block, along with the initiation of the kinematics recordings, a step signal was generated and fed into the EMG recording so that both signals could be synchronized offline.

C. Data processing

EMG data was filtered using a 4^{th} order Butterworth band-pass filter (10-500 Hz) to remove movement artifacts and high frequency noise. In addition, a 50 Hz comb filter was utilized in order to remove power line noise and its harmonics. Kinematic data was low-pass filtered with a 4^{th} order Butterworth filter (f_c = 1.5 Hz). The derivation of the positions and angles with respect to time was computed in order to obtain linear and angular velocity profiles, which were the variables to be predicted from EMG signals. The kinematic signal predicted from the decoder was filtered using a moving average with a backwards time window of

180 ms to improve movement smoothness towards online robot control.

Seven time-domain features typically used for myoelectric interfaces (Mean of absolute values, Variance, Waveform Length, Root-mean-square error, Willison Amplitude (WAMP), Zero crossing (ZC) and Slope sign changes (SSC)) [15] were extracted from each of the 10 EMG channels in 200 ms windows, resulting in a 70-element EMG feature set (7 features x 10 channels). The thresholds for the last three features were empirically selected and fixed to the same values for all the participants (TH_{WAMP} = 30 μV; TH_{ZC} = 30 μV; TH_{SSC} = 700 μV). Each of the EMG features of the generated set was normalized to zero mean and unit variance before being fed to the decoder. The testing data was normalized using the mean and standard deviation computed on the training dataset.

D. Algorithms

1) *Kalman filter*

A Kalman filter models the system by the state transition equation:

$$x_{t+1} = A_t x_t + w_t \tag{1}$$

Where x_t is the state at time t, A_t is the state transition matrix and w_t is the model white noise $\sim \mathcal{N}(0, Q)$.

The observations of the state are made through a measurement system which can be represented by the following linear equation:

$$y_t = C_t x_t + v_t \tag{2}$$

Where y_t is the observation or measurement at time t, x_t is the state at time t, C_t is the measurement matrix and v_t is additive measurement noise $\sim \mathcal{N}(0, R)$.

2) *Ridge regression*

The relationship between the dependent variable of length n, $y \in \Re^{1\times n}$, in this case velocity, and the independent variable, a p-dimensional EMG feature set $X \in \Re^{pxn}$, is modeled as follows:

$$y = \beta^T X + \beta_0 \quad \text{s.t.} \quad \sum_{j=1}^{p} \beta_j^2 \leq s \tag{3}$$

With $\beta^T \in \Re^{px1}$ being the vector of coefficients and β_0 the intercept term. The regularization consists of constraining the sum of squared coefficients with some value $s > 0$.

The solution is the one that minimizes the penalized residual sum of squares, which is expressed as:

$$\sum_{i=1}^{n}(y_i - \sum_{j=1}^{p} x_{ij}\beta_j)^2 + \lambda \sum_{j=1}^{p} \beta_j^2 \tag{4}$$

With λ being the regularization parameter. Since the penalized residual sum of squares in equation 4 is convex, it has a unique solution given by:

$$\beta_{ridge} = (X^T X + \lambda I_p)^{-1} X^T y \tag{5}$$

E. Decoding schemes

Three decoding schemes were implemented by using different training and testing conditions:

- *Within-session decoder* (WS): This decoder was trained and tested with data from the same session. It was implemented in order to have a metric of how good our decoder could work. Since we collected data during two sessions, we developed two types of decoders: one using only data from the first session S1 (WS1) and the other one only with data from the second session S2 (WS2).
- *Session-to-session decoder* (SS): This decoder was trained and validated in the first session S1 and tested in the next session S2. A performance drop due to the session-to-session transfer was expected when comparing its performance to the one of the WS decoder.
- *Re-calibrated session-to-session decoder* (RSS): This decoder was similar to the SS decoder explained above with the difference that a few minutes of data were collected at the beginning of S2 in order to re-calibrate the decoder. This was useful in order to check if this re-calibration phase could compensate for the expected performance drop due to the session-to-session transfer.

F. Cross-validation

All three of the decoding schemes were implemented for each task and DOF separately. The data from each session, task and DOF was divided into 5 blocks, each of them containing trials of all the trajectory types. These five blocks were divided into the training and test sets as follows:

For the WS decoding scheme, a 5-fold cross-validation (CV) was applied using only data from either S1 (for WS1) or S2 (for WS2). The values obtained from the testing phase of each CV-fold were averaged to compute the reported final performance. The SS decoding scheme, instead, consisted of a training phase with all 5 blocks of S1 and a testing phase with all 5 blocks of S2. For the RSS decoding scheme, all 5 blocks of S1 and the first block of S2 were included in the training set in order to re-calibrate the decoder. The remaining 4 blocks of S2 were assigned to the test set.

It should be mentioned that in the case of ridge regression, a nested CV was applied in all the decoding schemes because an optimum value for the regularization parameter had to be found. In each fold of the inner CV-loop, one of the blocks from the training set was employed as validation data in order to find the optimum regularization parameter. A grid search of values in the range $[10^{-7} - 10^{7}]$ was utilized to find the best parameter. After this, the decoder was once

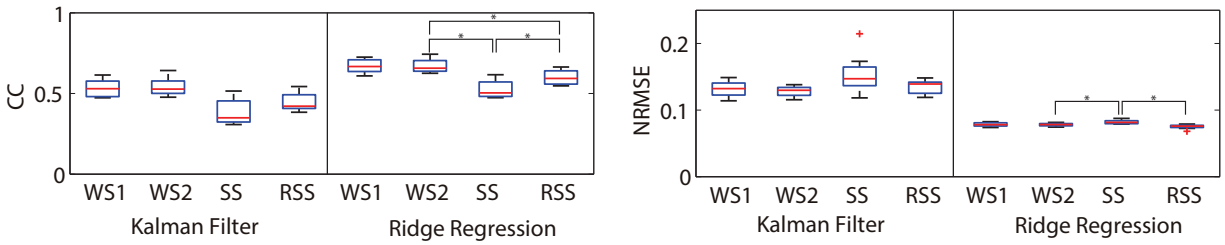

Fig. 2. Correlation coefficient (left) and normalized root mean squared error (right) for each combination of decoding scheme (WS1, WS2, SS or RSS) and algorithm (Kalman filter or ridge regression) after averaging over all subjects, tasks and involved DOFs. The median and the 25^{th} and 75^{th} percentiles are shown. Significant differences found between the decoding schemes using ridge regression are marked with an asterisk.

again trained with this optimized parameter and tested in the outer loop.

G. Performance evaluation

The correlation coefficient (CC) and the normalized root mean squared error (NRMSE) were employed as performance metrics. The reported performance values for each combination of decoding scheme and algorithm were computed as the average over the three tasks and the 8 participants. Each task's performance was in turn computed as the mean performance of the DOFs involved (i.e. actively used) in the corresponding task only.

Both for the CC and NRMSE values the following tests were applied:

Data was assumed to be normally distributed and a 2-way repeated measures Analysis of Variance (ANOVA) test with two factors (Algorithm and Decoding Scheme) was performed. The algorithm factor was comprised of two levels: Kalman filter and ridge regression while the decoding scheme factor consisted of three levels: WS2, SS and RSS.

This first test was used in order to find out which algorithm performed better overall and if that difference in performance was significant. Subsequent tests were then limited to the best algorithm. Secondly, a one-way repeated measures ANOVA was performed to test the effect of the decoding scheme factor only for the best algorithm. Post-hoc pairwise comparisons of the three decoding schemes were performed and controlled for multiple comparisons using Bonferroni correction.

For the best algorithm, a paired t-test comparing WS1 and WS2 decoding performance was also carried out in order to analyze the performance stability of the WS decoder and by extension, the reliability of session S1 and S2 data.

III. Results

For both metrics, the ANOVA resulted in a significant effect for both the algorithm (CC: $p = 10^{-6}$; NRMSE: $p = 10^{-5}$) and decoding scheme (CC: $p = 10^{-6}$; NRMSE: $p = 0.011$) factors while the interaction turned out to be non-significant (CC: $p = 0.075$; NRMSE: $p = 0.070$). The ridge regression algorithm performed significantly better than the Kalman filter and thereby, the subsequent tests were reduced to the comparison of the different decoding schemes using only ridge regression.

With the factor algorithm fixed at ridge regression, the one-way ANOVA test resulted in a significant decoding scheme effect in both cases (CC: $p < 10^{-6}$; NRMSE: $p = 10^{-5}$). Post-hoc Bonferroni corrected test results differed for each metric (see Fig. 2). For the CC, post-hoc tests revealed significant differences between the three decoding schemes. (WS2 vs SS: $p < 10^{-6}$; SS vs RSS: $p = 2.1 \cdot 10^{-4}$; WS2 vs RSS: $p = 3.1 \cdot 10^{-5}$). However, for the NRMSE metric, significant differences were found for the comparisons WS2 vs SS ($p = 4.5 \cdot 10^{-3}$) and SS vs RSS ($p = 7.5 \cdot 10^{-4}$) while the comparison WS2 vs RSS showed no significant difference ($p = 0.129$).

The paired t-test comparing WS1 and WS2 decoding schemes performance showed no significant difference for both CC ($p = 0.918$) and NRMSE ($p = 0.859$).

Additionally, for each of the three decoding schemes based on the ridge regression algorithm, the performance values (CC and NRMSE) for each of the DOFs separately were computed (see Fig. 3 and values in Table I). The performance values obtained for each DOF were consistent across decoding schemes. A significantly ($p = 10^{-6}$) lower CC for the distal DOFs (mean CC = 0.39) compared to the proximal DOFs (mean CC = 0.68) can be seen. However, the NRMSE stayed stable at a mean value of 0.077 (7.7%) for all the DOFs.

IV. Discussion

In this study, multiple decoding schemes and algorithms for the continuous mapping of EMG signals into upper limb kinematics were tested. The analysis included the decoding of distal and proximal DOFs during complex functional movements involving coordinated upper-arm and fore-arm muscle activity. Kalman filter and ridge regression techniques were compared across different decoding scenarios in order to test their ability to overcome the EMG non-stationarity as well as the variability in the performed movements. All these aspects are of great importance and have a direct impact on the clinical applications of EMG decoding.

The Kalman filter model has been extensively used before for myoelectric control applications. However, simple

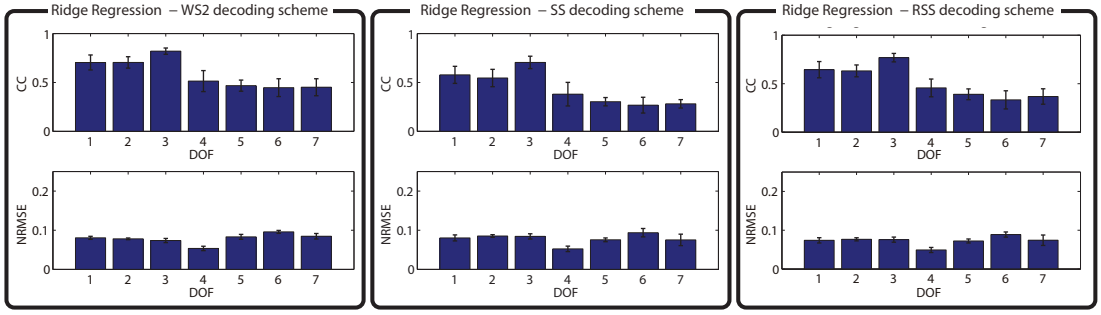

Fig. 3. Mean and standard deviation values of correlation coefficient (top) and normalized root mean squared error (bottom) for the decoded linear or angular velocities in each individual DOF, obtained with the WS2 (left), SS (middle) and RSS (right) decoding schemes. DOFs 1-2 correspond to linear velocities of: (1) p_x, (2) p_y; and DOFs 3-7 correspond to angular velocities of: (3) θ_{xy}; (4) ϕ_{wrist}; (5) δ_{thumb}; (6) ψ_{index}; (7) $\alpha_{3fingers}$.

TABLE I. MEAN AND STD VALUES OF CC AND NRMSE FOR EACH DOF AND DECODING SCHEMES USING ONLY RIDGE REGRESSION

	CC			**NRMSE**		
DOF	WS2	SS	RSS	WS2	SS	RSS
1	0.70 ($\pm$ 0.08)	0.58 ($\pm$ 0.09)	0.64 ($\pm$ 0.08)	0.081 ($\pm$ 0.004)	0.080 ($\pm$ 0.008)	0.074 ($\pm$ 0.007)
2	0.70 ($\pm$ 0.06)	0.55 ($\pm$ 0.09)	0.63 ($\pm$ 0.06)	0.078 ($\pm$ 0.002)	0.085 ($\pm$ 0.003)	0.077 ($\pm$ 0.004)
3	0.82 ($\pm$ 0.03)	0.70 ($\pm$ 0.06)	0.77 ($\pm$ 0.04)	0.074 ($\pm$ 0.005)	0.084 ($\pm$ 0.007)	0.076 ($\pm$ 0.007)
4	0.51 ($\pm$ 0.11)	0.38 ($\pm$ 0.12)	0.46 ($\pm$ 0.09)	0.054 ($\pm$ 0.006)	0.053 ($\pm$ 0.007)	0.049 ($\pm$ 0.007)
5	0.47 ($\pm$ 0.06)	0.30 ($\pm$ 0.04)	0.39 ($\pm$ 0.06)	0.083 ($\pm$ 0.006)	0.076 ($\pm$ 0.005)	0.072 ($\pm$ 0.005)
6	0.45 ($\pm$ 0.09)	0.27 ($\pm$ 0.08)	0.33 ($\pm$ 0.09)	0.096 ($\pm$ 0.004)	0.094 ($\pm$ 0.011)	0.089 ($\pm$ 0.007)
7	0.45 ($\pm$ 0.08)	0.28 ($\pm$ 0.04)	0.37 ($\pm$ 0.08)	0.085 ($\pm$ 0.007)	0.075 ($\pm$ 0.015)	0.074 ($\pm$ 0.013)

algorithms like ridge regression are often underestimated and therefore excluded from EMG decoding studies. Regularization methods impose a constraint to the model coefficients (i.e. control how large the coefficients are). This introduces the advantage of preventing overfitting and thus, of having a model with good generalization characteristics. This is highly desirable, especially in situations in which the decoder should be able to generalize to movements from which sufficient training data is not available. The results of the work presented here confirm our hypothesis that ridge regression generalizes to new EMG data better than the Kalman filter. Therefore, ridge regression constitutes a desirable algorithm for the continuous EMG decoding of upper limb kinematics.

Factors such as external interference, electrode shift and lift, electrode impedance changes, muscle fatigue, sweat and varying upper-limb positions alter the EMG signal distribution. Sources of variation like external interference can be mostly suppressed by filtering or electromagnetic shielding techniques. However, the remaining sources constitute a persistent issue in clinical practice and severely affect the performance of myoelectric decoders. In fact, we believe that in this particular study, one of the main factors affecting the performance stability could have been the variable positioning of the EMG electrodes from session-to-session since they were just placed within the general vicinity. A daily re-calibration phase was proposed as a solution to alleviate the effects of such non-stationarities. The additional time of re-calibrating the decoder and the cost of recording new data at the beginning of each session could be a concern for certain applications. Nevertheless, the performance comparisons between the three developed decoding schemes showed that there was a significant improvement in performance (a 14% increase in CC and a 8% reduction in NRMSE with respect to SS) when a re-calibration of the decoder was carried out. Moreover, the NRMSE values of the re-calibrated decoder were not significantly different from those achieved when training and testing the decoder with data from the same session (WS2 decoder). This implies that a re-calibration phase could reduce the error to the extent that the values would be just as low as if the decoder was trained using a larger amount of data only from the current session. It should also be mentioned that the calibration data length was 5 min, 1.5 min and 3 min for each task respectively and that it took a negligible amount of time to build the decoding model and choose the optimal regularization parameter, as opposed to other more complex algorithms. Therefore, the proposed approach was not very time and computationally demanding and served to significantly raise the performance. Nonetheless, the benefits and disadvantages of including a daily re-calibration phase should be carefully considered in order to choose the most suitable approach for each particular scenario.

The majority of recent studies in the field of myoelectric control interfaces are constrained to the decoding of a few distal or proximal DOFs. These devices could be employed for those cases in which impaired function of a few specific DOFs is present. However, the ability for interfaces to control multiple DOFs of the upper limb during dexterous and functional movements is necessary, especially for patients who are undergoing rehabilitation therapies for motor impairment of an entire extremity. Our protocol included the

decoding of coordinated multi-joint movements. While the NRMSE was stable at a very low value for all the DOFs, the lower CC values achieved for the distal DOFs might be due to the limited number of electrodes used for the decoding of distal DOFs. Extensors and flexor muscles of the forearm are often more difficult to target and it is usually hard to isolate the EMG activity from each recorded muscle. This makes the discrimination and decoding of individual finger movements more challenging. The minimum number of electrodes on the forearm that are necessary to attain an accurate decoding of distal DOF movements has been extensively investigated before [1], [4], [16], [17]. From the results presented in these previous studies, it can be concluded that a minimum of 12-16 electrodes are necessary to distinguish between multiple individual finger and wrist movements. Therefore, future studies should be performed with additional electrodes placed over the fore-arm in order to improve the decoding accuracy of distal DOFs.

V. Conclusion

This study addressed important aspects for the use of myoelectric control interfaces in clinical practice, which were: (i) the choice of a decoding algorithm with good generalization characteristics; (ii) the training procedure to follow in order to develop a decoder, which is robust to non-stationarities; and (iii) the decoding of coordinated distal and proximal DOF movements during complex functional tasks. From the results presented here, we concluded that a simple regularized algorithm such as ridge regression has good generalization characteristics for the EMG-based continuous decoding of multiple DOFs of the upper limb. Moreover, we demonstrated that by introducing a daily re-calibration phase the effects of the session-to-session non-stationarities could be significantly mitigated. Further studies including additional electrodes over the fore-arm should be performed in order to more accurately discriminate individual finger movements. Nevertheless, this pilot study is an important step towards the development of a robust myoelectric interface for the online control of coordinated multi-joint movements in robot-aided rehabilitation therapies.

Acknowledgment

This study was funded by the Baden-Württemberg Stiftung (GRUENS), the Indian-European collaborative research and technological development projects (INDIGO-DTB2-051), the Natural Science Fundation of China (NSFC 31450110072), EU COST action TD1006, Deutsche Forschungsgemeinschaft (DFG, Koselleck), Eva und Horst Köhler Stiftung, Volkswagen Stiftung and Bundes Ministerium für Bildung und Forschung BMBF MOTOR-BIC (FKZ 13GW0053). A. Sarasola-Sanz's work is supported by La Caixa-DAAD scholarship, E. López-Larraz's work by the Spanish projects HYPER-CSD2009-00067 and DGA-FSE (grupo T04) and N. Irastorza-Landa's work by the Basque Government and IKERBASQUE, Basque Foundation for Science, Bilbao, Spain.

References

[1] F. Tenore, A. Ramos, S. Fahmy, A.and Acharya, R. Etienne-Cummings, and N. Thakor, "Decoding of individuated finger movements using surface electromyography," *IEEE Transactions on Biomedical Engineering*, vol. 56, no. 5, pp. 1427 – 1434, 2009.

[2] S. W. Lee, K. Wilson, and D. Lock, B.A.and Kamper, "Subject-specific myoelectric pattern classification of functional hand movements for stroke survivors," *IEEE Transactions on Neural Systems and Rehabilitation Engineering*, vol. 19, no. 5, pp. 558 – 566, 2010.

[3] E. A. Corbett, E. J. Perreault, and K. P. Krding, "Mixture of time-warped trajectory models for movement decoding," *Advances in Neural Information Processing Systems 23 (NIPS)*, 2010.

[4] J. Hahne, F. BieBmann, N. Jiang, H. Rehbaum, D. Farina, F. Meinecke *et al.*, "Linear and nonlinear regression techniques for simultaneous and proportional myoelectric control," *IEEE Transactions on Neural Systems and Rehabilitation Engineering*, vol. 22, no. 2, pp. 269–279, 2014.

[5] R. Smith, F. Tenore, D. Huberdeau, R. Etienne-Cummings, and N. Thakor, "Continuous decoding of finger position from surface EMG signals for the control of powered prostheses." in *30th Annual International Conference of the IEEE Engineering in Medicine and Biology Society, EMBS*, 2008, pp. 197 – 200.

[6] P. Artemiadis and K. Kyriakopoulos, "A bio-inspired filtering framework for the EMG-based control of robots," *17th Mediterranean Conference on Control and Automation*, pp. 1155–1160, 2009.

[7] P. K. Artemiadis and K. J. Kyriakopoulos, "A switching regime model for the EMG-based control of a robot arm," *IEEE Transactions on Systems, Man, and Cybernetics*, vol. 41, no. 1, pp. 53–63, 2010.

[8] N. Sachs, E. Corbett, L. Miller, and E. Perreault, "Continuous movement decoding using a target- dependent model with EMG inputs," *Annual International Conference of the IEEE EMBC*, pp. 5432–5435, 2011.

[9] M. V. Liarokapis, P. K. Artemiadis, K. J. Kyriakopoulos, and E. S. Manolakos, "A learning scheme for reach to grasp movements: On EMG-based interfaces using task specific motion decoding models," *Biomedical and Health Informatics*, vol. 17, no. 5, pp. 915–921, 2013.

[10] A. Ramos-Murguialday, E. Garca-Cossio, A. Walter, W. Cho, D. Broetz, M. Bogdan, L. G. Cohen, and N. Birbaumer, "Decoding upper limb residual muscle activity in severe chronic stroke," *Annals of Clinical and Translational Neurology*, vol. 2, no. 1, pp. 1 – 11, 2015.

[11] M. Spüler, W. Rosenstiel, and M. Bogdan, "Adaptive SVM-based classification increases performance of a MEG-based brain-computer interface (BCI)," in *Artificial Neural Networks and Machine Learning–ICANN 2012*. Springer, 2012, pp. 669–676.

[12] A. E. Hoerl and R. W. Kennard, "Ridge regression: Biased estimation for nonorthogonal problems," *Technometrics*, vol. 12, no. 1, pp. 55–67, 1970.

[13] R. Kalman, "A new approach to linear filtering and prediction problems," *Journal of basic Engineering*, vol. 82, pp. 35 – 45, 1960.

[14] H. Zabaleta, D. Valencia, J. Perry, J. Veneman, and T. Keller, "Absolute position calculation for a desktop mobile rehabilitation robot based on three optical mouse sensors," *Annual International Conference of the IEEE Engineering in Medicine and Biology Society, EMBC*, pp. 2069 – 2072, 2011.

[15] M. Zecca, S. Micera, M. C. Carrozza, and P. Dario, "Control of multifunctional prosthetic hands by processing the electromyographic signal," *Critical Review in Biomedical Engineering*, vol. 30, pp. 4 – 6, 2002.

[16] S. Maier and P. van der Smagt, "Surface EMG suffices to classify the motion of each finger independently," *Proceedings of the International Conference of Motion and Vibration Control, MOVIC*, 2008.

[17] H. Daley, K. Englehart, L. Hargrove, and U. Kuruganti, "High density electromyography data of normally limbed and transradial amputee subjects for multifunction prosthetic control," *Journal of Electromyography and Kinesiology*, vol. 22, no. 3, pp. 478 – 484, 2012.

EMG Discrete Classification Towards a Myoelectric Control of a Robotic Exoskeleton in Motor Rehabilitation

N. Irastorza-Landa, A. Sarasola-Sanz, F. Shiman, E. López-Larraz, J. Klein, D. Valencia, A. Belloso, F.O. Morin, N. Birbaumer and A. Ramos-Murguialday

Abstract Myoelectric control constitutes a promising interface for robot-aided motor rehabilitation therapies. The development of accurate classifiers and suitable training protocols for this purpose are still challenging. In this study, eight healthy participants underwent electromyography (EMG) recordings while they performed reaching movements in four directions and five different hand movements wearing an exoskeleton on their right upper-limb. We developed an offline classifier based on a back-propagation artificial neural network (ANN) trained with the waveform length as time-domain feature extracted from EMG signals to classify discrete movements. A maximum overall classification performance of 75.54 % ± 5.17 and 67.37 % ± 8.75 were achieved for reaching and hand movements, respectively. We demonstrated that similar or better classification results could be achieved using a small number of electrodes placed over the main muscles involved in the movement instead of a large set of electrodes. This work is a first step towards a discrete decoding-based myoelectric control for a motor rehabilitation exoskeleton.

This study was funded by the GRUENS, the NSFC 31450110072, the DFG-Koselleck and the BMBF MOTOR-BIC (FKZ 13GW0053). A. Sarasola-Sanz's work is supported by the DAAD and N. Irastorza-Landa's work by the Basque Government.

N. Irastorza-Landa · A. Sarasola-Sanz · F. Shiman · E. López-Larraz · N. Birbaumer · A. Ramos-Murguialday (✉)
Institute of Medical Psychology and Behavioral Neurobiology,
University of Tübingen, Tubingen, Germany
e-mail: ander.ramos@med.uni-tuebingen.de

N. Irastorza-Landa
e-mail: nerea.irastorza-landa@medizin.uni-tuebingen.de

N. Irastorza-Landa · A. Sarasola-Sanz · F. Shiman
IMPRS for Cognitive and Systems Neuroscience, Tubingen, Germany

N. Irastorza-Landa
IKERBASQUE, Basque Foundation for Science, Bilbao, Spain

J. Klein · D. Valencia · A. Belloso · F.O. Morin · A. Ramos-Murguialday
TECNALIA, San Sebastian, Spain

J. Ibáñez et al. (eds.), *Converging Clinical and Engineering Research on Neurorehabilitation II*, Biosystems & Biorobotics 15,
DOI 10.1007/978-3-319-46669-9_29

1 Introduction

Myoelectric control constitutes a natural and intuitive interface for assistive and rehabilitative technologies for patients with motor impairment such as stroke patients. The development of kinematics-decoding models from electromyography still remains a challenge, especially in patients with an altered EMG activity. A dexterous EMG-based control of individual degrees of freedom (DoF) of an exoskeleton is therefore still a challenging approach. However, recent research findings classifying residual muscle activity related to motor intention during discrete movements in paralyzed limbs of chronic stroke patients suggest that EMG signals can be a promising source for the control of rehabilitation robots in these patients [1]. EMG classification of discrete movements during robot-aided motor rehabilitation tasks can serve as a way of coupling the motor intention reflected in the patients' residual EMG with the movement performed by the paralyzed limb. In this study we use ANNs for the discrete classification of upper-arm and hand/wrist movements using a reduced set of EMG electrodes. This work serves as a first step towards the implementation of a myoelectric control strategy for motor rehabilitation robots.

2 Materials and Methods

2.1 Experimental Protocol

Eight healthy right handed subjects (5 males, age 25 $\pm$ 2.74) were recruited for this study. Participants performed two different tasks while sitting and wearing a 7-DoF exoskeleton (Tecnalia, San Sebastian, Spain) on their right upper limb. Task A consisted of reaching movements (hand relaxed) from a predefined rest position towards four different goals indicated by targets of different colors around the workspace (see Fig. 1) and returning to the rest position. In task B, participants performed five hand/wrist movements: pronation, supination, pointing (index extension), cylindrical grasp and pinch grip. Each subject performed 50 reaching trials to each target and 30 trials of each hand/wrist movement. The timing of the tasks was instructed by imperative auditory cues and an inter-trial rest period was given to avoid fatigue. Ten bipolar Ag/AgCl electrodes from Myotronics-Noromed (Tukwila, WA, USA) were placed over the: (1) the abductor pollicis longus, (2) extensor carpi ulnaris, (3) extensor digitorium, (4) flexor carpi radialis, plamaris longus and flexor carpi ulnaris, (5) pronator teres, (6) long head of biceps, (7) external head of triceps, (8) anterior portion of deltoid, (9) lateral portion of deltoid and (10) posterior portion of deltoid. The ground monopolar electrode was placed over the right clavicle. The EMG signals were acquired at 2500 Hz using a bipolar amplifier (Brainproducts, Gilching, Germany). Kinematic data were acquired from the custom made exoskeleton at 18 Hz.

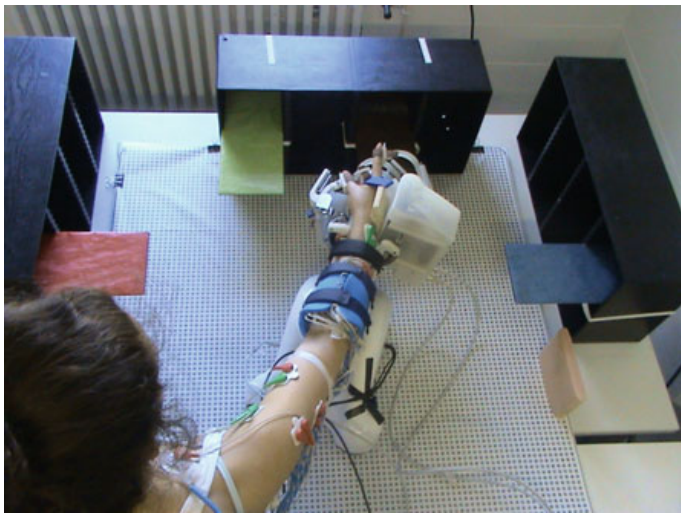

Fig. 1 A subject with EMG electrodes placed over the upper arm performing task A: starting from a predefined rest position, reaching movements towards four different directions indicated by targets of different colors (*red*, *green*, *brown*, *blue*) and return to rest position

2.2 Data Processing

The EMG signals were notch filtered, band-pass filtered between 10 Hz and 500 Hz using a 4th order butterworth filter and rectified. Kinematic data were low pass filtered at 1.5 Hz. EMG and kinematic data were synchronized offline and kinematic data were upsampled to the EMG data frequency. We epoched the EMG data recorded in task A in six classes based on the kinematic data: reaching movement towards four different directions (red, green, brown, blue targets), returning phase to rest position (returning trials from any target to the rest position were considered as a single class to simplify the future online control of the exoskeleton based on the classifier output) and resting phase (arm still at rest position). EMG data of task B were epoched into six classes: pronation, supination, pointing, grasping, pinch grip and resting phase (hand relaxed). Epoched EMG signals were baseline corrected and the waveform length (WL) feature was computed on sliding windows of 200 ms every 20 ms.

2.3 Classification Algorithm

ANNs have been broadly used for discrete decoding of upper arm, hand and individuated finger movements with high accuracies based on EMG [2], especially when using a high number of EMG electrodes [3]. Here we use an ANN classifier trained with the extracted WL feature for the pattern recognition of six movements (see Sect. 2.2). A multilayer perceptron (MLP) neural network was developed using a single hidden layer of three different numbers of nodes and the number of output neurons equal to the number of movements to be classified, six in each task type.

Two independent sets of networks were trained, validated and tested separately for the classification of movements of task A and B. Tan-sigmoid and softmax transfer functions were assigned for the hidden and output nodes, respectively, as commonly found in the literature [4]. The output neuron with the maximum probability value was selected as the classifier output. The network underwent training using the scaled conjugate gradient backpropagation algorithm. We used three different subsets of electrodes for movement classification: (i) all the electrodes (1–10), (ii) electrodes over muscles mainly involved in the movements following neurophysiology (6–10 for task A, 1-6 for task B), (iii) electrodes over muscles not involved in the movements (1–5 for task A, 7–10 for task B). For each task type and electrode set combination case, an inner fivefold cross validation (CV) was performed to find the best network parameters (i.e. number of nodes in the hidden layer) by searching the network with minimum validation mean square error results among all the networks trained for such case. The networks were trained using the best parameters and tested on a separate test dataset in an outer fivefold CV. The reported performance of the classifier was computed as the mean and standard deviation of the percentage of true positives (i.e. data points correctly classified) obtained with networks trained over the fivefolds to classify the independent test set in the outer CV.

3 Results

The mean and standard deviation of the classification success rate achieved for the 8 subjects in the classification of movements of task A and B are summarized in Table 1. The table presents the performance of the classifiers for each combination of task type and electrode set for classification and the chance level in each classification case.

Table 1 Classification success rates in %

Task	Electrodes placed over			
	All muscles	Muscles involved	Muscles not involved	Chance level
A	75.54 ± 5.17	73.63 ± 5.86	52.23 ± 5.54	16.7 %
B	66.74 ± 6.83	67.37 ± 8.75	39.42 ± 3.67	16.7 %

4 Discussion and Conclusions

In this work we show that it is possible to classify six functional arm and hand movements in healthy participants with accuracies above 67 % based on the EMG activity from six EMG bipolar electrodes only. Similar or better classification results could be achieved using only a small number of electrodes placed over the muscles mainly involved in the movement execution instead of a large set of electrodes. This finding suggests that a combination in parallel of these two classifiers could allow classifying upper-limb movements involving fore- and upper-arm muscles simultaneously. However, more data and further analysis are needed to prove this speculation since muscle activity changes depending on posture, substantially more in stroke patients [5], and online classification presents additional issues such as time delays.

Our future work will focus on the design and development of classifiers for fore- and upper-arm combined movements, the classification of residual EMG activity of stroke patients and the online implementation and testing of the classifier in a real-time scenario for the online electromyographic control of the rehabilitation exoskeleton.

References

1. A. Ramos-Murguialday, E. García-Cossio, A. Walter, W. Cho, D. Broetz, M. Bogdan, L.G. Cohen, N. Birbaumer, Detecting paretic arm motion intention through muscle activity decoding in severe chronic stroke. Ann. Clin. Transl. Neurol. **2**(1), 1–11 (2015). PMC. Web. 15 April 2016
2. M. Ison, P. Artemiadis, Beyond user-specificity for EMG decoding using multiresolution muscle synergy analysis. Conference: ASME 2013 Dynamic Systems and Control Conference, At Palo Alto, California (2013). doi:10.1115/DSCC2013-4070
3. F. Tenore, A. Ramos, A. Murguialday, A. Fahmy, R. Etienne-Cummings, N.V. Thakor, Towards real-time control of individuated finger movements using surface myoelectric signals. IEEE T Biomed. Eng. **56**(5), 1427 (2009)
4. F.H.Y. Chan, Y.-S. Yang, F.K. Lam, Y.-T. Zhang, P.A. Parker, Fuzzy EMG classification for prosthesis control. IEEE Trans. Rehab. Eng. **8**(3), 305–311 (2000)
5. E. García-Cossio, N. Birbaumer, A. Ramos-Murguialday, acilitation of completely paralyzed forearm muscle activity in chronic stroke patients, in *2013 6th International IEEE/EMBS Conference on Neural Engineering (NER)*, San Diego, CA, 2013, pp. 1545–1548

Hindawi Publishing Corporation
Advances in Human-Computer Interaction
Volume 2013, Article ID 369425, 9 pages
http://dx.doi.org/10.1155/2013/369425

Review Article

Controlling Assistive Machines in Paralysis Using Brain Waves and Other Biosignals

Paulo Rogério de Almeida Ribeiro,[1,2,3] Fabricio Lima Brasil,[1,2,4] Matthias Witkowski,[1,2] Farid Shiman,[1,2] Christian Cipriani,[5] Nicola Vitiello,[5] Maria Chiara Carrozza,[5] and Surjo Raphael Soekadar[1,2]

[1] *Institute of Medical Psychology and Behavioral Neurobiology and MEG Center, University of Tübingen, Silcherstraße 5, 72076 Tübingen, Germany*
[2] *Applied Neurotechnology Lab, Department of Psychiatry and Psychotherapy, University of Tübingen, Calwerstraße 14, 72076 Tübingen, Germany*
[3] *International Max Planck Research School for Neural Information Processing, Österbergstraße 3, 72074 Tübingen, Germany*
[4] *International Max Planck Research School for Neural & Behavioral Sciences, Österbergstraße 3, 72074 Tübingen, Germany*
[5] *The BioRobotics Institute, Scuola Superiore Sant'Anna, V.le R. Piaggio 34, 56025 Pontedera, Italy*

Correspondence should be addressed to Surjo Raphael Soekadar; surjo.soekadar@uni-tuebingen.de

Received 9 January 2013; Accepted 24 April 2013

Academic Editor: Christoph Braun

The extent to which humans can interact with machines significantly enhanced through inclusion of speech, gestures, and eye movements. However, these communication channels depend on a functional motor system. As many people suffer from severe damage of the motor system resulting in paralysis and inability to communicate, the development of brain-machine interfaces (BMI) that translate electric or metabolic brain activity into control signals of external devices promises to overcome this dependence. People with complete paralysis can learn to use their brain waves to control prosthetic devices or exoskeletons. However, information transfer rates of currently available noninvasive BMI systems are still very limited and do not allow versatile control and interaction with assistive machines. Thus, using brain waves in combination with other biosignals might significantly enhance the ability of people with a compromised motor system to interact with assistive machines. Here, we give an overview of the current state of assistive, noninvasive BMI research and propose to integrate brain waves and other biosignals for improved control and applicability of assistive machines in paralysis. Beside introducing an example of such a system, potential future developments are being discussed.

1. Introduction

The way humans interact with computers has changed substantially in the last decades. While, for many years, the input from the human to the machine was mainly managed through keystrokes, then later through hand movements using a computer mouse, other potential input sources have been opened up allowing more intuitive and effortless control, for example, based on speech [1], gestures [2], or eye movements [3], all depending on a functional motor system.

As cardiovascular diseases increase and people live longer, an increasing number of people suffer from conditions that affect their capacity to communicate or limit their mobility [4], for example, due to stroke, neurodegenerative disorders, or hereditary myopathies. Motor disability can also result from traumatic injuries, affecting the central or peripheral nervous system or can be related to amputations of the upper or lower extremities. While these handicapped people would benefit the most from assistive machines, their capacity to interact with computers or machines is often severely impeded.

Among the most important causes of neurological disabilities resulting in permanent damage and reduction of

motor functions or the ability to communicate are stroke, multiple sclerosis (MS), spinal cord injury (SCI), brachial plexus injury (BPI), and neurodegenerative diseases, such as amyotrophic lateral sclerosis (ALS) or dementia [4].

Stroke is the leading cause of long-term disability in adults and affects approximately 20 million people per year worldwide [5, 6]. Five millions remain severely handicapped and dependent on assistance in daily life [4]. Nearly 30% of all stroke patients are under the age of 65 [7]. Other diseases resulting in paralysis at such early age include MS, affecting more than 2.5 million people worldwide [8], or SCI with 12.1 to 57.8 cases per million [9, 10]. BPI, the disruption of the upper limb nerves leading to a flaccid paralysis of the arm, affects thousands of people every year [11]. Furthermore, every year there are approximately 2,000 new traumatic upper limb amputations in Europe [12].

While there is major progress in the development of assistive apparatuses built for instance to compensate for a lost or paralyzed limb for example, lightweight and versatile prostheses or exoskeletons [13–16], intuitive and reliable control of such devices is an enormous challenge.

Previous surveys on the use of artificial hands revealed that up to 50% of the amputees are not using their prosthetic hand regularly, mainly due to low functionality, poor cosmetic appearance, and low controllability [17].

Since early on, the use of electromyographic (EMG) signals for prosthetic control, for example, from the amputee's stump or contralateral chest muscles, was an important concept [18, 19]. However, its broader success is still limited due to many practical reasons that are valid for all assistive systems that depend on recording biosignals, primarily the effort and costs to provide good signal quality, a fast and effective calibration process, and, last but not least, the benefit of the system in the user's everyday life. Furthermore, increasing the signal-to-noise ratio or the specificity of such recordings by means of techniques such as the electric nerve stimulation [20] is possible but increases the overall system complexity [21]. Adding sensory qualities during utilization of prosthetic devices increasing the bidirectional interaction between users and the machine improves the functionality of assistive systems [22]. Here, however, the same limitation applies as to the motor domain that the majority of such systems depend on an intact peripheral sensory system.

Thus, the development and provision of assistive machines that are independent of the peripheral nervous system's integrity represent a promising and appealing perspective, particularly, if controlled intuitively and without requiring extensive training to gain reliable control.

2. Brain-Computer and Brain-Machine Interfaces: A General Overview

Since it was discovered that brain waves contain information about cognitive states [23, 24] and can be functionally specific [25, 26], the idea to use such signals for direct brain control of assistive machines became a major driving force for the development of the so-called brain-computer or brain-machine interfaces (BCI/BMI) [27]. Such interfaces allow direct translation of electric or metabolic brain activity into control signals of external devices or computers bypassing the peripheral nervous and muscular system.

Table 1: Categories of brain-computer and brain-machine interfaces.

Based on: **recording site of brain signals**	
Brain signal used	*Recording technique*
Invasive	
Single spike	Single cell recordings
Multiunit activity	Multiunit arrays (MUA)
Local field potentials (LFP)	Electrocorticogram (ECoG)
Noninvasive	
Electric brain potentials	Electroencephalography (EEG)
Neuromagnetic fields	Magnetoencephalography (MEG)
BOLD	Functional magnetic resonance imaging (fMRI)
Oxy/deoxyhemoglobin	Near-infrared spectroscopy (NIRS)
Based on: **mode of operation**	
Active	Asynchronous control
	Synchronous control
Reactive	N.A.
Passive	N.A.
Based on: **purpose**	
Assistive/biomimetic	Restorative/biofeedback
Used for restoration of	*Tested in the treatment of*
Communication	Stroke
Paralysis	Chronic pain
	Tinnitus
	Dementia
	Depression
	Schizophrenia

As neural or metabolic brain activity can be recorded from sensors inside or outside the brain, BCI/BMI is categorized as invasive or noninvasive systems [28]. Other categorizations relate to the specific brain signal used for BCI/BMI control or the mode of operation (see Table 1).

Invasively recorded brain signals that were successfully used for BCI/BMI control include single-spike or multiunit activity and local field potentials (LFP) [29]. These signals are necessarily recorded from inside the skull, while electric or magnetic brain oscillations reflecting pattern formation of larger cell assemblies' activity [30] can also be recorded from outside the skull using electro- or magnetoencephalography (EEG/MEG). Each method offers access to specific unique properties of brain activity [31]. These noninvasive techniques allow, for example, detection and translation of slow cortical potentials (SCP), changes of sensorimotor rhythms (SMR), or event-related potentials (ERP), for example, the P300, translating them into control signals for external devices or computers. More recently, online interpretation of changes in metabolic brain activity [32, 33] was introduced for BCI/BMI application offering high spatial (in the range of mm), but low temporal, resolution (in the range of seconds). These systems

use functional magnetic resonance imaging (fMRI) [32] or near-infrared spectroscopy (NIRS) [33, 34], both measuring changes in brain tissue's blood-oxygenation-level dependent (BOLD) signals.

In 1969, Fetz demonstrated that single neurons in precentral cortex can be operantly conditioned by delivery of food pellets [35]. Since then, operant conditioning of cortical activity was demonstrated in various paradigms [36], requiring, though, opening of the skull and insertion of electrodes into the brain with the risk of bleedings and infections [37, 38]. An intermediate, semiinvasive approach uses LFP recorded by epidural electrocorticography (ECoG) [29, 39]. LFP reflects neural activity of an area of up to 200 μm^2 comprising hundreds of thousands of neurons with numerous local recurrent connections and connections to more distant brain regions [40], while brain oscillations recorded noninvasively (e.g., using EEG or MEG) contain information of millions of neurons [41].

To control assistive devices or machines in paralysis, the following noninvasively recorded neurophysiologic signals were successfully used up to now: (1) slow cortical potentials (SCP) [42, 43], (2) sensorimotor rhythms (SMRs) and its harmonics [44, 45], and (3) event-related potentials (ERPs), for example, P300 [46].

The use of SCP in BCI/BMI applications goes back to Birbaumer and his coworker's work in the late 1970s showing that operant control of SCPs (slow direct-current shifts occurring event-related after 300 ms to several seconds) is possible while exhibiting strong and anatomically specific effects on behavior and cognition [47–49]. A tight correlation of central SCPs and blood-oxygen level-dependent (BOLD) signals in the anterior basal ganglia and premotor cortex was found [50] suggesting a critical role of the basal ganglia-thalamo-frontal network for operant control of SCP.

In contrast to SCPs, SMRs are recorded over the sensorimotor cortex usually at a frequency between 8 and 15 Hz. In analogy to the occipital alpha and visual processing [51], the SMR (or rolandic alpha) shows a clear functional specificity, disappearing during planned, actual, or imagined movements [52]. Accordingly, a close association with functional motor inhibition of thalamocortical loops was suggested [53]. Depending on the context, the SMR is also called μ-rhythm [54] or rolandic alpha and was extensively investigated by the Pfurtscheller group in Graz [55] and the Wolpaw group in Albany [56, 57].

Another well-established and tested BCI/BMI controller is the P300-based ERP-BCI introduced by Farwell and Donchin [58]. While SCP- and SMR-controls are learned through visual and auditory feedback often requiring multiple training sessions before reliable control is achieved, the P300-BCI needs no training at all. While, in the classical P300-ERP-BCI paradigm, the user focuses his attention to a visual stimulus, other sensory qualities such as tactile [59] or auditory stimuli [60, 61] were successfully implemented in ERP-BCI. Information rates of ERP-BCI can reach 20–30 bits/min: [62].

In terms of operation mode, active, passive, and reactive BCI/BMI applications can be distinguished [63]. While active and reactive BCI/BMI require the user's full attention to generate voluntary and directed commands, passive BCI/BMI relates to the concept of cognitive monitoring introducing the assessment of the users' intentions, situational interpretations, and emotional states [64].

In active BCI/BMI applications, two forms of control can be distinguished: synchronous and asynchronous control [65]. In synchronous control, translation of brain activity follows a fixed sequence or cue. The user is required to be fully attentive, while in asynchronous or uncued control, a specific brain signal is used to detect the user's intention to engage in BCI/BMI control [65, 66].

3. Brain-Machine Interfaces in Neurorehabilitation of Paralysis

BMI used in neurorehabilitation follows two different strategies: while assistive or biomimetic BMI systems strive for continuous high-dimensional control of robotic devices or functional electric stimulation (FES) of paralyzed muscles to substitute for lost motor functions in a daily life environment [67–69], restorative or biofeedback BMI systems aim at normalizing of neurophysiologic activity that might facilitate motor recovery [70–74]. Insofar, restorative or biofeedback BMI can be considered as "training-tools" to induce use-dependent brain plasticity increasing the patient's capacity for motor learning [44, 75].

These two approaches derive from different research traditions and are not necessarily related to the invasiveness of the approach: in the early 80s of the last century, decoding of different movement directions from single neurons was successfully demonstrated [76]. Since then, reconstruction of complex movements from neuronal activity was pursued, using both invasive and noninvasive methods.

Firing patterns acquired through single cell recordings from the motor cortex [77] or parietal neuronal pools [78] in animals were remarkably successful for reconstruction of movement trajectories. Monkeys learned to control computer cursors towards moving targets on a screen activating neurons in motor, premotor, and parietal motor areas. It was shown that 32 cells were sufficient to move an artificial arm and perform skillful reaching movements enabling a monkey to feed himself [67]. Learned control of movements based on single cell activity was also shown using neurons outside the primary or secondary motor representations [79]. In 2006, successful implantation of densely packed microelectrode arrays in two quadriplegic human patients was demonstrated, enabling them to use LFP in order to move a computer cursor in several directions [68]. Most recently, a study using two 96-channel intracortical microelectrodes placed in the motor cortex of a 52-year-old woman with tetraplegia demonstrated robust seven-dimensional movements of a prosthetic limb [80].

In contrast to this work aiming at assistive appliance of invasive and noninvasive BMI technology, the development of restorative/biofeedback BMI systems is tightly associated with the development and successes of neurofeedback (NF) and its use to purposefully upregulate or downregulate brain activity—a quality that showed to have some beneficial effect

in the treatment of various neurological and psychiatric disorders associated with neurophysiologic abnormalities [71]. In NF, subjects receive visual or auditory online feedback of their brain activity and are asked to voluntarily modify, for example, a particular type of brainwave. Successful modification becomes contingently rewarded. NF was successfully used in the treatment of epilepsy [81, 82], ADHD [83–85], chronic pain syndrome [86]. The rational to use this approach in the context of neurorehabilitation is based on data indicating that stroke patients with best motor recovery are the ones in whom ipsilesional cortical function is closer to that found in healthy controls [87]. A negative correlation between impairment and activation in ipsilesional M1 during hand motions has been documented [88]. Thus, a larger clinical study was performed at the University of Tübingen in Germany and the National Institute of Neurological Disorders and Stroke (NINDS, NIH) in USA with over 30 chronic stroke patients testing the hypothesis that augmentation of ipsilesional brain activity would improve motor recovery [89, 90]. In this study, all participating patients suffered from complete hand paralysis and were unable, for example, to grasp. The study showed that one month of daily ipsilesional BMI training combined with goal-directed physiotherapy resulted in significant motor improvements, while random BMI-feedback did not. Further analysis of neurophysiological parameters indicated that motor evoked potentials (MEP) from the ipsilesional hemisphere reflecting the integrity of the corticospinal tract could predict motor recovery of the trained patients [91]. Currently, further improvements of this training paradigm, for example, related to the feedback or specificity and effectiveness of training [44], for example, using electric brain stimulation to enhance neuroplasticity [92], are being tested.

4. Noninvasive Assistive Brain-Machine Interfaces in Paralysis

Both invasive and noninvasive BCI and BMI found their way into assistive systems, for example, allowing communication in locked-in patients [42] or restoration of movement in patients with paralysis [28, 93]. The Graz group was the first to use volitional SMR modulation for control of electric stimulation of a quadriplegic patient's paralyzed hand [69, 94]. While the patient imagined a movement, the associated modulation of SMR was translated into functional electric stimulation (FES) of his upper limb muscles resulting in grasping motions. After this proof-of-concept study, numerous publications addressed the different aspects that are important to allow intuitive and seamless control of biomimetic devices [20] or FES [95] in a daily life environment [96]. While many challenges were successfully mastered in the last years, three major aspects were not satisfyingly solved yet: (1) intuitive, asynchronous BCI/BMI control, (2) 100% reliability, and (3) unambiguous superiority (in terms of information transfer rate, ITR, and necessary preparation effort) over the use of other biosignals (e.g., related to speech, gestures, or eye movements).

These aspects do not apply to BCI use for communication in complete paralysis, for example, complete locked-in-state (CLIS) in ALS, as no asynchronous mode is necessary, reliability is secondary, and no other biosignals are available anymore [97].

A system that is unreliable in daily does not only limit its practicality, but limits its practicality, but would be also associated with ethical difficulties [98, 99]. While there are good arguments suggesting that invasive BCI/BMI can provide a higher ITR [100], it is still unclear how much meaningful information, for example, for reconstruction of hand movements, can be extracted from noninvasively recorded brain signals [101]. Recently, work by Contreras-Vidal's group at the University of Houston suggested that slow-frequency EEG (oscillations with a frequency of up to 4 Hz) might provide as much information as invasive recordings [102, 103], for example, for reconstruction of three-dimensional hand movements [103]. Currently, implementation of this approach in closed-loop paradigms is being pursued. Nevertheless, it is conceivable that the only viable solution to satisfyingly solve those three aspects will be the inclusion of other biosignals into a system merging different biosignal sources to detect user's intentions and integrating this information into the current context of the user to further increase intuitive control and assure reliability of the system. Such systems that merge brain control with other biosignals were recently summarized under the term "brain-neural computer interaction" (BNCI) systems receiving notable funding through the 7th Framework Program for Research and Technological Development (FP7) of the European Union.

Particularly promising in this context is integrating eye movements using electrooculography (EOG) or eye tracking into prosthetic control. At the University of Tübingen, a first prototype system was conceptualized that allows asynchronous BCI/BMI control while solving the reliability issue by using eye tracking, EOG, and computer vision-based object recognition. A computer equipped with a 3D camera recognizes objects placed on a table. The system detects when the user fixates any of the objects recognized as graspable, for example, a cup or ball. Once an object is fixated with the eyes, the BCI/BMI mode switches on, detecting whether the user wants to grasp the object. A robotic hand or exoskeleton (both developed by the BioRobotics Institute, Scuola Superiore Sant'Anna, Pisa, Italy) performs the grasping motion (Figure 1). The motion becomes interrupted if the user does not fixate the object anymore as measured by eye tracking and EOG (see Figure 2). This assures that no action of the system depends exclusively on brain wave control that might be susceptible to inaccuracies. Such system, integrating perceptual and contextual computing developed in the field of human-computer interaction (HCI) research into BCI applications, promises to overcome many limitations of brain control alone, mainly the reliability issue, likewise broadening the repertoire of modern HCI research to infer user state and intention from brain activity.

As trauma or stroke can affect motor and body functions very differently in each individual, proper and fast calibration for inclusion into seamless BNCI control is often impeded. Thus, inclusion of eye movements is the most promising biosignal in this context so far. Particularly as visual interaction plays a key role when planning, executing, and

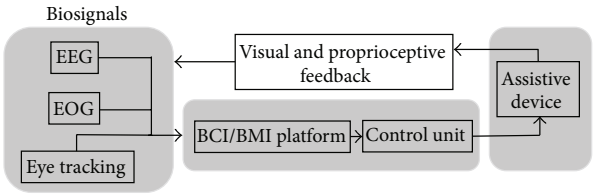

Figure 1: Organization of the University of Tübingen' prototype system controlling assistive devices using brain waves and eye movements.

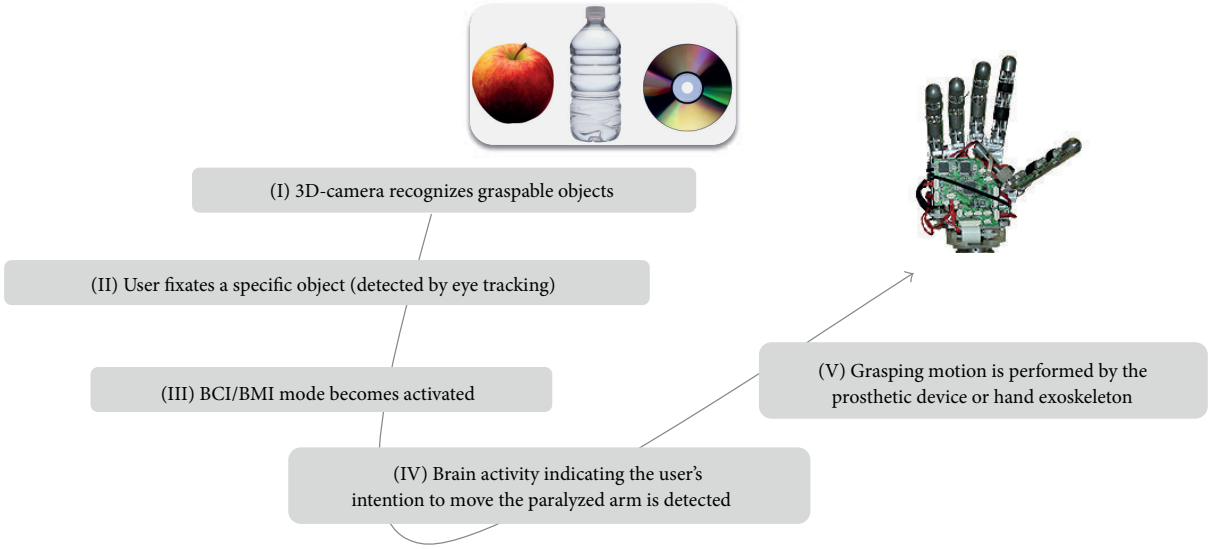

Figure 2: Illustration of the processing chain for performing grasping motions of an assistive system using brain waves and eye movements. The grasping motion stops once the user does not fixate the object with his eyes anymore.

adapting motor control. Beside electric biosignals such as EOG and EMG, other measures that can be used for BNCI control include magnetic, mechanic, optic, acoustic, chemical, and thermal biosignals. These biosignals, however, are more susceptible for artifacts and exhibit larger variability depending on the environmental conditions. Future research, however, might find novel ways to advantageously include such biosignals into BNCI control and application.

The organisms' behavior measurable in these various biosignals reflects conscious and unconscious processes that can be inferred and purposefully used for BNCI control. In case of eye movement control, changing fixation of an object can point to inattention, distraction, or volitional (conscious) act to interrupt unwanted output of the BNCI for example.

Practicality of such approach is limited when, for instance, eyesight or eyeball control is impaired due to a disease or trauma. This can be the case in multiple sclerosis, traumatic brain injury, stroke, or neurodegenerative disorders such as ALS. ALS may lead to CLIS, where classical semantic conditioning might be the only way to sustain a communication channel [104] while inclusion or use of other biosignals seemed not particularly helpful [94]. Also, inclusion of other biosignals often increases preparation time for placing and calibrating the required biosensors further limiting practicality. This is particularly relevant when the system requires handicapped persons to place and handle the sensors in a home environment. Nevertheless, these technical limitations might dissolve in the course of near-future research and development.

An important conceptual advantage of including other biosignals into BCI control relates to the improved reliability, which not only increases usability in daily life, but also the degree of self-efficacy, a dimension that should not be underestimated in acceptance of such technology, but also in the context of restorative/biofeedback BCI training for example. Here, the fact that a patient experiences full control of a completely paralyzed limb might facilitate overcoming "learned nonuse" and motivate the user to engage in behavioral physiotherapy [105].

5. Conclusion

BCI/BMI systems promise to enhance applicability of assistive technology in humans with a compromised or damaged motor system. While information transfer rates of noninvasive BCI/BMI are sufficient for communication, for example, in locked-in-state, versatile control of prosthetic devices

using brain waves will require major research and development efforts to provide intuitive, asynchronous control sufficiently reliable in daily life environments. Many reasons suggest that using the combination of brain waves with other biosignals might entail many attractive solutions to control assistive, noninvasive technology even after severe damage of the central or peripheral nervous system.

Authors' Contribution

Paulo Rogério de Almeida Ribeiro and Fabricio Lima Brasil contributed equally to this work.

Acknowledgments

This work was supported by the EU Project WAY FP7-ICT-2011-288551, the Italian Project AMULOS (Industria 2015, MI01 00319), the Regional Project EARLYREHAB (Regione Toscana, Health Regional Research Programme 2009), the German Federal Ministry of Education and Research (BMBF, 01GQ0831, and 16SV5840), and the Deutsche Forschungsgemeinschaft (DFG SO932-2), Open Access Publishing Fund of the University of Tübingen, as well as CNPq/DAAD (National Council for Scientific and Technological Development—Brazil; German Academic Exchange Service—Germany) scholarships.

References

[1] S. Furui, "50 years of progress in speech and speaker recognition research," *ECTI Transactions on Computer and Information Technology*, vol. 1, no. 2, p. 64, 2005.

[2] H. S. Yoon, J. Soh, Y. J. Bae, and H. Seung Yang, "Hand gesture recognition using combined features of location, angle and velocity," *Pattern Recognition*, vol. 34, no. 7, pp. 1491–1501, 2001.

[3] M. R. Ahsan, M. I. Ibrahimy, and O. O. Khalifa, "EMG signal classification for human computer interaction: a review," *European Journal of Scientific Research*, vol. 33, no. 3, pp. 480–501, 2009.

[4] W. H. O., *World report on disability*: World Health Organization, 2011.

[5] N. S. Ward and L. G. Cohen, "Mechanisms underlying recovery of motor function after stroke," *Archives of Neurology*, vol. 61, no. 12, pp. 1844–1848, 2004.

[6] S. MacMahon, "Introduction: the global burden of stroke," in *Clinician's Manual on Blood Pressure and Stroke Prevention*, J. Chalmers, Ed., pp. 1–6, Science Press, London, UK, 2002.

[7] N. I. O. N. Disorders and Stroke, *Stroke: hope through research*, National Institute of Neurological Disorders and Stroke, National Institutes of Health, 1999.

[8] T. C. Frohman, D. L. O'Donoghue, and D. Northrop, *A Practical Primer: Multiple Sclerosis for the Physician Assistant*, Southwestern Medical Center, Dallas, Tex, USA, 2011.

[9] F. W. A. Van Asbeck, M. W. M. Post, and R. F. Pangalila, "An epidemiological description of spinal cord injuries in The Netherlands in 1994," *Spinal Cord*, vol. 38, no. 7, pp. 420–424, 2000.

[10] F. Martins, F. Freitas, L. Martins, J. F. Dartigues, and M. Barat, "Spinal cord injuries—epidemiology in Portugal's central region," *Spinal Cord*, vol. 36, no. 8, pp. 574–578, 1998.

[11] W. Pondaag, M. J. A. Malessy, J. G. Van Dijk, and R. T. W. M. Thomeer, "Natural history of obstetric brachial plexus palsy: a systematic review," *Developmental Medicine & Child Neurology*, vol. 46, no. 2, pp. 138–144, 2004.

[12] S. Banzi, E. Mainardi, and A. Davalli, "Analisi delle strategie di controllo per protesi di arto superior in pazienti con amputazioni transomerali o disarticolati di spalla," in *Biosys, ANIPLA*, pp. 290–300, 2005.

[13] J. L. Pons, "Rehabilitation exoskeletal robotics. The promise of an emerging field," *IEEE Engineering in Medicine and Biology Magazine*, vol. 29, no. 3, pp. 57–63, 2010.

[14] N. Vitiello, T. Lenzo, S. Roccella et al., "NEUROExos: a powered elbow exoskeleton for physical rehabilitation," *IEEE Transactions on Robotics*, vol. 29, no. 1, pp. 220–235, 2013.

[15] A. Chiri, N. Vitiello, F. Giovacchini, S. Roccella, F. Vecchi, and M. C. Carrozza, "Mechatronic design and characterization of the index finger module of a hand exoskeleton for post-stroke rehabilitation," *IEEE/ASME Transactions on Mechatronics*, vol. 17, no. 5, pp. 884–894, 2012.

[16] J. Iqbal, N. G. Tsagarakis, A. E. Fiorilla, and D. G. Caldwell, "A portable rehabilitation device for the hand," in *Proceedings of the 32nd Annual International Conference of the IEEE Engineering in Medicine and Biology Society (EMBC '10)*, pp. 3694–3697, September 2010.

[17] D. J. Atkins, D. C. Y. Heard, and W. H. Donovan, "Epidemiologic overview of individuals with upper-limb loss and their reported research priorities," *Journal of Prosthetics and Orthotics*, vol. 8, no. 1, pp. 2–11, 1996.

[18] B. Peerdeman, D. Boere, H. Witteveen et al., "Myoelectric forearm prostheses: state of the art from a user-centered perspective," *Journal of Rehabilitation Research and Development*, vol. 48, no. 6, pp. 719–737, 2011.

[19] M. Zecca, S. Micera, M. C. Carrozza, and P. Dario, "Control of multifunctional prosthetic hands by processing the electromyographic signal," *Critical Reviews in Biomedical Engineering*, vol. 30, no. 4-6, pp. 459–485, 2002.

[20] R. Rupp and H. J. Gerner, "Neuroprosthetics of the upper extremity—clinical application in spinal cord injury and challenges for the future," in *Operative Neuromodulation*, vol. 97 of *Acta Neurochirurgica Supplements*, pp. 419–426, 2007.

[21] A. Fougner, O. Stavdahl, P. J. Kyberd, Y. G. Losier, and P. A. Parker, "Control of upper limb prostheses: terminology and proportional myoelectric control—a review," *IEEE Transactions on Neural Systems and Rehabilitation Engineering*, vol. 20, no. 5, pp. 663–677, 2012.

[22] D. J. Weber, R. Friesen, and L. E. Miller, "Interfacing the somatosensory system to restore touch and proprioception: essential considerations," *Journal of Motor Behavior*, vol. 44, no. 6, pp. 403–418, 2012.

[23] W. J. Ray and H. W. Cole, "EEG alpha activity reflects attentional demands, and beta activity reflects emotional and cognitive processes," *Science*, vol. 228, no. 4700, pp. 750–752, 1985.

[24] W. Klimesch, "EEG alpha and theta oscillations reflect cognitive and memory performance: a review and analysis," *Brain Research Reviews*, vol. 29, no. 2-3, pp. 169–195, 1999.

[25] G. E. Chatrian, M. C. Petersen, and J. A. Lazarte, "The blocking of the rolandic wicket rhythm and some central changes related to movement," *Electroencephalography and Clinical Neurophysiology*, vol. 11, no. 3, pp. 497–510, 1959.

[26] E. G. Walsh, "'Visual attention' and the alpha-rhythm," *The Journal of Physiology*, vol. 120, no. 1-2, pp. 155–159, 1953.

[27] J. R. Wolpaw, N. Birbaumer, D. J. McFarland, G. Pfurtscheller, and T. M. Vaughan, "Brain-computer interfaces for communication and control," *Clinical Neurophysiology*, vol. 113, no. 6, pp. 767–791, 2002.

[28] N. Birbaumer, "Breaking the silence: brain-computer interfaces (BCI) for communication and motor control," *Psychophysiology*, vol. 43, no. 6, pp. 517–532, 2006.

[29] G. Schalk and E. C. Leuthardt, "Brain-computer interfaces using electrocorticographic signals," *IEEE Reviews in Biomedical Engineering*, vol. 4, pp. 140–154, 2011.

[30] F. Lopes da Silva, "Neural mechanisms underlying brain waves: from neural membranes to networks," *Electroencephalography and Clinical Neurophysiology*, vol. 79, no. 2, pp. 81–93, 1991.

[31] J. Malmivuo, "Comparison of the properties of EEG and MEG in detecting the electric activity of the brain," *Brain Topography*, vol. 25, no. 1, pp. 1–19, 2012.

[32] N. Weiskopf, R. Veit, M. Erb et al., "Physiological self-regulation of regional brain activity using real-time functional magnetic resonance imaging (fMRI): methodology and exemplary data," *NeuroImage*, vol. 19, no. 3, pp. 577–586, 2003.

[33] R. Sitaram, H. Zhang, C. Guan et al., "Temporal classification of multichannel near-infrared spectroscopy signals of motor imagery for developing a brain-computer interface," *NeuroImage*, vol. 34, no. 4, pp. 1416–1427, 2007.

[34] T. Nagaoka, K. Sakatani, T. Awano et al., "Development of a new rehabilitation system based on a brain-computer interface using near-infrared spectroscopy," in *Oxygen Transport to Tissue XXXI*, vol. 662 of *Advances in Experimental Medicine and Biology*, pp. 497–503, 2010.

[35] E. E. Fetz, "Operant conditioning of cortical unit activity," *Science*, vol. 163, no. 3870, pp. 955–958, 1969.

[36] E. E. Fetz, "Volitional control of neural activity: implications for brain-computer interfaces," *The Journal of Physiology*, vol. 579, no. 3, pp. 571–579, 2007.

[37] E. Behrens, J. Schramm, J. Zentner, and R. König, "Surgical and neurological complications in a series of 708 epilepsy surgery procedures," *Neurosurgery*, vol. 41, no. 1, pp. 1–10, 1997.

[38] A. M. Korinek, J. L. Golmard, A. Elcheick et al., "Risk factors for neurosurgical site infections after craniotomy: a critical reappraisal of antibiotic prophylaxis on 4578 patients," *British Journal of Neurosurgery*, vol. 19, no. 2, pp. 155–162, 2005.

[39] D. Moran, "Evolution of brain-computer interface: action potentials, local field potentials and electrocorticograms," *Current Opinion in Neurobiology*, vol. 20, no. 6, pp. 741–745, 2010.

[40] J. Linke, S. H. Witt, A. V. King et al., "Genome-wide supported risk variant for bipolar disorder alters anatomical connectivity in the human brain," *NeuroImage*, vol. 59, no. 4, pp. 3288–3296, 2012.

[41] D. Turner, P. Patil, and M. Nicolelis, "Conceptual and technical approaches to human neural ensemble recordings," in *Methods for Neural Ensemble Recordings*, M. A. L. Nicolelis, Ed., Boca Raton, Fla, USA, 2nd edition, 2008.

[42] N. Birbaumer, N. Ghanayim, T. Hinterberger et al., "A spelling device for the paralysed," *Nature*, vol. 398, no. 6725, pp. 297–298, 1999.

[43] T. Elbert, B. Rockstroh, W. Lutzenberger, and N. Birbaumer, "Biofeedback of slow cortical potentials. I," *Electroencephalography and Clinical Neurophysiology*, vol. 48, no. 3, pp. 293–301, 1980.

[44] S. R. Soekadar, M. Witkowski, J. Mellinger, A. Ramos, N. Birbaumer, and L. G. Cohen, "ERD-based online brain-machine interfaces (BMI) in the context of neurorehabilitation: optimizing BMI learning and performance," *IEEE Transactions on Neural Systems and Rehabilitation Engineering*, vol. 19, no. 5, pp. 542–549, 2011.

[45] C. Neuper, G. R. Müller-Putz, R. Scherer, and G. Pfurtscheller, "Motor imagery and EEG-based control of spelling devices and neuroprostheses," *Progress in Brain Research*, vol. 159, pp. 393–409, 2006.

[46] G. R. Müller-Putz and G. Pfurtscheller, "Control of an electrical prosthesis with an SSVEP-based BCI," *IEEE Transactions on Biomedical Engineering*, vol. 55, no. 1, pp. 361–364, 2008.

[47] N. Birbaumer, T. Elbert, A. G. M. Canavan, and B. Rockstroh, "Slow potentials of the cerebral cortex and behavior," *Physiological Reviews*, vol. 70, no. 1, pp. 1–41, 1990.

[48] N. Birbaumer, L. E. Roberts, W. Lutzenberger, B. Rockstroh, and T. Elbert, "Area-specific self-regulation of slow cortical potentials on the sagittal midline and its effects on behavior," *Electroencephalography and Clinical Neurophysiology*, vol. 84, no. 4, pp. 353–361, 1992.

[49] N. Birbaumer, H. Flor, W. Lutzenberger, and T. Elbert, "Chaos and order in the human brain," *Electroencephalography and Clinical Neurophysiology*, vol. 44, pp. 450–459, 1995.

[50] T. Hinterberger, R. Veit, B. Wilhelm, N. Weiskopf, J. J. Vatine, and N. Birbaumer, "Neuronal mechanisms underlying control of a brain—computer interface," *European Journal of Neuroscience*, vol. 21, no. 11, pp. 3169–3181, 2005.

[51] P. Eberlin and D. Yager, "Alpha blocking during visual afterimages," *Electroencephalography and Clinical Neurophysiology*, vol. 25, no. 1, pp. 23–28, 1968.

[52] R. C. Howe and M. B. Sterman, "Cortical-subcortical EEG correlates of suppressed motor behavior during sleep and waking in the cat," *Electroencephalography and Clinical Neurophysiology*, vol. 32, no. 6, pp. 681–695, 1972.

[53] C. Neuper and G. Pfurtscheller, "Event-related dynamics of cortical rhythms: frequency-specific features and functional correlates," *International Journal of Psychophysiology*, vol. 43, no. 1, pp. 41–58, 2001.

[54] H. Gastaut, "Electrocorticographic study of the reactivity of rolandic rhythm," *Revue Neurologique*, vol. 87, no. 2, pp. 176–182, 1952.

[55] G. Pfurtscheller, C. Neuper, and N. Birbaumer, "Human brain-computer interface (BCI)," in *Motor Cortex in Voluntary Movements. A Distributed System for Distributed Functions*, pp. 367–401, 2005.

[56] J. R. Wolpaw and D. J. McFarland, "Control of a two-dimensional movement signal by a noninvasive brain-computer interface in humans," *Proceedings of the National Academy of Sciences of the United States of America*, vol. 101, no. 51, pp. 17849–17854, 2004.

[57] J. R. Wolpaw, "Brain-computer interfaces as new brain output pathways," *The Journal of Physiology*, vol. 579, no. 3, pp. 613–619, 2007.

[58] L. A. Farwell and E. Donchin, "Talking off the top of your head: toward a mental prosthesis utilizing event-related brain potentials," *Electroencephalography and Clinical Neurophysiology*, vol. 70, no. 6, pp. 510–523, 1988.

[59] A. Chatterjee, V. Aggarwal, A. Ramos, S. Acharya, and N. V. Thakor, "A brain-computer interface with vibrotactile biofeedback for haptic information," *Journal of NeuroEngineering and Rehabilitation*, vol. 4, article 40, 2007.

[60] I. Käthner, C. A. Ruf, E. Pasqualotto, C. Braun, N. Birbaumer, and S. Halder, "A portable auditory P300 brain-computer interface with directional cues," *Clinical Neurophysiology*, vol. 124, no. 2, pp. 327–338, 2012.

[61] M. Schreuder, B. Blankertz, and M. Tangermann, "A new auditory multi-class brain-computer interface paradigm: spatial hearing as an informative cue," *PLoS ONE*, vol. 5, no. 4, Article ID e9813, 2010.

[62] A. Lenhardt, M. Kaper, and H. J. Ritter, "An adaptive P300-based online brain-computer interface," *IEEE Transactions on Neural Systems and Rehabilitation Engineering*, vol. 16, no. 2, pp. 121–130, 2008.

[63] T. O. Zander and C. Kothe, "Towards passive brain-computer interfaces: applying brain-computer interface technology to human-machine systems in general," *Journal of Neural Engineering*, vol. 8, no. 2, Article ID 025005, 2011.

[64] T. Zander and S. Jatzev, "Context-aware brain-computer interfaces: exploring the information space of user, technical system and environment," *Journal of Neural Engineering*, vol. 9, no. 1, Article ID 016003, 2012.

[65] G. R. Müller-Putz, R. Scherer, G. Pfurtscheller, and R. Rupp, "Brain-computer interfaces for control of neuroprostheses: from synchronous to asynchronous mode of operation," *Biomedizinische Technik*, vol. 51, no. 2, pp. 57–63, 2006.

[66] S. G. Mason and G. E. Birch, "A brain-controlled switch for asynchronous control applications," *IEEE Transactions on Biomedical Engineering*, vol. 47, no. 10, pp. 1297–1307, 2000.

[67] M. Velliste, S. Perel, M. C. Spalding, A. S. Whitford, and A. B. Schwartz, "Cortical control of a prosthetic arm for self-feeding," *Nature*, vol. 453, no. 7198, pp. 1098–1101, 2008.

[68] L. R. Hochberg, M. D. Serruya, G. M. Friehs et al., "Neuronal ensemble control of prosthetic devices by a human with tetraplegia," *Nature*, vol. 442, no. 7099, pp. 164–171, 2006.

[69] G. Pfurtscheller, C. Guger, G. Müller, G. Krausz, and C. Neuper, "Brain oscillations control hand orthosis in a tetraplegic," *Neuroscience Letters*, vol. 292, no. 3, pp. 211–214, 2000.

[70] N. Birbaumer and L. G. Cohen, "Brain-computer interfaces: communication and restoration of movement in paralysis," *The Journal of Physiology*, vol. 579, no. 3, pp. 621–636, 2007.

[71] N. Birbaumer, A. Ramos Murguialday, C. Weber, and P. Montoya, "Neurofeedback and brain-computer interface: clinical applications," *International Review of Neurobiology*, vol. 86, pp. 107–117, 2009.

[72] J. J. Daly and J. R. Wolpaw, "Brain-computer interfaces in neurological rehabilitation," *The Lancet Neurology*, vol. 7, no. 11, pp. 1032–1043, 2008.

[73] D. Broetz, C. Braun, C. Weber, S. R. Soekadar, A. Caria, and N. Birbaumer, "Combination of brain-computer interface training and goal-directed physical therapy in chronic stroke: a case report," *Neurorehabilitation and Neural Repair*, vol. 24, no. 7, pp. 674–679, 2010.

[74] A. Caria, C. Weber, D. Brötz et al., "Chronic stroke recovery after combined BCI training and physiotherapy: a case report," *Psychophysiology*, vol. 48, no. 4, pp. 578–582, 2010.

[75] W. Wang, J. L. Collinger, M. A. Perez et al., "Neural interface technology for rehabilitation: exploiting and promoting neuroplasticity," *Physical Medicine and Rehabilitation Clinics of North America*, vol. 21, no. 1, pp. 157–178, 2010.

[76] A. P. Georgopoulos, A. B. Schwartz, and R. E. Kettner, "Neuronal population coding on movement direction," *Science*, vol. 233, no. 4771, pp. 1416–1419, 1986.

[77] M. A. L. Nicolelis, D. Dimitrov, J. M. Carmena et al., "Chronic, multisite, multielectrode recordings in macaque monkeys," *Proceedings of the National Academy of Sciences of the United States of America*, vol. 100, no. 19, pp. 11041–11046, 2003.

[78] H. Scherberger, M. R. Jarvis, and R. A. Andersen, "Cortical local field potential encodes movement intentions in the posterior parietal cortex," *Neuron*, vol. 46, no. 2, pp. 347–354, 2005.

[79] D. M. Taylor, S. I. H. Tillery, and A. B. Schwartz, "Direct cortical control of 3D neuroprosthetic devices," *Science*, vol. 296, no. 5574, pp. 1829–1832, 2002.

[80] M. Velliste, A. McMorland, E. Diril, S. Clanton, and A. Schwartz, "State-space control of prosthetic hand shape," in *Proceedings of the Annual International Conference of the IEEE Engineering in Medicine and Biology Society (EMBC '12)*, pp. 964–967, 2012.

[81] A. R. Seifert and J. F. Lubar, "Reduction of epileptic seizures through EEG biofeedback training," *Biological Psychology*, vol. 3, no. 3, pp. 157–184, 1975.

[82] B. Kotchoubey, U. Strehl, C. Uhlmann et al., "Modification of slow cortical potentials in patients with refractory epilepsy: a controlled outcome study," *Epilepsia*, vol. 42, no. 3, pp. 406–416, 2001.

[83] N. Birbaumer, T. Elbert, B. Rockstroh, and W. Lutzenberger, "Biofeedback of slow cortical potentials in attentional disorders," in *Cerebral Psychophysiology: Studies in Event-Related Potentials*, pp. 440–442, 1986.

[84] U. Strehl, U. Leins, G. Goth, C. Klinger, T. Hinterberger, and N. Birbaumer, "Self-regulation of slow cortical potentials: a new treatment for children with attention-deficit/hyperactivity disorder," *Pediatrics*, vol. 118, no. 5, pp. e1530–e1540, 2006.

[85] T. Fuchs, N. Birbaumer, W. Lutzenberger, J. H. Gruzelier, and J. Kaiser, "Neurofeedback treatment for attention-deficit/hyperactivity disorder in children: a comparison with methylphenidate," *Applied Psychophysiology and Biofeedback*, vol. 28, no. 1, pp. 1–12, 2003.

[86] M. Lotze, W. Grodd, N. Birbaumer, M. Erb, E. Huse, and H. Flor, "Does use of a myoelectric prosthesis prevent cortical reorganization and phantom limb pain?" *Nature Neuroscience*, vol. 2, no. 6, pp. 501–502, 1999.

[87] T. Platz, I. H. Kim, U. Engel, A. Kieselbach, and K. H. Mauritz, "Brain activation pattern as assessed with multi-modal EEG analysis predict motor recovery among stroke patients with mild arm paresis who receive the Arm Ability Training," *Restorative Neurology and Neuroscience*, vol. 20, no. 1-2, pp. 21–35, 2002.

[88] C. Calautti, M. Naccarato, P. S. Jones et al., "The relationship between motor deficit and hemisphere activation balance after stroke: a 3T fMRI study," *NeuroImage*, vol. 34, no. 1, pp. 322–331, 2007.

[89] E. Buch, C. Weber, L. G. Cohen et al., "Think to move: a neuromagnetic brain-computer interface (BCI) system for chronic stroke," *Stroke*, vol. 39, no. 3, pp. 910–917, 2008.

[90] A. Ramos-Murguialday, D. Broetz, M. Rea et al., "Brain-machine-interface in chronic stroke rehabilitation: a controlled study," *Annals of Neurology*, 2013.

[91] F. Brasil, M. R. Curado, M. Witkowski et al., "MEP predicts motor recovery in chronic stroke patients undergoing 4-weeks of daily physical therapy," in *Human Brain Mapping Annual Meeting*, Beijing, China, 2012, 33WTh.

[92] J. M. Carmena and L. G. Cohen, "Brain-machine interfaces and transcranial stimulation: future implications for directing

functional movement and improving function after spinal injury in humans," in *Spinal Cord Injuries E-Book*, vol. 109 of *Handbook of Clinical Neurology*, chapter 27, pp. 435–444, 2012.

[93] C. R. Hema, M. Paulraj, S. Yaacob, A. H. Adom, and R. Nagarajan, "Asynchronous brain machine interface-based control of a wheelchair," in *Software Tools and Algorithms for Biological Systems*, pp. 565–572, 2011.

[94] G. Pfurtscheller, G. R. Müller, J. Pfurtscheller, H. J. Gerner, and R. Rupp, "'Thought'—control of functional electrical stimulation to restore hand grasp in a patient with tetraplegia," *Neuroscience Letters*, vol. 351, no. 1, pp. 33–36, 2003.

[95] A. H. Do, P. T. Wang, A. Abiri, C. King, and Z. Nenadic, "Brain-computer interface controlled functional electrical stimulation system for ankle movement," *Journal of NeuroEngineering and Rehabilitation*, vol. 8, no. 1, article 49, 2011.

[96] M. Tavella, R. Leeb, R. Rupp, and J. D. R. Millán, "Towards natural non-invasive hand neuroprostheses for daily living," in *Proceedings of the 32nd Annual International Conference of the IEEE Engineering in Medicine and Biology Society (EMBC '10)*, pp. 126–129, September 2010.

[97] A. R. Murguialday, J. Hill, M. Bensch et al., "Transition from the locked in to the completely locked-in state: a physiological analysis," *Clinical Neurophysiology*, vol. 122, no. 5, pp. 925–933, 2011.

[98] J. Clausen, "Ethische Aspekte von Gehirn-Computer-Schnittstellen in motorischen Neuroprothesen," *International Review of Information Ethics*, vol. 5, pp. 25–32, 2006.

[99] J. Clausen, "Man, machine and in between," *Nature*, vol. 457, no. 7233, pp. 1080–1081, 2009.

[100] J. L. Collinger, B. Wodlinger, J. E. Downey et al., "High-performance neuroprosthetic control by an individual with tetraplegia," *The Lancet*, vol. 381, no. 9866, pp. 557–564, 2013.

[101] S. T. Grafton and C. M. Tipper, "Decoding intention: a neuroergonomic perspective," *NeuroImage*, vol. 59, no. 1, pp. 14–24, 2012.

[102] A. Presacco, L. W. Forrester, and J. L. Contreras-Vidal, "Decoding intra-limb and inter-limb kinematics during treadmill walking from scalp electroencephalographic (EEG) signals," *IEEE Transactions on Neural Systems and Rehabilitation Engineering*, vol. 20, no. 2, pp. 212–219, 2012.

[103] T. J. Bradberry, R. J. Gentili, and J. L. Contreras-Vidal, "Reconstructing three-dimensional hand movements from noninvasive electroencephalographic signals," *The Journal of Neuroscience*, vol. 30, no. 9, pp. 3432–3437, 2010.

[104] N. Birbaumer, G. Gallegos-Ayala, M. Wildgruber, S. Silvoni, and S. R. Soekadar, "Direct brain control and communication in paralysis," *Brain Topography*. In press.

[105] S. R. Soekadar and N. Birbaumer, "Improving the efficacy of ipsilesional brain-computer interface training in neurorehabilitation of chronic stroke," in *Brain-Computer Interface Research: A State-of-the-Art Summary*, C. Guger, B. Allison, and G. Edlinger, Eds., Springer, 2013.